CAPACITIVE PRESSURE TRANSDUCER SYSTEM

by

Gerard J. Born
Enoch J. Durbin
Robert S. Quinn

Department of Aerospace and Mechanical Sciences
Princeton University

July, 1967

TABLE OF CONTENTS

ACKNOWLEDGEMENT

This work was supported by the National Aeronautics and Space Administration Contract NASA 8-5343. The authors wish to express their appreciation for the technical guidance and understanding support of Mr. James Power, scientist at the Astrionics Laboratory, George C. Marshall Space Flight Center, Huntsville, Alabama.

LIST OF FIGURES

LIST OF SYMBOLS

a	radius of diaphragm
A	amplifications
A_D	surface area of the diaphragm
b	phase lag factor
C_o	capacitance of one side of the transducer
ΔC_o	change in capacitance of the transducer
c	speed of sound
d_o	electrode-diaphragm spacing when diaphragm is in equilibrium
Δd_o	center deflection of diaphragm
d	diaphragm-electrode space when the diaphragm is deflected
db	decibels
e_n	noise voltage
E	Young's Modulus
$E(s)$	Laplace transform of error signal
F_m	mechanical force
F_g	gravitational force
F_{es}	electrostatic force
g	gravitational constant
$G(s)$	forward loop transfer function
$H(s)$	feedback loop transfer function
h	thickness of diaphragm
k	dielectric constant
K'	gauge constant

K	sensitivity constant
K_i	slope at operating point
k	mechanical spring constant
k'	electrical spring constant
K_1	open loop gain
K_{2i}	closed loop gain (uncompensated)
K_{3i}	compensated closed loop gain
ℓ	length of tubing
m	mass per unit area
m_1	phase lead factor
M_m	resonance ratio
P	pressure
P_D	pressure disturbance
P_c	pressure change in reservoir (air cavity)
P_o	standard atmospheric pressure
P_{es}	electrostatic pressure
R'	radius of electrode
r	radius
R_L	load resistance
R_1	damping constant
s	Laplace operator
S	cross sectional area of air cavity
t	time
T	tension lbs/in
V_o	output voltage from bridge
V_E	bridge excitation voltage

V	volume of air cavity
V_i	operating voltage
v	output voltage of forward loop
$Y_{os(max)}$	maximum overshoot
ϵ_o	permittivity constant
η_o	center deflection of diaphragm
η	deflection of diaphragm as measured from equilibrium position
Δ	differential change
Ω	frequency of bridge excitation
ω_{nD}	natural frequency of diaphragm RAD./SEC.
ω_{nR}	natural frequency of resonator
ω'_{nD}	closed loop frequency
ξ_D	damping ratio of diaphragm
ξ'_D	closed loop damping
μ	weight/unit volume
ρ	mass/unit volume
ϕ	sensitivity constant
α	constant
γ	constant
σ	Poisson's Ratio
β_i	feedback constant
τ	time constant
θ	phase angle
ω	frequency
ϵ	error

INTRODUCTION

In recent years advanced research and technology in science and engineering have created a need for newly improved and highly intricate instrumentation. In particular, in the Aerospace field, one of the many new demands on instrumentation has been for the development of a pressure transducer with an extended frequency response that is capable of accurately measuring very low pressures.

In the measurement of very low pressures, microscopic changes in the properties of the sensing material become extremely important. Many of the pressure transducers that are presently being used for low pressure measurements provide an indirect measure of pressure changes. That is, in these instruments the pressure of a gas is determined as a quantitative measure of the microscopic changes of the properties (such as thermal and electrical changes) of a particular material to which the gas is exposed. The major disadvantage of this indirect measurement is that the degree of change of the properties of the sensing element is not only dependent upon gas pressure, but also upon the composition of the gas and to the effects of environmental changes such as temperature changes. Hence, in utilizing these instruments, it becomes necessary to provide a corrrection factor for each gas and for different environmental conditions.

A more precise measurement can be obtained if the gas pressure is directly measured by a mechanical sensing device. The advantage of a direct measurement is that the pressure measurements are independent of the nature of the gas.

In the low pressure range, the McLeod gauge has been the only mechanical device capable of accurately measuring pressures as low as 10^{-2}mm of mercury. However, in the last twenty years capacitive pressure transducers have been designed for the measurement of very low pressures. This type of transducer utilizes the concept by which a physical quantity, in this case a pressure, deflects a sensing element producing a capacitance change. The transducer consists of a pressure sensitive metallic diaphragm symmetrically placed between two fixed electrodes thus forming a differential capacitor. This differential element makes up the two active arms of a bridge network which is excited by an AC source of several kc/sec. The application of pressure to the diaphragm displaces the diaphragm from its equilibrium position thus causing a differential change of capacitance. This capacitance change produces a bridge error or output voltage which is amplified and fed to a phase sensitive detector that determines the direction of unbalance and develops a DC voltage. The final output voltage can then be used:

1. in a forward or open loop system and directly recorded;
2. or in a feedback or closed loop system.

Capacitive pressure transducers originally utilized a thin plate as their sensing element and operated as an open loop system. A thin plate is a diaphragm which has a restoring force due to its stiffness (Modulus of Elasticity). The sensitivity of a thin plate is inversely proportional to its stiffness or mechanical spring constant. Consequently, since these pressure transducers utilized thin plates that had a high modulus of

elasticity they were not very sensitive to constant accelerating forces; however, they also exhibited a poor sensitivity to low pressures.

These instruments experienced a high frequency response because the natural frequency of a thin plate is proportional to the square root of its stiffness. Furthermore, because the sensing element was very stiff, it experienced only small deflections. Consequently, these pressure transducers had a high degree of linearity.

In order to increase the instrument's sensitivity to low pressures, the sensing element was made very thin and was weakly stressed. In essence, it became a weakly stressed membrane and its stiffness became negligible compared to its tension.

The sensitivity of a membrane is inversely proportional to its tension. Hence, by utilizing a weakly stressed membrane, the instrument's sensitivity to low pressures increased. However, by making the weakly stressed sensing element very thin both its mass and mechanical spring constant decreased; hence, its sensitivity to constant accelerating forces did not change.

Furthermore, because of being weakly stressed and very thin, the sensing element experiences larger deflections when disturbed by a differential force. This decreased the linearity of the instrument because the transducer was only linear for very small deflections. However, because the frequency of a membrane is proportional to the square root of its tension a weakly stressed membrane had a low frequency response. This

was a disadvantage in that it gave the system a slow response but it was also an advantage because it made the system insensitive to high frequency disturbances such as high frequency vibration in an aircraft. Other difficulties were also caused by the adverse effects of the associated circuitry which were costly and complex.

In an attempt to eliminate some of these disadvantages, the concept of the highly stressed membrane was developed. By increasing the tension of the membrane, its frequency response increased, resulting in a fast time response. In addition, a mechanically stressed membrane experiences smaller deflections. Thus, the instrument's range of linearity increased.

However, since the sensitivity of a membrane is inversely proportional to its tension (stiffness), a highly stressed membrane is less sensitive to low pressures. In fact, if a highly stressed membrane is as stiff as a thin plate, its pressure sensitivity would be equal to the pressure sensitivity of a thin plate. However, because the mass of the membrane is very small, a highly stressed membrane is less sensitive to constant accelerating forces than a thin plate. Consequently, utilizing a highly stressed membrane has improved the instrument's signal to noise ratio; the ratio of percent of deflection due to a pressure force to the percent of deflection due to a constant accelerating force has increased.

A disadvantage of a highly stressed membrane is that environmental effects such as temperature changes effect the calibration of the instrument by altering the tension of the membrane. Hence, in order to obtain accurate pressure measurements, it is necessary to monitor other

parameters in the system. Consequently, by utilizing a highly stressed membrane, the performance of the transducer is dependent upon the mechanical properties of the sensing element.

It was anticipated that by employing a weakly stressed membrane in a feedback loop, the sensing element could be electrostatically stiffened. By replacing the mechanical stiffness of the sensing element by a stiff electrical spring the system's performance would be made independent of the mechanical properties of the membrane and its linearity would be increased. Furthermore, its acceleration sensitivity would be less than sensitivity of a thin plate. It is the purpose of this report to analyze and design closed loop capacitive pressure transducers to achieve this goal.

This report begins with the theoretical design analysis of a forward loop capacitive pressure transducer. Next, an analysis is made to evaluate the effects of closing the loop by introducing an electrostatic feedback loop around the transducer. A closed loop system, utilizing a weakly stressed diaphragm, is theoretically designed. The investigation of this closed loop system involves a frequency and dynamic response synthesis of the system and an analog simulation study. The final portion of this report discribes the construction of a closed loop system which is used to experimentally verify the theoretical results.

This report also contains four appendices which deal respectively with: the theoretical investigation of diaphragm; theory of acoustic resonators; determination of the transfer function of a capacitance bridge network with two active differential arms; and the theoretical analysis of a variable capacitor relating a differential displacement to the resulting differential change in capacitance.

CHAPTER I

Theory

A. Capacitive Pressure Transducer

Figure 1 represents a cross section of a symmetrical capacitive transducer. It consists of a thin metallic circular diaphragm. The diaphragm is clamped along its perphery under a radial tension T. The disphragm has an effective radius "a" measured from the inside edge of the clamp and an infinitesimal thickness h. It is centrally placed a distance d_o between two stationary electrodes of radius R'. The diaphragm is placed symmetrically between the electrodes because this configuration leads to the simplest analysis and represents the optimal design. The transducer constructed in this manner forms a differential parallel capacitor.

If the transducer was stationary and the diaphragm not ferromagnetic, three forces can act on the diaphragm.

1. Mechanical force: caused by a disturbing pressure ΔP

$$F_m = \pi a^2 \Delta P \qquad 1$$

2. Gravitation force: caused by tilting the diaphragm from its vertical position by an angle θ

$$F_G = (\pi a^2) \rho g h \sin\theta \qquad 2$$

For this study the effect of the gravitational force on the diaphragm will be considered negligible and omitted from the analysis.

3. Electro-static force: caused by the application of a voltage V to one or both sides of the differential capacitor while the diaphragm is grounded

$$F_{e.s.} = (\pi R'^2) \frac{k\epsilon_o}{2d_o^2} V^2 \qquad \text{(non-linear)} \qquad 3$$

When acted upon by one of these disturbing forces, the resultant motion of the diaphragm is dependent upon its mechanical characteristics. Appendix A contains a detailed study on the theory of diaphragms. From equations in this Appendix, it is assumed that the diaphragm used in this study is characterized as a membrane. When the diaphragm is subjected to a uniform pressure disturbance P_D, membrane theory shows that the resultant deflection is assumed to vary linearly with pressure provided $\frac{\Delta d_o}{d_o} \leq 0.01$.
This relationship is expressed by Equation A-52

$$\eta = \eta_o \left[1 - \left(\frac{r}{a}\right)^2 \right] \qquad \text{A-52}$$

where η_o, the center deflection is

$$\eta_o = \Delta d_o = \frac{a^2 \Delta P}{4T} \qquad \text{A-51}$$

and η is the deflection measured from the equilibrium position of the diaphragm.

When measured from the surface of the fixed electrodes, the electrode spacing becomes

$$d = d_o \pm \Delta d_o \left[1 - \left(\frac{r}{a}\right)^2 \right] \qquad 4$$

where the plus or minus signs depend on whether the diaphragm is deflected towards or away from the reference electrode.

B. Capacitance Bridge

Figure 4 is a simplified diagram of a capacitance bridge with two active arms excited by a constant frequency a.c. source. The two variable capacitors correspond to the two sides of the differential pressure transducers. The capacitance of each of the four elements is equal to the capacitance of one side of the differential transducer with the diaphragm in its undeflected state. Equation D-2 in Appendix D expresses the capacitance of this parallel plate capacitor as

$$C_o = \frac{k\epsilon_o A}{d_o} = \frac{k\epsilon_o \pi R'^2}{d_o} \qquad \text{D-2}$$

When the diaphragm is in its equilibrium position, all of the bridge elements are of equal capacitance and the bridge is considered to be balanced. The balancing relationship, as taken from Appendix C, is

$$C_1 C_4 = C_3 C_2 \qquad \text{C-3}$$

When this equation is satisfied, there is no output voltage from the bridge. But when the diaphragm is subjected to a disturbing force, it is displaced a distance Δd_o from its equilibrium. Since the capacitance of this symmetrical differential capacitor is inversely proportional to the electrode spacing, a differential change in the spacing, $\pm\Delta d_o$, will result in a differential change in capacitance, ΔC_o, on each side of the transducer. Appendix D derives an equation relating the variation in electrode spacing Δd_o to the resulting capacitance change ΔC_o for a variable capacitor. To a first order approximation in $\frac{\Delta d_o}{d_o}$ this relationship is given by Equation D-11

$$\Delta C_o = \pm \frac{1}{2} K' C_o \frac{\Delta d_o}{d_o} \qquad \text{D-11}$$

The resulting change in capacitance off balances the bridge and produces an output voltage from the bridge. The expression relating the bridge output voltage, V_o, to the capacitive change, ΔC_o, is derived in Appendix C and is

$$\frac{V_o}{V_E} = \frac{1}{2} \frac{\Delta C_o}{C_o} \left[\frac{1}{1 + \frac{1}{\Omega R_L C_o}} \right] \qquad \text{C-17}$$

CHAPTER II

FORWARD LOOP ANALYSIS

A. Design of the Forward Loop

Figure 5 shows a schematic representation of the uncompensated forward loop system. It consists of the capacitive pressure transducer, the capacitance bridge circuit and an amplifier. The system is also represented in block diagram form in Figure 6 .

The first two transfer functions $G_1(s)$ and $G_2(s)$ of the forward loop system are related to the transducer. An analysis of the dynamics of the transducer considers the transducer as consisting of two coupled sections. The first section is the length of tubing leading to the transducer and the air cavity that exists between the electrode and the diaphragm. The second section is the diaphragm. The motion of the air in the cavity is coupled to the motion of the diaphragm by the volume of air in the cavity (which mutually acts on both sections).

Appendix B explains that the air cavity acts like an acoustical resonator and shows that the motion of the air in the enclosure is described by a simple second order differential equation

$$\frac{1}{\omega_{nR}^2}\ddot{P}_c + \frac{2\zeta_R}{\omega_{nR}}\dot{P}_c + P_c = P_D \qquad \text{B-23}$$

or expressed as a transfer function

$$G_1(s) = \frac{P_c(s)}{P_D(s)} = \frac{1}{\frac{s^2}{\omega_{nR}^2} + \frac{2\zeta_R}{\omega_{nR}}s + 1} \qquad \text{B-26}$$

where

$$\omega_{nR} = c\sqrt{\frac{S}{\ell V}} \qquad \text{B-24}$$

$$\zeta_R = \frac{8\mu\ell}{2\pi r^4}\sqrt{\frac{\pi r^2 V}{\rho \ell \gamma P_o}} \qquad \text{B-25}$$

This Appendix explains that because of the long length of tubing leading to the cavity, the damping is principally caused by the viscous friction in the tubing, while the damping due to radiation loss from the cavity is comparably negligible.

The volume of air in the cavity couples the pressure disturbance to the diaphragm. Its motion disturbs the diaphragm from its equilibrium position. Appendix A contains a detailed study on diaphragms. From equations in this Appendix, the diaphragm is assumed to have the characteristics of a membrane. This will be proven in a later section. From membrane theory, the motion of the diaphragm, when acted upon by a disturbing pressure force, is expressed by a second-order differential equation with the following transfer function

$$G_2(s) = \frac{\Delta d_o(s)}{P_c(s)} = \frac{\phi}{\frac{S^2}{\omega_{nD}^2} + \frac{2\zeta_D}{\omega_{nD}} S + 1} \qquad 5$$

where

$$\omega_{nD} = \omega_{nM} = \frac{2.405}{a}\sqrt{\frac{T}{m}} \qquad \text{A-13}$$

$$\zeta_D = \sqrt{\frac{R_i^2 a^2}{23.2 T m}} \qquad \text{(obtained from Equations A-22 and A-13)} \qquad 5\text{-}a$$

The gain K is evaluated under steady state conditions in this same Appendix and is found to be equal to

$$\phi = \frac{a^2}{4T} \qquad \text{A-51}$$

At this point, the analysis can be simplified if the coupling between the two transfer functions, $G_1(s)$ and $G_2(s)$, can be eliminated. The dynamics of these two second order systems can be uncoupled if their natural frequencies (or resonance region) are in widely separated regions in the frequency domain. Hence, if ω_{nR}, the natural frequency of $G_1(s)$, can be made several times larger than ω_{nD}, then in effect the two systems are uncoupled. From Equation B-24 it is observed that ω_{nR} increases as the cavity volume decreases. Hence, in order to increase ω_{nR} the transducer should be designed for a minimum internal cavity volume. This dimension is most easily changed by varying the electrode spacing d_o. Theoretically, this spacing can be made infinitesimally small, but for practical applications, this is not possible. There is a relation between the electrode spacing of a parallel plate capacitor and the voltage applied across the gap. This is known as Paschen's Law and must be considered in choosing the minimum allowable electrode spacing.

Hence, when operating in the frequency range of the diaphragm, the dynamics of the system are unaffected by $G_1(s)$ if $\omega_{nR} \gg \omega_{nD}$. Furthermore, by this requirement, it can be assumed that $\frac{1}{\omega_{nR}} \ll 1$. Hence, for the operating frequency range encountered in this analysis, the transfer function for the resonator may be approximated as

$$G_1(s) = \frac{P_c(s)}{P_o(s)} \simeq 1 \qquad 6$$

Consequently, by the above requirements, the pressure transducer can be represented by a second order transfer function whose damping and frequency are characteristic only of the diaphragm.

As previously stated in Chapter I, the transducer is a differential capacitor making up two arms of a capacitance bridge network which is excited by an A.C. source. The capacitance C_o of each side of this variable differential parallel plate capacitor is given by the Equation D-2. When disturbed by a pressure difference, the motion of the diaphragm results in a differential change in capacitance ΔC_o on both sides of the transducer. This capacitive unbalance on each side of the differential capacitor $(c_o + \Delta c_o,\ c_o - \Delta c_o)$ produces an output signal from the bridge. From Appendix C the expression relating the output signal to the differential change in capacitance is expressed as

$$\frac{V_o}{V_E} = \frac{1}{2}\frac{\Delta C_o}{C_o}\left[\frac{1}{1+\frac{1}{\Omega R_L C_o}}\right] \qquad \text{C-17}$$

Appendix D derives an expression relating the capacitive change ΔC_o on one side of the symmetrical transducer to the deflection of the diaphragm Δd_o. This relationship is expressed as

$$\Delta C_o = \pm\frac{1}{2}\frac{\Delta d_o}{d_o} C_o K' \qquad \text{D-11}$$

where

$$K' = 2 - \left(\frac{R'}{a}\right)^2 \qquad \text{D-12a}$$

Substituting Equation D-11 into Equation C-17 the following equation is obtained relating the diaphragm deflection to the resulting bridge output signal

$$\frac{V_o}{\Delta d_o} = \frac{V_E K'}{4 d_o}\left[\frac{1}{1+\frac{1}{\Omega R_L C_o}}\right] = \frac{V_E K'}{4 d_o}\left[\frac{1}{1+\frac{\alpha}{\Omega}}\right] \qquad \text{C-19}$$

where

$$V_E = V_E \sin \Omega t$$

$$\alpha = \frac{1}{R_L C_o}$$

Now as a design requirement, it is desirable to isolate the frequency response of the transducer from the possible unstabilizing effects of other elements in the forward loop. The frequency of the transducer is fixed by the characteristics of the diaphragm. Hence, it is necessary to design the other elements in the loop such that their frequency is much larger than ω_{nD}. It would be preferable to set $\alpha \gg \omega_{nD}$, but by referring to Appendix C, it is seen that when Equation C-19 is transformed to bode form, the system's loop gain is attenuated by the factor α. Since it will be required to have a maximum output signal, an attenuation in gain is not desired. On this basis, the bridge circuit must be designed such that $\alpha < \omega_{nD}$.

Now α, as defined, is inversely proportional to R_L and C_o. Since C_o is fixed by the geometry of the transducer, R_L is the only variable control on α. Hence, it is observed from Equation 7 that in order to decrease α it is necessary for R_L to be very large. Fortunately another requirement is to have a maximum output voltage from this bridge. This also requires R_L to be very large in order to prevent loading of the bridge.

Figure 34 is a Thevenin equivalent circuit for the capacitance bridge. Note that since all four capacitors in the bridge circuit are equal, the equivalent capacitance is also C_o.

In designing a measuring system it is desirable to eliminate errors such as noise, inherent in the electrical circuitry. Equation 8 gives the general equation for finding the noise voltage of a circuit.

$$e_N^2 = \frac{4KT}{2\pi}\int_0^\infty R(\omega)\,d\omega \qquad 8$$

K = Boltzmann's Constant

T = Temp. (degree Kelvin)

$R(\omega)$ corresponds to the real component of the total impedance of the circuit. For the Thevenin equivalent circuit under discussion,

$$Z\,(\text{IMPEDENCE}) = \frac{R_L}{1+j\omega C_o R_L} \quad ; \quad R(\omega) = \frac{R_L}{\sqrt{1+(\omega C_o R_L)^2}} \qquad 9$$

Hence, when this expression is substituted into Equation 8, the noise voltage for this circuit is evaluated as

$$e_N^2 = \frac{KT}{C_o} \qquad 10$$

For all practical purposes, the value of this term is small and can be neglected from the analysis.

A further simplification can be made in this analysis by requiring the bridge to be excited by a high frequency A.C. signal. Since $\alpha < \omega_{nD}$, it can be shown that by setting Ω, the frequency of the A.C. source, much larger than ω_{nD}, the following approximation can be made

$$\Omega \gg \alpha$$

thus

$$\frac{\alpha}{\Omega} \ll 1$$

By this assumption, Equation C-19 can be rewritten as

$$\frac{V_o}{\Delta d_o} = \frac{K'}{4d_o} V_E$$

C-29

where $V_E = V_E \sin \Omega t$. Since the output will be rectified, it is only necessary to consider the absolute magnitude of V_E. Thus, the transfer function $G_3(s)$ relating the rectified bridge output to the displacement of the diaphragm is expressed as

$$G_3(s) = \frac{V_o(s)}{\Delta d_o(s)} = \frac{K' V_E}{4 d_o}$$

Hence, by requiring $\Omega \gg \alpha$, the output becomes insensitive to changes of the bridge excitation frequency. This approximation has also been demonstrated in Appendix C where the proof is worked out in the time domain.

The fourth element, $G_4(s)$ in the forward loop amplifies the output voltage from the bridge. Hence, the rectified output voltage of the system is expressed as

$$v = A V_o$$

where

$$G_4(s) = \frac{V(s)}{V_o(s)} = A \qquad 12$$

By combining Equations 5, 6, 11, 12 an expression for the complete forward loop transfer function is obtained. This expression relates the output voltage v to input pressure disturbance P_D as follows

$$G(s) = G_1(s) G_2(s) G_3(s) G_4(s) = \frac{V(s)}{P_D(s)} = \frac{P_i(s)}{P_D(s)} \frac{\Delta d_o(s)}{d_o(s)} \frac{V_o(s)}{\Delta d_o(s)} \frac{V(s)}{V_o(s)}$$

$$G(s) = \frac{V(s)}{P_D(s)} = A \frac{K' V_E}{4 d_o} \frac{a^2}{4T} \left[\frac{1}{\frac{s^2}{\omega_{no}^2} + \frac{2\zeta}{\omega_{no}} s + 1} \right] \qquad 13$$

In conclusion, the mathematical model for the forward loop system has been reduced to a second order differential equation characteristic of the motion of the membrane. The forward loop gain defined as

$$K_1 = \left[\frac{a^2}{4T} \right] \left[\frac{K' V_E}{4 d_o} \right] A = \phi \gamma A \qquad 14$$

Summary of the Forward Loop Design Requirements

(1) Want a minimum cavity volume for the transducer in order that

A. $\omega_{nR} \gg \omega_{nD}$

B. $G_1(s) \simeq 1$

C. Consequently $G_1(s)$ and $G_2(s)$ do not have coupled modes.

(2) Want R_L very large

A. Maximum output signal

$\alpha < \omega_{nD}$

(3) Want $\Omega \gg \alpha$ such that

A. $G_3(s) \simeq$ gain

B. $G_3(s)$ will be insensitive to small frequency variations

(4) Maximum Gain

B. Construction of the Forward Loop

The forward loop system of the capacitance pressure transducer consists of four main parts: the diaphragm, the electrodes, the diaphragm housing, and the bridge network. The design requirements for this system have been given in the previous section and its construction will now be considered.

A. Diaphragm

The diaphragm is made from a 1/2 mil mylar film with a 1/4 mil of aluminum vacuum deposited on each side. Consequently, h, the thickness of the metallic diaphragm is 1 mil. The diaphragm is circularly clamped under a radial tension, T, of 0.10 lbs/in or 17.5 newtons/m. Its effective radius, a, is 0.75 in. The natural frequency, ω_{no}, of the diaphragm is a function of its mechanical and physical properties. Section A-5 of Appendix A derives a graphical method of determining the "Fundamental Natural Frequency of a Stretched, Circular, Clamped, Flat Diaphragm."

As outlined in that section, the first step in determining the natural frequency of the diaphragm is to evaluate Equation A-45

$$\frac{a^2 T}{m} \quad \frac{12\rho(1-\sigma^2)}{(E+T)h^2} \qquad \text{(A-45)}$$

For the diaphragm under study

σ = POISSON'S RATIO = 0.40

E = TENSILE (YOUNGS) MODULUS = 5.5×10^5 psi

$m = \frac{\mu}{g} h = \rho h$

μ = WEIGHT DENSITY = 1.38 (62.4) = 86 lb/in^3

Substituting these values and the dimensions given above into Equation A-45, it is evaluated as 1025. With the aid of Figure 29 and Table 2 the frequency of this diaphragm is theoretically found to be 100 c/s. From this analysis, it will be assumed that this diaphragm has the characteristics of a membrane. However, experiments on the diaphragm found it to have a frequency of only 60 c/s and a damping of 0.1 (see Figure 31). This experimentally determined value will be considered the correct frequency of the diaphragm and will be used for the theoretical analysis.

B. Electrodes

As previously explained, two circular aluminum electrodes are used in this system. Each electrode has a 0.75" radius and has an input port consisting of a 4" length of copper tubing 0.25" diameter located along their central axis.

The electrodes are symmetrically placed at a fixed distance d_o from both sides of the diaphragm. In accordance with the requirements set in Chapter 2, it is necessary to minimize the electrode-diaphragm spacing. It was determined that setting d_o = 4 mils satisfies the design requirements. The only restriction now is on the maximum voltage that can be applied across this air gap. From Paschen's curve given in Figure 2, it is seen that the maximum voltage is a function of the plate separations and the air pressure.

C. Diaphragm Housing

In order to establish the desired diaphragm-electrode space, a teflon ring 4 mils thick is centrally placed on each side of the clamped diaphragm. The ring has an I.D = 1.5 IN. and an O.D = 2 IN. By tightly clamping the electrodes against each ring, an internal cavity with a volume of $4\ \text{mils}\,(\pi a^2) = 7.1\times10^{-3}\ \text{IN}$ is created on each side of the diaphragm. The inlet port on the electrodes makes each cavity accessible for pressure measurements. As described in Appendix B, when a long length of tubing is connected to these ports an acoustical resonator is formed on each side of the diaphragm.

From Equation B-24 the natural frequency for the acoustical system is calculated as 3000 c/s . Thus, by choosing an electrode-diaphragm spacing of 4 mils the internal cavity volume is minimized. Hence, as seen from Equation B-24 ω_{nR} becomes much larger than ω_{no}. As explained in Chapter II this satisfies the requirement needed to uncouple the dynamics of the acoustical system from the dynamics of the diaphragm.

D. Bridge Network

As previously explained in Chapters I and II, the electrical circuitry of the forward loop consists of a capacitance bridge network with two active arms. The diaphragm-electrode configuration described above represents a differential capacitance pressure transducer. The two sides of this variable capacitor make up the two active elements of the capacitance bridge. This arrangement is schematically represented in Figure 4 . The capacitance of each side of the transducer is equal

and is a function of its geometry. For the above dimensions, the capacitance of each side of the transducer can be evaluated from Equation D-2 as

$$C_o = \frac{k\epsilon_o \pi a^2}{d_o} = 100 \times 10^{-12} \text{ FARADS}$$

However, experimental tests on the transducer found it to have a capacitance of 240 μμf. In order that all four capacitive elements in the bridge network are equal, the two fixed capacitors are also chosen as 240 μμf.

The last design requirement on the circuitry is for Ω, the frequency of the A.C. bridge excitation, to be much larger than α. Now α is expressed as

$$\alpha = \frac{1}{R_L C_o}$$

R_L is chosen as 30 mega-ohms and C_o is given above. For these values, α is evaluated as 300 rad/sec. Hence, by choosing Ω = 20 kc, $\Omega \gg \alpha$ or $\frac{\alpha}{\Omega} \ll 1$ and the approximations made in Chapter II are valid.

CHAPTER III

Closed Loop Analysis

Table 3 summarizes some of the important characteristics of an open loop capacitive pressure transducer for three different types of sensing elements. Now, it can be generally stated that although a forward or open loop system has the advantage of featuring a simple and stable operation, it can also have some undesirable features. One negative consequence of an open loop system is the dependence of the controlled output on the calibration of the intermediate components. Another disadvantage is that the output varies due to load changes, external disturbances and noise within the system.

The question now arises as to if it is possible to design a system to minimize these disadvantages. Now, in general, if a system's requirements cannot be satisfied by an open loop system, the desired accuracy of control can be obtained by employing a closed loop system. In this type of system, the output is determined, fed-back and compared with the system's input. The difference between the actual state (output) and the desired state (input) is the error or actuating signal. This signal is used to drive the actual state towards the desired state.

The important differences between closed loop operation and open loop operation lie in the feedback path. The effects of feedback which can also be classified as advantages can be summarized as follows:

1. Because the closed loop system is accuated by the error signal, it continues to function until the error is reduced to zero. Thus, feedback continuously reduces and eliminates the effects of errors present in the loop and consequently maintains a high degree of accuracy for the loop.

2. Due to this increase in accuracy for a closed loop system, it is unnecessary to periodically calibrate the instrument.

3. Feedback reduces the effects of nonlinearities which occur in the loop.

4. Feedback increases the bandwidth of the open loop system thus improving its dynamic response and reducing its time constant.

5. If the open loop gain is very large, it can be shown that in a closed loop system, the input-output characteristic of the system is mainly a function of the feedback element. Thus, by using a closed loop system, the forward loop characteristics are, in a sense, replaced by the feedback characteristics.

Although a closed loop system offers several advantages over an open loop system, its major disadvantage is complexity. Furthermore, a suitable margin of stability for the system must be obtained.

Now the ultimate design goal in this report is to produce a pressure transducer with an extended frequency response that is capable of accurately measuring very low pressures. From the above discussion and as discussed in the introduction, it appears that it is possible to achieve this goal by utilizing a capacitive pressure transducer with a weakly stressed membrane in a closed loop system.

A practical method of closing the loop is by electrostatic feedback. In such a scheme the output signal from the bridge after being amplified and rectified is fed back to the electrode on the high pressure side of the transducer. With the diaphragm at ground potential, this voltage creates an electrostatic force, F_{es}, which opposes the pressure force on the diaphragm. The effects of these two opposing forces on the diaphragm are to effectively stiffen the diaphragm thereby increasing its frequency response.

By following a procedure similar to that outlined in Section 1 of Appendix D, an expression for the total electrostatic force, F_{es}, on a deflected diaphragm can be obtained as follows

$$F_{es} = \int_0^{R'} \frac{k\epsilon_0 (\pi R'^2)\, 2\pi r}{2(d_0 \pm \eta)^2}\, dr \qquad 15$$

WHERE

$$\eta = \eta_0 \left[1 - \left(\frac{r}{a}\right)^2\right]$$

Now to a first order approximation in $\frac{\Delta d_0}{d_0}$, the above integral becomes

$$F_{es} = F_0 \left[1 - K' \frac{\Delta d_0}{d_0}\right] \quad ; \quad K' = 2 - \left(\frac{R'}{a}\right)^2 \qquad 16$$

where

$$F_0 = \frac{k\epsilon_0 (\pi R'^2)}{2 d_0^2} V^2$$

is the electrostatic force of attraction between the undeflected (or nulled) diaphragm and the electrode.

When the electrostatic force equals the pressure force, the diaphragm is nulled; i.e., $\Delta d_0 = 0$ and the following relationship holds

$$\Delta P = \frac{F_{es}}{A_D} = \frac{F_0}{A_D} \qquad 17$$

where A_D = surface area of the diaphragm. Hence, with the system set up in this manner, the differential pressure force is nonlinearly related to the square of the rectified output voltage.

To simplify this analysis, it is preferable to linearize the above relationship. If a voltage is applied to both electrodes of the transducer, it is possible to obtain a linear pressure scale for the

instrument instead of a quadratic one. This can be accomplished as follows. With the diaphragm in its null position, an equal voltage, V_i, is applied to the fixed electrodes of the transducers. When the differential pressure deflects the diaphragm, unbalancing the bridge, the diaphragm movement is opposed by an electrostatic force resulting from an increase of voltage on one fixed electrode and a decrease on the other. The differential change in voltage is denoted by v.

To a first order in $\frac{\Delta d_o}{d_o}$ the net electrostatic force on the diaphragm is

$$\Delta F_{es} = \frac{(\pi R'^2) k \epsilon_o}{2 d_o} \left\{ (V_i + v)^2 \left[1 - K' \frac{\Delta d_o}{d_o} \right] - (V_i - v)^2 \left[1 + K' \frac{\Delta d_o}{d_o} \right] \right\} \qquad 18$$

$$\Delta F_{es} = \frac{2 k \epsilon_o (\pi R'^2)}{d_o^2} \left\{ V_i v - V_i^2 \left[1 + \left(\frac{v}{V_i} \right)^2 \right] K' \frac{\Delta d_o}{d_o} \right\} \qquad 19$$

Since the voltage required to compensate the maximum pressure differential cannot exceed V_i, it follows

$$\frac{1}{2} \left[1 + \left(\frac{v}{V_i} \right)^2 \right] \leq 1 \qquad 20$$

In fact, V_i will be chosen such that $v \ll V_i$.

Now from Equation D-11, C-30 and 12, the following expression is obtained

$$\frac{v}{\left(\frac{A V_E K'}{4} \right)} = \frac{\Delta d_o}{d_o} \qquad 21$$

If $\frac{A V_E K'}{4} \gg v$ then Equation 21 is less than unity. This assumption toegther with Equation 20 makes the second term in Equation 19 negligible. Hence Equation 19 can be written as

$$\Delta F_{es} = \frac{2 k \epsilon_o \pi R'^2 V_i}{d_o^2} v \qquad 22$$

Since V_i is a constant, Equation 22 can be written as

$$\Delta F_{es} = 2K_i v \qquad \text{WHERE} \quad K_i = \frac{k\epsilon_o \pi R^2 V_i}{d_o^2} \qquad 23$$

Therefore, by applying a voltage V_i to both electrodes, a linear pressure scale is obtained for the transducer which directly relates the differential pressure disturbance to the rectified output signal.

Another method of demonstrating that this technique would result in a linear pressure scale is to choose an operating point V_i along the nonlinear curve expressed by Equation 3 and perform a linear perturbation analysis about the operating point. By carrying out this analysis, it becomes obvious that the constant K_i in Equation 23 corresponds to the slope of the nonlinear curve at the operating point. This slope then has to be multiplied by 2 as in Equation 23 because there is an electrostatic force being contributed by both sides of the differential capacitor. Throughout the remainder of the analysis, the constant K_i in Equation 23 shall be interpreted from a graphical linearization of Equation 3 .

Since this transducer measures differential pressures, ΔP, the operating voltage V_i may be chosen as any value as long as $v \ll V$. (Note: V_i cannot exceed the limit set by Paschen's Law.) The particular operating voltage only determines the slope of linear pressure scale and consequently the sensitivity of the pressure - output voltage scale.

Now, in particular, three operating voltages, V_i, are considered along the nonlinear curve. Figures 7, 8 , and 9 are plots of Equation 3 respectively showing the three operating voltages at

10v, 100v, and 500v. The constant, K_i, as previously explained, corresponds to the slope of the tangent line at each operating point and these values are respectively obtained from Figures 7 , 8 and 9 as (8.2×10^{-4}), (8.2×10^{-3}) and $(41. \times 10^{-2})$. These values will be referred to respectively as K_{10}, K_{100}, and K_{500}.

Recall from the open loop analysis that for small deflection of the membrane, the displacement is linearly proportional to the disturbing pressure by the following expression

$$\Delta d_o = \frac{a^2}{4T} \Delta P \qquad \text{A-51}$$

In the forward loop analysis ΔP is the input pressure disturbance, but in the closed loop system ΔP becomes the actuating error signal. The error signal for this system is the difference between the input disturbing pressure, P_D, and the feedback "electrostatic pressure" P_{es}. The electrostatic pressure is created by the electrostatic force acting on the surface area, A_D, of the diaphragm. Hence, ΔP is a difference of pressures and is expressed as

$$\Delta P = P_D - P_{es} \qquad 24$$

Thus, for a closed loop system, Equation A-51 becomes

$$\Delta d_o = \frac{a^2}{4T} \left[P_D - P_{es} \right] \qquad 25$$

$$\Delta d_o = \frac{a^2}{4T} \left[P_D - \frac{\pi R'^2}{\pi a^2} \frac{k \epsilon_o 2 V_i}{d_o^2} v \right] \qquad 26$$

From this expression it is obvious that the "electrostatic pressure" being fed back is expressed as

$$P_{es} = \frac{F_{es}}{A_D} = \frac{1}{\pi a^2} \frac{\pi R'^2 k \epsilon_0 2 V_i}{d_o^2} v \qquad 27$$

Hence, the feedback transfer function H(s) is

$$H(s) = \frac{P_{es}(s)}{v(s)} = \frac{2K_i}{A_D} = \beta_i \qquad 28$$

Combining Equations 5, 6, 11, 12, and 28 the input-output relationship or the closed loop transfer function for this system is expressed as

$$\frac{V(s)}{P_D(s)} = \frac{G(s)}{1+G(s)H(s)} = \frac{\dfrac{A\phi\gamma}{\frac{s^2}{\omega_{nD}^2} + \frac{2\zeta_D}{\omega_{nD}}s + 1}}{\left[1 + \dfrac{A\phi\gamma\beta_i}{\frac{s^2}{\omega_{nD}^2} + \frac{2\zeta_D}{\omega_{nD}}s + 1}\right]} \qquad 29$$

where $G(s) = G_1 G_2 G_3 G_4$

From Equation 29 the characteristic equation for this closed loop system is

$$1 + \frac{A\phi\gamma\beta_i}{\frac{s^2}{\omega_{nD}^2} + \frac{2\zeta_D}{\omega_{nD}}s + 1} = 0 \qquad 30$$

expanding

$$s^2 + 2\zeta_D\omega_{nD}s + \omega_{nD}^2(1 + \phi\gamma\beta_i A) = 0 \qquad 31$$

From Equation 31 the closed loop frequency, ω'_{nD} and the damping, ζ'_D, for this system are respectively found to be

$$\omega'_{nD} = \omega_{nD}\sqrt{1 + \phi\gamma\beta_i A} \qquad 32$$

$$\zeta'_D = \frac{\zeta_D}{\sqrt{1 + \phi\gamma\beta_i A}} \qquad 33$$

Hence, it is observed that the effect of closing the loop around the system has resulted in an increase in frequency of the weakly stressed diaphragm but a decrease in damping for the system.

A further insight on the effects on feedback on the weakly stressed diaphragm can be obtained by expressing the second order equation in Equation 31 in its equivalent mechanical form (mass, spring, damper). Substituting the following expression into Equation 31

$$\omega_{nD} = \sqrt{\frac{k}{m}} \qquad \zeta_D = \frac{B}{2\sqrt{km}} \qquad 34 \text{ AND } 35$$

where

k = mechanical spring constant of diaphragm lb/in.

B = damping constant

m = mass of diaphragm

it is rewritten as

$$1 + \frac{A\phi\gamma\beta_i}{\frac{m}{k}s^2 + \frac{B}{k}s + 1} = 0 \qquad 36$$

or

$$s^2 + \frac{B}{m}s + \frac{k + k\phi\gamma A\beta_i}{m} = 0 \qquad 37$$

Note: 1. From Equation 14

$$\phi = \frac{a^2}{4T} = \frac{IN^2}{lb/IN.}$$

2. Similarly

$$k = \frac{lb}{IN.}$$

3. Hence, ϕ can be expressed as

$$\phi = \frac{C_1}{k}$$ where

C_1 is a constant in units of in^2. and

k is the mechanical spring constant for the diaphragm.

Consequently, in Equation 37

$$k\phi A\gamma\beta_i = k\frac{C_1}{k}A\gamma\beta_i = C_1 A\gamma\beta_i$$

Hence, the characteristic equation is rewritten as

$$S^2 + \frac{B}{m}S + \frac{k + C_1 A\gamma\beta_i}{m} = 0 \qquad 38$$

From this equation the closed loop frequency and damping for this system are respectively found as

$$\omega'_{nD} = \sqrt{\frac{k + C_1 A\gamma\beta_i}{m}} \qquad 39$$

$$\zeta'_D = \frac{1}{2}\frac{B}{\sqrt{k + C_1 A\gamma\beta_i}} \qquad 40$$

This result is identical to Equation 32 and 33 .

It is observed from these results that feedback has electrically increased the spring constant of the weakly stressed diaphragm. From Equation 38 the new spring constant k' for the closed loop system is seen to be

$$k' = k + C_1 A\gamma\beta_i \qquad 41$$

Since the diaphragm in the forward loop is weakly stressed, its mechanical spring constant k is a very small value. Consequently, if the loop gain is large

$$k \ll C_1 A\gamma\beta_i \qquad 42$$

Hence, Equation 41 can be expressed as

$$k' = C_1 A\gamma\beta_i$$

Similarly, k in Equations 39 and 40 is also negligible. Hence, the conclusion is reached that by employing a weakly stressed diaphragm in this closed loop system, the mechanical stiffness of the

diaphragm is replaced by an "electrical spring". This is a good accomplishment because this feedback loop has electrostatically eliminated the mechanical properties of the diaphragm which result in nonlinear behavior in the forward loop system. In effect, in a closed loop system the weakly stressed diaphragm is used as a boundary between the opposing electrostatic and pressure forces. Consequently, this alleviates the need to recalibrate the instrument if undesirable effects slightly alter the properties of the sensing element in the forward loop. Theoretically, the only errors in the system should be attributed to the linear approximation of this nonlinear physical law.

Observe that closing the loop around the forward loop system did not change the order of the system. Therefore, the open loop transfer function of this closed loop system is still a second order system and is expressed as

$$G_1 G_2 G_3 G_4 H = \frac{K_{2i}}{\left[\frac{S^2}{\omega_{nD}^2} + \frac{2\zeta_D}{\omega_{nD}} S + 1\right]} \qquad 43$$

where K_{2i}, the new open loop gain is expressed as

$$K_{2i} = \phi \gamma \beta_i A \qquad 44$$

As previously explained the second order system in Equation 43 is characteristic of the dynamics of the diaphragm (membrane).

From Chapter II the frequency and damping ratio for this second order equation were calculated as

$$\zeta_{nD} = 60\ \%$$

$$\omega_{nD} = 377\ \text{RAD/sec}$$

$$\zeta_D = 0.10$$

Figure 11 shows the frequency response for the open loop transfer function expressed by Equation 43 (for unity gain).

CHAPTER IV

Closed Loop Stability Compensation

From the results of the previous chapter, it is concluded that it is highly advantageous to use a weakly stressed diaphragm in a closed loop system. It was demonstrated that the introduction of feedback around the forward loop did not increase the order of the system. Consequently, the open loop transfer function for the closed loop system remains a second order equation as expressed by Equation 43

Although a closed loop second order system of this sort is theoretically stable, its frequency plot shows that its phase response asymptotically approaches 180° in the high frequency region (Figure 11). In designing a control system, the phase margin, that is the phase at the frequency at which the amplitude response crosses the 0^{db} line, is a good practical criterion of system stability. As a rule, a sufficiently stable system requires at least a 30° to 45° phase margin.

Referring to the open loop response in Figure 11 it is observed that the maximum frequency at which the amplitude plot could cross the zero db line and satisfy the above requirement is 70 c/s.

The stability of the system can be improved by extending the frequency at which this phase margin occurs; i.e., extending the frequency range of the system. This is readily accomplished by introducing a phase lead into the resonance and high frequency region of the system and thus extending its frequency range. To achieve this increase in stability, it is necessary to "compensate" the closed loop system. This is accomplished by inserting into the loop a complex transfer function, $G(j\omega)$, which has a positive phase angle in the high frequency region.

The ideal compensation element would be a pure differentiating function, but this cannot be obtained by the use of passive networks. Therefore, use is made of a element with a transfer function approaching that of a differentiating element. It is called a "phase lead" element or a "differential controller" and its transfer function is generally of the form

$$G_5(s) = \frac{1}{m_1} \frac{1 + m_1 \tau_1 s}{1 + \tau_1 s} \qquad m_1 > 1 \qquad 44$$

where τ_1 , is the time constant of the network and the quantity "m_1" is the "phase lead factor" or "time constant ratio."

Figure 12 shows a plot of this function for several values of m_1. It can be seen from these plots that the amount of phase lead is determined by the phase lead factor. This relationship between θ_{max} and "m_1" is expressed as

$$\theta_{MAX} = \sin^{-1} \frac{m_1 - 1}{m_1 + 1} \qquad 45$$

and is plotted in Figure 13 . The frequency at which the maximum phase angle occurs is

$$\omega_M = \frac{1}{\tau_1 \sqrt{m_1}} \qquad 46$$

Above this frequency, the phase lead decreases as the gain increases. Hence, it is observed that this element acts as a pure differentiator only in a limited range.

In defining a phase lead controller for this system, care must be taken in the selection of "m" and τ_1 . Examining Equation 44 , it is noted that phase lead compensation extends the frequency range of the system. That is, the feedback system becomes "m" time faster. But the open loop gain is attenuated by the same factor. Thus, it becomes necessary to add an additional gain factor elsewhere in the system to make up for the attenuation brought on by this element.

Since it is desired to extend the location of the 45° phase margin into the high frequency region of the system, a phase lead factor resulting in at least a 45° phase lead is required. From Figure 13 it is seen that this requirement is met for values of $\frac{1}{m_1} \leq .17$ or $m_1 \geq 5.8$ Care must also be taken in choosing the time constant τ_1 , or in other words, the break frequency of this compensating network defined as $\omega_1 = \frac{1}{\tau_1}$. It is important that this break frequency is not placed far to the right of the frequency of the second order term. A large separation in break frequencies would result in sharp fluctuations in the phase plot which would tend to drive the system towards instability (180°) in the response region.

Three values of "m_1" are examined; 10, 20, 100 and for each case resulting open loop response is plotted for several values of ω_1 . The frequency responses of the resulting compensation systems are shown in Figures 14a , 14b , and 14c for each of the three cases. Figure 14 identifies the curves in these plots.

Although Figure 14c indicates that a lead factor of 100 results in large increase of the frequency range of the system, it also means that an additional amplification of 100 must be added to the system to correct for the attenuation of 100 of this element. Thus, although it is desirable from the frequency standpoint to use a very large m_1, there are practical limitations on this value. As demonstrated above, the attenuating effect of this element increases as the phase lead factor increases and this loss in gain must be made up for elsewhere in the loop. Hence, in practice, it is customary to use the value of m_1 ranging from 4 to 10 and in extreme cases, 20.

Based on these requirements, response number 2 in Figure 14a represents the most satisfactory response for the system. For this response $m_1 = 10$ and $\tau_1 = \frac{1}{628}$ or $\omega_1 = 628$ r/s (100 c/s). As seen from the plot a phase lead compensation with these characteristics extends the frequency range of the open loop system to 1400 c/s or 8800 r/s and results in a nearly constant phase response of -135° ranging from 100 c/s to 500 c/s

Now in final form, the open loop transfer function for the compensated system becomes

$$G_1(s)G_2(s)G_3(s)G_4(s)G_5(s)H(s) = \frac{A\phi\gamma\beta_i}{m_1}\left[\frac{1}{\frac{s^2}{\omega_{n0}^2} + \frac{2\zeta_0}{\omega_{n0}}s + 1}\right]\left[\frac{1+m_1\tau_1 s}{1+\tau_1 s}\right] \qquad 47$$

where the open loop gain is now

$$K_{3i} = A \phi \gamma \beta_i \frac{1}{m}, \qquad 48$$

The frequency response of this transfer function, for unity gain, is plotted in Figure 11 .

CHAPTER V

Analysis of the Total Loop Gain

The open loop gain for the compensated system expressed by Equation 47 is

$$K_{3i} = A \phi \gamma \beta_i \frac{1}{m_1} \qquad 48$$

where

$$\phi = \frac{a^2}{4T}$$

$$\beta_i = \frac{2K_i}{A_D} = \frac{2k\epsilon_0(\pi R'^2)V_i}{(\pi a^2)d_0}$$

$$\gamma = \frac{K' V_E}{4 d_0}$$

Substituting these expressions into Equation 48 it can be rewritten as

$$K_{3i} = \frac{V_E K' K_i A V_i R'^2}{8\pi T d_0 m_1 a^2} \qquad 49$$

For the values given in previous chapters A_D, K', ϕ and γ are calculated as

$V_E = 1.4$ v R.M.S.

$A_D = \pi a^2 = 1.765\,in^2 = 11.4 \times 10^{-4}\ m^2$

$K' = 2 - \left(\frac{R'}{a}\right)^2 = 1$

$\phi = 52.0 \times 10^{-6}\ m^3/NT$

$\gamma = 3.44 \times 10^3\ v/m$

These values are a function of the construction of the instrument and will be considered as open loop constants independent of the feedback path.

The feedback gain, β_i, is characteristic of the linearized feedback path. In Chapter IV three operating points were considered for the linearized closed loop (feedback) analysis. Corresponding to each operating point was a particular gain K_i. These were calculated as

$$K_{10} = 8.2 \times 10^{-4}$$
$$K_{100} = 8.2 \times 10^{-3}$$
$$K_{500} = 41 \times 10^{-2}$$

Hence, for $\beta_i = 2 \frac{K_i}{A_D}$

$$\beta_{10} = 1.44$$
$$\beta_{100} = 14.4$$
$$\beta_{500} = 720.0$$

The subscripts indicate the particular operating point. Corresponding to each β_i, there is also a particular amplifier setting A_i for the forward loop. Hence the open loop gain K_{3i} is now reduced to a function of the particular operating point on the nonlinear curve. Substituting the above values into Equation 48 , the open loop gain is written as

$$K_{3i} = \phi \gamma \frac{1}{m_1} \beta_i A_i$$
$$K_{3(10)} = A_{10}(0.0258)$$
$$K_{3(100)} = A_{100}(0.258)$$
$$K_{3(500)} = A_{500}(12.9)$$

The selection of the open loop gain settings result in a compromise between stability and performance. The open loop gain is either chosen small in order to be safe with respect to stability, hence, the servo is soft and not very accurate, or the servo is stiffened by increasing

the gain in order to improve the static accuracy but at a loss of stability.

As seen from above, the final value of the open loop gain is controlled by the variable amplification factor A_i.

The analysis of the open loop gain shall now be considered in two parts. The first part involves an analysis of the frequency response of the system to determine the amplifier settings. The second part is a stability and performance synthesis on the dynamic response of the system.

A. Frequency Response Analysis

Figure 11 shows a frequency plot of the compensated closed loop system for unity gain. In Chapter V it was explained that the introduction of phase lead compensation would increase the stability and extend the frequency range of the original uncompensated system. By extending the frequency range in this manner, the frequency at which the amplitude response could cross the 0^{db} line corresponding to a 45^{o} phase margin was increased. Now, with the appropriate gain adjustment, the maximum frequency at which a 45^{o} phase margin can occur is 1400 c/s

The gain required for the amplitude plot to cross the 0^{db} line at $\omega = 1400$ c/s is the open loop gain for the compensated system. To find this gain, it is first necessary to evaluate the amplification factor A_i for each operating point. This is accomplished by first expressing $\phi \gamma \frac{1}{m_1} \beta_i$ in decibel units. These values are then

added to the amplitude response curve shown in Figure 11 . This curve is presently plotted for a unity gain factor. This procedure is sketched in Figure 16 a, b and c. Now, the vertical distance this plot must be moved again such that it crosses the zero db line at 1400 c/s represents the amplification A_i associated with each particular operating point.

From Figure 16 it is seen that the resulting amplifications are

$$A_{10} = 3,370.0$$
$$A_{100} = 337.0$$
$$A_{500} = 6.4$$

Table 1 summarizes these results and computes the total open loop gain for each operating point. The open loop gain for all three cases is 87. This should be expected since each of the cases have identical stability requirements.

Hence, the open loop transfer function for the compensated closed system is written as

$$G(s)H(s) = \frac{87}{\frac{S^2}{(377)^2} + \frac{2\zeta_0}{(377)}S + 1}\left[\frac{\frac{S}{628} + 1}{\frac{S}{6280} + 1}\right] \qquad 50$$

B. Dynamic Analysis

A convenient means of synthesizing the dynamic response of a linear control system is by using analog simulation. Figure 17 represents the analog circuit of the closed loop control system.
The open loop transfer function of this circuit is given by Equation 50. Figure 17 lists the potentiometer settings required to simulate the

exact dynamic response of the system. The system is time scaled such that $\tau = 1000t$.

Figure 19 shows the time response of this system (Gain = 87) for a step input. Now as a rule, a good control system should be designed for

$$1.2 < M_m < 1.5$$

where M_m, the resonance ratio, is the maximum output to input ratio of the system when by a sinusoidal input. For a second order system, the resonance ratio is a function of the damping ratio, ξ. This relationship is given by Equation 51 and is plotted in Figure 23 .

$$M_m = \frac{1}{2\xi\sqrt{1-\xi^2}} \qquad 51$$

This functional dependence is also observed from the amplitude frequency response shown in Figure 11 for a second order system.

For a second order system, the time response to a step input is

$$Y(t) = 1 + \frac{e^{-\xi\omega_n t}}{\sqrt{1-\xi^2}} \sin\left[\omega_n\sqrt{1-\xi^2}\,t + \cos^{-1}(-\xi)\right] \qquad 52$$

This response is plotted in Figure 18 for several damping ratios. From this plot, it is observed that there also exists a relationship between the maximum response Y_{max} (or maximum overshot $Y_{os(max)}$) and ξ for a step input. By differentiating Equation 52 and equating the equation to zero the time, t_m, at which Y_{max} occurs is found to be

$$t_m = \frac{\pi}{\omega_n\sqrt{1-\xi^2}} \qquad 53$$

An expression for Y_{max} is obtained by substituting Equation 53 into Equation 52 .

$$Y_{MAX} = 1 + e^{-\frac{\zeta\pi}{\sqrt{1-\zeta^2}}} \qquad 54$$

or

$$Y_{os(MAX)} = Y_M - 1 = e^{-\frac{\zeta\pi}{\sqrt{1-\zeta^2}}} \qquad 55$$

This result is plotted in Figure 22 . For a good servo system, the maximum overshot for a step input should be

$$0.20 < Y_{os(MAX)} < 0.32$$

This corresponds to a damping of

$$0.35 < \zeta < 0.45$$

Since the step response of this system, shown in Figure 19 , resembles the step response of a second order system, it may be assumed that Equation 51 and 55 , as derived for a second order system, can also be used to analyze the dynamic response of this system.

From Figure 19 $Y_{os(max)} = .575$. Thus, based on the above assumption, the appropriate values of ζ and M_m as taken from Figures 22 and 23 are respectively 0.16 and 3.175. Since this time response does not satisfy the stability requirements stated above, it is necessary to modify the present system to obtain the desired response.

This is easily done on the analog computer by varying the systems total loop gain. It is found that a decrease in loop gain results in a decrease in $Y_{os(max)}$ and consequently a decrease in ζ and M_m. Figures 20a to 20d respectively show the time response for gain settings of 87(3/4), 87(1/2), 87(1/4) and 87(1/10). Optimum stability and dynamic conditions

occur in Figure 20c for a loop gain of 87(1/4). For this response $Y_{os(max)} = .25$ and from Figures 24 and 23, ξ and M_m are to be respectively 0.40 and 1.38.

Although decreasing the loop gain results in the desired time response and improves dynamic stability, it reduces the static accuracy of the system. The static or steady state error, ϵ, of the system is defined by the final value theorem as

$$\epsilon = \lim_{s \to 0} s E(s) \qquad 56$$

where

$$E(s) = \frac{R(s)}{1 + G(s) H(s)} \quad ; \quad G(s) = G_1 G_2 G_3 G_4 G_5 \qquad 57$$

For $R(s) = \frac{1}{s}$ (step input) the steady state error for this system reduces to

$$\epsilon = \frac{1}{1 + A_i \phi \gamma \beta_i \frac{1}{m_1}} \simeq \frac{1}{\text{LOOP GAIN}} \qquad 58$$

Thus, as the low frequency or D.C. gain (loop gain) decreases, errors tend to predominate in the system as seen from Equation 58. It is required that this control system operate with less than a 0.01 static error. For the present gain of 87(1/4) the static error is 0.046 and is consequently insufficient for the desired accuracy of the system.

In order to improve the system performance, it is necessary to increase the low frequency gain. The static error can be decreased by a factor "b" (i.e., low frequency or loop gain increased by b) if a complex element having a value "b" at low frequencies and unity at high frequencies is introduced into the system. It is important that the phase and amplitude

characteristics of this element do not affect the resonance or high frequency region of the system because the desired stability and optimum dynamic response have already been established for these regions.

An element that produces this type of control is called an "integral controller" or "phase lag compensator." Its transfer function with an additional gain, b, is expressed as

$$G_c(s) = b\,\frac{1+\tau_2 s}{1+b\tau_2 s} \qquad 59$$

$$b = \frac{\omega_2}{\omega_2'}$$

$$\omega_2 = \frac{1}{\tau_2}$$

$$\omega_2' = \frac{1}{b\tau_2}$$

The amplitude frequency response of this element is plotted in Figure 10 for several values of b. The frequency phase response for a lag compensator is the negative of the phase response for a lead network. Hence, Figure 12.b is applicable to a lag element if the phase angles are considered negative and b = m. The time constant of this lag network, $\frac{1}{\tau_2}$, is chosen such that $\omega_2 = \frac{1}{\tau_2} = 125.6$ rad/sec in order that the phase lag characteristic of this element does not affect the resonance region of the system. By choosing b = 4 and consequently $\omega_2' = 31.4$ rad/sec the total loop gain of the system is again equal to 87. The dynamic response of this system is shown in Figure 21.a.

As b increases or ω_2' decreases, the amount of low frequency gain amplification increases. Figures 21.a to 21.d respectively show the dynamic response of the system for values of b = 4, 8, 10, and 16 or ω_2' = 31.4, 15.7, 12.56, and 7.85 rad/sec. An analysis of these plots shows that Figure 21.d represents the optimum state of the system. For this response b = 16 and consequently the low frequency gain or open loop gain of the

system is equal to (87/4)(16) = 348. This results in a static error of .00288 which meets the performance specification of the system.

Thus, the closed loop system has been designed for optimum dynamic stability and performance characteristics. The final form of the open loop transfer function for the system is written as

$$G_1G_2G_3G_4G_5G_6H = 348\left[\frac{1}{\frac{S^2}{(377)^2}+\frac{2(.1)}{377}S+1}\right]\left[\frac{1+\frac{S}{628}}{1+\frac{S}{6280}}\right]\left[\frac{1+\frac{S}{7.85}}{1+\frac{S}{125.6}}\right] \qquad 60$$

The open frequency response of this system is plotted in Figure 24. The dynamic or time response of the closed loop system to a step input is shown in Figure 21d.

In summary, a closed loop capacitive type low pressure transducer has been theoretically designed having the following characteristics

Radial tension in the membrane	=	0.10 lb/in
Natural frequency of the diaphragm	=	60 c/s
Closed loop damping ratio	=	0.40
Resonance ratio M_m	=	1.38
Maximum overshot; $Y_{os(max)}$	=	0.25 per cent
Accuracy	=	0.003
Frequency	=	1000 c/s
Open loop gain	=	348

CHAPTER VI

Experiments

The purpose of the experiments is to verify the theoretical results obtained in the previous chapters. A closed loop capacitive pressure transducer utilizing a weakly stressed membrane has been constructed.

Experimental Set-Up

The forward loop section of the system consists of the capacitive pressure transducer and the bridge network as outlined in Chapter II. The uncompensated closed loop experimental system is schematically shown in Figure 32. As seen from this figure, the A.C. error signal from the bridge is applied to an isolation amplifier and an A.C. amplifier which has a combined gain of about 15.

In the phase sensitive detector, the amplified error signal from the bridge is compared with the reference signal. As shown in the figure, the reference signal is derived from the bridge excitation source. This unit yields a D.C. output voltage proportional to its amplified A.C. input. The polarity of the D.C. output voltage is determined by the phase relationship between the error signal and the reference voltage. This D.C. voltage is then amplified and fed back to the transducer.

The cathode followers shown in the system are used for impedance matching. Furthermore, each electrode has a D.C. bias of 150 volts, that determines the operating point for local linearization of the system as explained in Chapter III.

Open Loop Experiments

Several clamped circular diaphragms were constructed which had natural frequencies in the order of 50 to 100 c/s. Figure 31 shows a typical dynamic response for the open loop pressure transducers. The closed loop experiments utilized a diaphragm which had a natural frequency of approximately 100 c/s.

Experimental System

Each element in the loop was designed to have a small time constant as compared to the time constant of the diaphragm. The ripple from the rectified excitation voltage of 20 kc/s was filtered out by setting the break frequency of the detector at 1000 c/s and the break frequency of the two D.C. amplifiers at 10 kc/s.

This closed loop system was found to be stable for a gain less than 0.2. However, at 0.2 the system oscillated at a frequency of 5 kc/s which corresponded to the time constant of the capacitive bridge circuit. At this gain, the closed loop system worked as an R.C. oscillator and oscillated at its natural frequency of 5 kc/s. To verify that this was due to an electrical time constant and not to a mechanical time constant, the variable capacitors of the pressure transducers were replaced by two fixed capacitors. It was found that this system also oscillated at about 5 kc/s.

To reduce the open loop gain at 5 kc/s, the break frequency of the two D.C. amplifiers were also set at 1000 c/s.

The block diagram for this experimental system is shown in Figure 15. Dynamic tests were performed on this system by exciting the diaphragm

with an electrical step of 8 volts (or equivalently 0.4 microns). The system was found to be stable for gains of less than 2. However, at a gain of approximately 2, the system oscillated at about 160 c/s. This result was confirmed from the plot of the frequency response of this system, due to the electrical construction of the bridge circuit.

However, the results of this experiment verified the philosophy of the previous chapters and a new bridge system was designed. The block diagram of this system is shown in Figure 32.

Basically, in this system one side of the capacitor transducer is used as the measuring element. The other side is used as the feedback side. In this manner, the measuring element and feedback element were mechanically separated. Testing the closed frequency response was done by applying a pressure step input to one side of the transducer (with both sides of the diaphragm at atmospheric pressure). The closed loop frequency response was measured by the rise time of the closed loop system. Figure 33 gives an example of the response when the open loop gain was set at 10.

CONCLUSION

In this report, it was found that the frequency of a membrane is directly proportional to the square root of its radial tension while its sensitivity is inversely proportional to its tension. Hence, it is concluded that in designing a capacitive pressure transducer for an open loop system, one is faced with a "sensitivity-frequency response" dilemma. The open loop analysis showed that if a capacitive pressure transducer utilizes a highly stressed diaphragm as its sensing element, the system will have a high frequency response but a low pressure sensitivity. While on the other hand, if a high frequency response is not required, the system can be made very sensitive to low pressure by utilizing a weakly stressed diaphragm.

Furthermore, it was found that regardless of how the diaphragm was stressed, the performance of the open loop system was dependent upon its mechanical properties. This resulted in a limited range of linearity for the system and required the monitoring of other parameters such as temperature changes in order to determine their influence on characteristics of the diaphragm and if necessary provide a correction factor because of their effects.

It was theoretically and experimentally established in this report that by employing a weakly stressed diaphragm in a feedback system, the system's performance could be made independent of the mechanical properties of the diaphragm.

A closed loop system was designed in which the amplified and rectified transducer output voltage was fed back to the high pressure side of the diaphragm. This created an electrostatic force of attraction which opposed the pressure force on the diaphragm, thus nulling the diaphragm. The effect of these two opposing forces acting on the diaphragm electrically stiffened the diaphragm. Furthermore, it was found that by having a high loop gain, the weak spring constant of the low stressed diaphragm is replaced by a stiffer "electrical spring." Hence, it is concluded that by employing a weakly stressed diaphragm in a closed loop system, the mechanical "spring" properties of the diaphragm are electrically eliminated. Furthermore, it was found that by closing the loop, the frequency of the system increased as the square root of one plus the loop gain while the damping for the system decreased by the same factor.

Table 3 gives a comparison of the properties of an open loop highly stressed diaphragm and a closed loop low stressed diaphragm. In general, the properties of both systems are identical. The difference between the two systems is in the measurement range. For the upper measurement range, for example 10^{-3} mm Hg to atmospheric pressure, the open loop measuring system is clearly preferable over the closed loop measuring system (less complicated). For the lower measurement range (say lower than 10^{-3} mm Hg pressure), the closed loop pressure measuring system will start to have an advantage over the open loop measuring system. The open loop sensitivity of a weakly stressed diaphragm can be made larger than that of a strongly stressed diaphragm; consequently,

the resolution of a closed loop measuring system can be improved compared to that of the open loop pressure measuring system.

In conclusion, the closed loop diaphragm pressure transducer should be used for the lower end of the pressure measurement range, or in the case when a better resolution is desired in the lower end of the pressure measurement range.

REFERENCES

1. Gille, J.C., Pelegin, M.J., Decaulne, P., Feedback Control Systems, McGraw-Hill Book Co., Inc., New York, 1959.

2. Opstelten, J.J. and Warmoltz, N., "Double-Sided Micromanometer", Applied Scientific Research, Section B, Volume 4, 1954.

3. Rony, P.R. and Lamers, K.W., "Differential Micromanometer", University of California, Lawrence Radiation Laboratory, UCRL-11218 Parts 1 and 2, October 16, 1964.

4. Kinsler, L.E. and Frey, A.R., Fundamentals of Acoustics, John Wiley and Sons, Inc., 1950.

5. McLachlan, N.W., Theory of Vibrations, Dover Publications, Inc., New York, 1951.

6. Patterson, J.L., "A Miniature Electrical Pressure Gage Utilizing a Stretched Flat Diaphragm", NACA TN2659, April, 1952.

7. Mason, W.P., Electromechanical Transducers and Wave Filter, D. Van Nostrand Co., Inc., New York, 1942.

8. Rayleigh, (Lord), Theory of Sound, Dover Publications, New York, 1945.

9. Crandall, Irving B., Theory of Vibrating Systems and Sounds, D. Van Nostrand Co., Inc., New York, 1926.

10. Weidemann, Hans, "Inertia of Dynamic Pressure Arrays", N.A.C.A. TM998, 1941.

11. Delio, G.J., Schwent, G.V., Cesaro, R.S., "Transient Behavior of Lumped-Constant Systems for Sensing Gas Pressures", N.A.C.A. TN1988, 1949.

12. Truxal, J.G., Control Engineer's Handbook, McGraw-Hill Book Co., New York, 1958.

13. Lilly, J.C., Legallais, V., and Cherry, R., "A Variable Capacitor", Journal of Applied Physics, Vol. 18 (July, 1947), pp. 613 - 628.

14. Cope, J.O., "Direct Reading Diaphragm-Type Pressure Transducers", Rev. Sci. Inst., 33 No. 9, 980, 1962.

15. Opstelten, J.J. and Warmoltz, N., "A Double Sided Micro Anemometer", Appl. Sci. Res. Sect., B4-329, 1955.

16. Zaalberg, J.J. and Zelst, V., "Circuit for Condensor Microphones with Low Noise Level", Phillips Technical Review Rev. 9 357, 1947.

APPENDIX A

ANALYSIS OF DIAPHRAGMS

A1. Membranes - Equation of Motion of a Circular Membrane

Surfaces whose stiffness is negligible compared with the restoring forces due to tension are called membranes. The theoretical membrane is assumed to be a perfectly flexible, uniform and infinitesimally thin solid lamina stretched in all directions by a force which is unaffected by the motion of the membrane. It can be looked upon as a two dimensional generalization of a string.

Before formulating the equations of motion of a circularly clamped membrane, it is expedient to make the following assumptions to simplify the analysis:

a) Vibration occurs "in vacuo."

b) There is absence of loss (no internal or external damping).

c) The system is elastic and its force-displacement characteristics are linear.

d) The maximum displacement is small.

e) Deformation due to gravity is negligible.

f) The circular membrane vibrates with circular symmetry.

Consider an element of area $dS = rdrd\theta$ of the membrane in Figure 26. The radial force acting across the arc $rd\theta$ is given by $dF_r = Trd\theta$ where T is the tension in newtons per meter of length. The vertical component dF_y of this force is

$$dF_y = Tr\,d\theta \sin\Phi \qquad \text{A-1}$$

and by assumption d

$$\sin\Phi \simeq \tan\Phi = \frac{\partial y}{\partial r}$$

or

$$dF_y = Tr\frac{\partial y}{\partial r}d\theta = Td\theta\left[r\frac{\partial y}{\partial r}\right] \qquad A\text{-}2$$

The net vertical force acting upon the surface element rdrdθ due to tension parallel to the radius is

$$(dF_y)_{r+dr} - (dF_y)_r = Td\theta\left[\left(r\frac{\partial y}{\partial r}\right)_{r+dr} - \left(r\frac{\partial y}{\partial r}\right)_r\right] = T\frac{\partial}{\partial r}\left(r\frac{\partial y}{\partial r}\right)dr\,d\theta \qquad A\text{-}3$$

Similarly, the net force in the y direction due to tension perpendicular to the radius is given by

$$Tdr\left[\left(\frac{\partial^2 y}{\partial r\,\partial\theta}\right)_{\theta+d\theta} - \left(\frac{\partial^2 y}{\partial r\,\partial\theta}\right)_{\theta}\right] = \frac{T}{r}\frac{\partial^2 y}{\partial\theta^2}\,dr\,d\theta \qquad A\text{-}4$$

However, since y is not a function of θ for the case of circular symmetry, this force is zero.

The net force on the element must equal its mass, mrdrdθ, (where m is in units of mass per unit area) times its acceleration. Thus, by equating forces

$$mr\,dr\,d\theta\frac{\partial^2 y}{\partial t^2} = T\frac{\partial}{\partial r}\left(r\frac{\partial y}{\partial r}\right)dr\,d\theta \qquad A\text{-}5$$

and

$$\frac{m}{T}\frac{\partial^2 y}{\partial t^2} = \frac{1}{r}\frac{\partial}{\partial r}\left[r\frac{\partial y}{\partial r}\right]$$

where

$$\frac{1}{r}\frac{\partial}{\partial r}\left[r\frac{\partial y}{\partial r}\right] = \frac{\partial^2 y}{\partial r^2} + \frac{1}{r}\frac{\partial y}{\partial r} = \nabla_r^2 y$$

is the Laplacian operator in polar form for a function having circular symmetry. Now letting $d_1 = \sqrt{\frac{T}{m}}$ the dynamic equation of motion becomes

$$\frac{\partial^2 y}{\partial t^2} = d_1^2\nabla_r^2 y \qquad A\text{-}6$$

A2. Undamped Natural Frequency of a Clamped, Circular Membrane

A solution for equation (A-6) can be obtained by assuming that in any particular mode of vibration the motion is harmonic and can be expressed as

$$y = \eta e^{j\omega t} \qquad \text{A-7}$$

where $\eta = \eta(r)$ is a function of the radius and ω is the frequency of the mode. Substituting into equation (A-6), a second order ordinary differential equation is obtained, characterizing the motion of the membrane.

$$\frac{d^2\eta}{dr^2} + \frac{1}{r}\frac{d\eta}{dr} + K^2\eta = 0 \qquad \text{A-8}$$

where

$$K^2 = \frac{\omega^2}{d_1^2}$$

Equation (A-8) is a particular form of Bessel's differential equation whose complete solution with two arbitrary constants is of the form

$$\eta(r) = A J_0(Kr) + B Y_0(Kr) \qquad \text{A-9}$$

or

$$y(r,t) = \left[A J_0(Kr) + B Y_0(kr) \right] e^{j\omega t} \qquad \text{A-9}_2$$

where $J_0(Kr)$ is the Bessel function of the first kind and of zero order and $Y_0(Kr)$ is a Bessel function of the second kind and zero order.

In particular, the analysis is of a circularly clamped membrane with the following boundary conditions

i) $\eta = \eta_0$ at $r = 0$

ii) $\eta = 0$ at $r = a$

At the center, where r = 0, $Y_o(Kr)$ is undefined by virtue of its singularity. From its series form it can

$$Y_p(Kr) \simeq \frac{2^p (p-1)!}{\pi} (Kr)^{-p}$$

be seen that it becomes infinite at r = 0 and hence will not satisfy equation (A-9) under condition (i) unless B = 0.

Now $J_o(Kr)$ can also be represented in series form as

$$J_p(Kr) \simeq \frac{1}{2^p p!} (Kr)^p$$

or

$$J_o(kr) = 1 - \frac{(kr)^2}{2} + \frac{(kr)^4}{2^4 (2!)^2} - \cdots\cdots$$

Hence, at r = 0 $J_o(0) = 1$. Therefore, from (i) $A = \eta_o$ and the solution becomes

$$\eta(r) = \eta_o J_o(Kr) \qquad \text{A-10}$$

or

$$y(r,t) = \eta_o J_o(Kr) e^{j\omega t} \qquad \text{A-10a}$$

From condition (ii) and equation (A-10) is obtained an equation for the frequency of a vibrating membrane

$$J_o(Ka) = 0 \qquad \text{A-12}$$

Thus, Ka must always satisfy this equation; i.e., it must be a zero of this Bessel function. The plot of this function resembles a damped cosine wave; hence, there exists an infinite number of roots to equation (A-12) which occur at $Ka \simeq 2.405, 5.52, 8.654\ldots\ldots$ Thus, the frequency of the fundamental mode becomes

$$Ka = 2.405$$

$$\frac{\omega_{nM}}{d_1} = 2.405$$

$$f_{nM} = \frac{\omega_{nM}}{2\pi} = \frac{2.405}{2\pi a}\sqrt{\frac{T}{m}} \qquad \text{A-13}$$

A3. Damped Vibration of a Membrane

In order to make the discussion of the circular membrane more realistic, it is necessary to consider the effects of damping forces on the system. These forces include an internal frictional, the forces resulting from the radiation of energy in the form of sound waves and to the viscous damping of the surrounding medium.

Assume that the damping force per unit area (damping pressure P_r) is proportional to its velocity

$$P_r = -R_1 \frac{\partial y}{\partial t} \qquad A\text{-}14$$

where R_1 is a damping constant independent of r and y, but dependent upon frequency. The introduction of this damping force into the system alters the original equation of motion. Equation (A-6) now becomes

$$\frac{\partial^2 y}{\partial t^2} + \frac{R_1}{m}\frac{\partial y}{\partial t} = d_1^2 \nabla_r^2 y \qquad A\text{-}15$$

Again assuming harmonic motion

$$y = \eta e^{\gamma_1 t} \qquad A\text{-}16$$

a second order differential equation is obtained of the form

$$\frac{d^2\eta}{dr^2} + \frac{1}{r}\frac{d\eta}{dr} + K^2\eta = 0 \qquad A\text{-}17$$

where γ_1 must satisfy the equation

$$\gamma_1^2 + \frac{R}{m}\gamma_1 + K^2 d_1^2 = 0 \qquad A\text{-}18$$

Equation (A-17) is identical with equation (A-8); therefore, its solution, as before, is $A\,J_0(Kr)$. The same boundary condition also holds; thus, once again, the equation $J_0(Ka) = 0$ is satisfied by the same previously determined values of Ka, i.e., Ka = 2.405, 5.520....

For damped vibrations, however, the allowed frequencies are not given by $\omega_{nM} = \frac{Kd_1}{a}$ but instead are determined by the imaginary part of γ_1.

Solving equation (A-18), γ_1 is expressed as

$$\gamma_1 = -\frac{R_1}{2m} \pm J\sqrt{K^2 d_1^2 - \frac{R_1^2}{4m^2}} \qquad \text{A-19}$$

The general solution of equation (A-15) is now

$$y = A e^{-\frac{Rt}{2m}} J_0(Kr) e^{J\omega' t} \qquad \text{A-20}$$

where

$$\omega'_{nM} = \sqrt{K^2 d_1^2 - \frac{R_1^2}{4m}} = K d_1 \sqrt{1 - \frac{R_1^2}{4K^2 T m}} \qquad \text{A-21}$$

The fundamental frequency is obtained by setting $K = \frac{2.405}{a}$.

$$f'_{nM} = \frac{\omega'_{nM}}{2\pi} = \frac{2.405}{2\pi a}\sqrt{\frac{T}{m}}\left[1 - \frac{R_1^2 a^2}{23.2 T m}\right]^{1/2} \qquad \text{A-22}$$

Thus, it is concluded that the amplitude of vibration of the membrane is exponentially damped and that the frequency of oscillation is slightly less than for the corresponding undamped case.

A4. Thin Plate

A stretched diaphragm in which the restoring force is due entirely to its stiffness, as opposed to tension, is called a thin plate. Theoretically, a thin plate consists of a perfectly elastic, homogeneous material that has a uniform thickness considered small in comparison to its other dimensions.

The analysis of the thin plate will be limited to the symmetrical vibrations of a clamped circular diaphragm. The assumptions, as previously stated for a membrane, will also be valid for the thin plate.

The mathematical derivation of the equation of motion of a thin plate is more involved than that for a membrane. Therefore, a rigorous development will not be present here, but merely the resulting equations will be stated. The steps in formulating this equation as well as others

used in the discussion of the diaphragm can be found in the treatise by Rayleigh (Reference 8).

As taken from the above reference, the equation of motion of a thin plate is:

$$-\frac{1}{c_1^2}\frac{\partial^2 y}{\partial t^2} = \nabla_r^4 y \qquad \text{A-23}$$

where

$$c_1^2 = \frac{E h^2}{12\rho(1-\bar{\sigma}^2)}$$

E = Young's Modulus

h = thickness

ρ = volume density = $\frac{\text{mass}}{\text{unit vol.}}$

$\bar{\sigma}$ = Poisson's Ratio

Again the assumption is made that the motion in any mode is harmonic as described by equation (A-7)

$$y(r,t) = \eta(r)\, e^{j\omega t}$$

Substituting this expression into equation (A-23), the equation becomes

$$\nabla_r^4 \eta = \frac{\omega^2}{c_1^2}\eta$$

or

$$\nabla_r^4 \eta = K_3^4 \eta \qquad \text{where} \quad K_3^4 = \left(\frac{\omega}{c_1}\right)^2 \qquad \text{A-24}$$

Expressing in operator form, the differential equation becomes

$$\left(\nabla_r^4 - K_3^4\right)\eta = 0 \qquad \text{A-24a}$$

Now the linear operator is commutative; thus, equation (A-24) can be factored giving

$$\left(\nabla_r^2 + K_3^2\right)\left(\nabla_r^2 - K_3^2\right)\eta = 0$$

or

$$r^2\frac{\partial^2\eta}{\partial r^2} + r\frac{\partial\eta}{\partial r} \pm K_3^2 r^2 \eta = 0 \qquad \text{A-25}$$

Therefore, η can be a solution of either $(\nabla r^2 + K_3^2)\eta = 0$ or $(\nabla r^2 - K_3^2)\eta = 0$.

The complete solution of equation (A-25) is the sum of these two solutions. Noting that the first of these equations is identical in form with equation (A-8), its solution will also be the same, namely,

$$\eta = A J_0(K_3 r) \qquad \text{A-26}$$

The solution of the second equation is obtained from the first by replacing K by jK and is written as

$$\eta = B J_0(jK_3 r)$$

or

$$\eta = B I_0(K_3 r) \qquad \text{A-27}$$

which is the so-called hyperbolic Bessel function whose independent variable has imaginary values. Thus, the solution of equation (A-25) is

$$\eta = A J_0(K_3 r) + B I_0(K_3 r) \qquad \text{A-28}$$

Since equation (A-28) only contains two, rather than four arbitrary constants, it is not the complete solution of the differential equation. But, as with the membrane, the remaining constants are zero by the condition that at r = 0 the amplitude of vibration must remain finite.

To evaluate the constants, A and B, two boundary conditions are necessary. Again considering the case of a rigidly clamped diaphragm, the following two conditions for a thin plate are obtained

i) at $r = a$; $\eta = 0$

ii) at $r = a$; $\frac{d\eta}{dr}$ = slope = 0

When the first of these conditions is applied to equation (A-28) the following relation is obtained

$$0 = A J_0(K_3 a) + B I_0(K_3 a) \qquad \text{A-29}$$

and applying the second condition to the equation

$$0 = A\frac{dJ_0(K_3a)}{dr} + B\frac{dI_0(K_3a)}{dr} \qquad \text{A-30}$$

but since

$$\frac{dJ_0(K_3a)}{dr} = -KJ_1(K_3a) \quad \text{AND} \quad \frac{dI_0(K_3a)}{dr} = KI_1(K_3a)$$

the equation (A-30) takes the form

$$0 = -AK_3J_1(K_3a) + BK_3I_1(K_3a) \qquad \text{A-30a}$$

Rearranging terms in equations (A-29, A-30a) and dividing one by the other, a frequency equation is obtained which must be satisfied by particular values of Ka for a solution to exist.

$$\frac{J_0(K_3a)}{J_1(K_3a)} = -\frac{I_0(K_3a)}{I_1(K_3a)} \qquad \text{A-31}$$

Now since both the Bessel functions I_0 and I_1 are positive for all values of Ka, a solution occurs only when J_0 and J_1 are of opposite sign. From a table of Bessel functions, it can be seen that the equation is satisfied by

$$K_3a = 3.20\ ,\ 6.30\ ,\ 9.44\ ,\ \ldots\ .$$

or approximately by

$$K_3a \simeq n\pi \qquad n = 1, 2, 3, \ldots$$

Now from equation (A-24)

$$K_3^4 = \left(\frac{\omega}{c_1}\right)^2$$

$$= \frac{\omega^2\, 12\rho(1-\sigma^2)}{Eh^2}$$

or

$$\omega_{np} = K_3^2\sqrt{\frac{Eh^2}{12\rho(1-\sigma^2)}} \qquad \text{A-32}$$

where upon setting $K_3 = \frac{3.20}{a}$ the fundamental frequency is given by

$$f_{np} = \frac{\omega_{np}}{2\pi} = \frac{(3.20)^2}{2\pi}\frac{h}{a^2}\sqrt{\frac{E}{12\rho(1-\sigma^2)}} \qquad \text{A-33}$$

A5. General Case: Graphical Solution for the Fundamental Natural Frequency of a Stretched, Circular, Clamped Flat Diaphragm

Experiments show that, although membranes and thin plates exist in theory, they are not easily achieved in practice. Unless a diaphragm is extremely thin or stretched very tightly, deviations occur from the theoretical results calculated for membranes due to the inherent stiffness of the material of the diaphragm. For this reason, a general case must be considered which takes into account restoring forces in the diaphragm due to both tension and stiffness.

Once again, the derivation of the equations of motion for this general case is quite complicated and thus will not be included here. The equation of motion as taken from Reference 7 is:

$$\frac{(E+T)h^2}{12\rho(1-\sigma^2)}\nabla_r^4 y - \frac{T}{m}\nabla_r^2 y - \frac{P}{m} + \frac{\partial^2 y}{\partial t^2} = 0 \qquad \text{A-34}$$

where P is now a traverse pressure or a resultant disturbing force on the diaphragm and the added term T to Young's modulus occurs because the added tension increases the effective modulus. Again, a symmetrical condition is assumed and thus no variation will occur when θ, the polar angle, is varied.

If a harmonic motion is assumed in all modes, i.e., $y(r,t) = \eta(r)e^{j\omega t}$ equation (A-34) can be written as

$$\frac{(E+T)h^2}{12\rho(1-\sigma^2)}\nabla_r^4 \eta - \frac{T}{m}\nabla_r^2 \eta - \frac{P}{m} - \omega^2\eta = 0 \qquad \text{A-34a}$$

Note that from this general equation, the equation of motion for a stretched membrane can be obtained by letting $h \to 0$ and similarly by letting $T \to 0$, and the equation of motion of an unstretched thin plate is obtained.

As previously seen, due to the boundary condition that the center deflection of the diaphragm is finite, Bessel functions of the second kind are not permissible. This condition thus eliminates two of the four arbitrary constants needed to solve equation (A-34a). A solution of (A-34a) then is of the form

$$\eta = A J_0(K_1 r) + B J_0(K_2' r) - \frac{P}{\omega^2 m} \qquad \text{A-35}$$

where K_1 and K_2' satisfy the equation

$$\frac{(E+T)h^2}{12\rho(1-\sigma^2)} K^4 + \frac{T}{m} K^2 - \omega^2 = 0 \qquad \text{A-36}$$

letting

$$c_1 = \frac{(E+T)h^2}{12\rho(1-\sigma^2)} \quad ; \quad d_1 = \frac{T}{m}$$

the two solutions are

$$K_1 = \sqrt{\frac{\sqrt{d_1^2 + 4c_1\omega^2} - d_1}{2c_1}} \qquad \text{A-37}$$

$$K_2' = j\sqrt{\frac{\sqrt{d_1^2 + 4c_1\omega^2} + d_1}{2c_1}} \qquad \text{A-38}$$

Substituting equations (A-37, A-38) into equation (A-35) and using the condition for a clamped diaphragm that $\eta = \frac{d\eta}{dr} = 0$ when $r = a$ to evaluate the constants A and B, Mason (Reference 7) obtained the following expression for displacement of the diaphragm:

$$\eta = \frac{P}{\omega^2 m}\left[\frac{K_2 I_1(K_2 a) J_0(K_1 r) + K_1 J_1(K_1 a) I_0(K_2 r)}{J_0(K_1 a) K_2 I_1(K_2 a) + K_1 J_1(K_1 a) I_0(K_2 a)}\right] \qquad \text{A-39}$$

where

$$K_2 = -jK'_2$$

Now theoretically at a undamped natural frequency ω_n the center deflection of the diaphragm becomes infinite. Applying this theoretical condition to equation (A-39), it is seen that for the equation to be satisfied, the following condition must hold

$$J_0(K_1a)K_2I_1(K_2a) + K_1J_1(K_1a)I_0(K_2a) = 0 \qquad A-40$$

If $x = K_1a$ and $z = K_2a$ the frequency equation (A-40) takes the form

$$\frac{I_0(z)}{zI_1(z)} = \frac{-J_0(x)}{xJ_1(x)} \qquad A-41$$

To find values of x and z to satisfy equation (A-41), a plot is made of $-\frac{J_0(x)}{x\,J_1(x)}$ vs x as shown in Figure 27. Also plotted in this figure are two plots of $\frac{I_0(z)}{z\,I_1(z)}$ vs z. One plot corresponds to x = z and the other to x = 0.1z. The intersection of the curves gives values of x and z which satisfy equation (A-41) for the particular cases where $\frac{x}{z} = 1$ and $\frac{x}{z} = 0.1$.

Thus, from a cross plot of $\frac{J_0(x)}{x\,J_1(x)}$ and $\frac{I_0(z)}{z\,I_1(z)}$ values of x and z satisfying equation (A-41) can be found for various ratios of x to z. The ratio $\frac{x}{z}$ in expanded form is

$$\frac{x}{z} = \frac{(K_1a)}{(K_2a)} = \sqrt{\frac{\sqrt{d_1^2 + 4c_1\omega_n^2} - d_1}{\sqrt{d_1^2 + 4c_1\omega_n^2} + d_1}} \qquad A-42$$

Now the general case under study is of a diaphragm whose characteristic is between a theoretical membrane at one extreme and a thin plate as the other extreme. This thus sets limits on the values of $\frac{x}{z}$ which are necessary to consider. For a membrane (no bending stiffness) $c_1 = 0$ and

one limit is $\frac{x}{z} = 0$ while for a thin plate (no tension) $d_1 = 0$ and $\frac{x}{z} = 1$. Hence, it can be seen from Figure 27 that, at the fundamental natural frequency, x is limited in value to the range from $x = 2.405$ ($\frac{x}{z} = 0$ and $z = \infty$) to $x = z = 3.196$. Table 2 gives values of x and z from expanded plots of $-\frac{J_0(x)}{x J_1(x)}$ vs x and $\frac{I_0(z)}{z I_1(z)}$ vs z for various values of $\frac{x}{z}$ in this range.

In order to graphically find the fundamental natural frequency, another plot is required. From previously defined expressions for x and z the following equations are obtained

$$X^2 = \frac{a^2}{2c_1}\left[\sqrt{d_1^2 + 4\omega_n^2 c_1} - d_1\right]$$

$$Z^2 = \frac{a^2}{2c_1}\left[\sqrt{d_1^2 + 4\omega_n^2 c_1} + d_1\right]$$

and

$$Z^2 - X^2 = \frac{a^2 d_1^2}{c_1} \qquad \text{A-43}$$

$$X^2 Z^2 = \frac{a^4 \omega_{nD}^2}{c_1}$$

hence

$$XZ = \frac{a^2 \omega_{nD}}{\sqrt{c_1}} \qquad \text{A-44}$$

Substituting the previously defined values of c_1 and d_1 into equations (A-43) and (A-44) yields

$$Z^2 - X^2 = \frac{a^2 T}{m} \frac{12\rho(1-\sigma^2)}{(E+T)h^2} \qquad \text{A-45}$$

$$XZ = \frac{2a^2 \omega_{nD}}{h}\sqrt{\frac{3\rho(1-\sigma^2)}{(E+T)}} \qquad \text{A-46}$$

Table 1 also contains tabulated values of expressions (A-45) and (A-46) for various values of x and z within our range of interest. Figure 28 shows a plot of equation (A-45) plotted against equation (A-46) for their respective values given in Table A-1. Hence, the plot shown in Figure 28 is a graphical solution of equation (A-34) for the fundamental natural frequency of any circular, clamped, flat diaphragm under radial tension.

Summary: Steps to follow in using the graphical method (Reference).

1) Calculate $\frac{a^2 T}{m} \quad \frac{12\rho(1-\sigma^2)}{(E+T)\,h^2}$ (equation A-45) from the initial tension and the diaphragm constants.

2) With the value calculated in step (1), obtain the value of $\frac{2a^2}{h}\omega_{n\rho}\sqrt{\frac{3\rho(1-\sigma^2)}{(E+T)}}$ (equation A-46) from the graphical solution plotted in Figure 28

3) Calculate $\frac{2a^2}{h}\sqrt{\frac{3\rho(1-\sigma^2)}{(E+T)}}$.

4) Divide the value obtained in step (2) by the value obtained in step (3) to obtain the fundamental natural frequency of the diaphragm.

A6. Static Deflection of a Diaphragm

Equation (A-47) gives an expression for the displacement, η, of a diaphragm with tension and stiffness. If η is treated as a small quantity, as originally assumed, then the expression for the displacement as given in Reference (7), is reduced to

$$\eta = \frac{P}{T}\left[\frac{\left\{a\sqrt{\frac{(E+T)h^3}{12T(1-\sigma^2)}}\left[I_0\left(r\sqrt{\frac{12T(1-\sigma^2)}{(E+T)h^3}}\right) - I_0\left(a\sqrt{\frac{12T(1-\sigma^2)}{(E+T)h^3}}\right)\right]\right\}}{I_1\left(a\sqrt{\frac{12T(1-\sigma^2)}{(E+T)h^3}}\right)} + \frac{a^2-r^2}{4}\right] \qquad \text{A-47}$$

In the case of a thin plate $T \to 0$ and the static deflection becomes

$$\eta = \frac{12(1-\sigma^2)}{Eh^3}\left[\frac{r^4+a^4}{64} - \frac{a^2r^2}{32}\right] \qquad \text{A-48}$$

In the case of a theoretical membrane, $h \to 0$ or the natural stiffness is quite small compared to the tension; the amplitude of vibration is

$$\eta = \frac{P}{T}\left[\frac{a^2-r^2}{4}\right] \qquad \text{A-49}$$

This equation may be written as

$$\eta = \frac{a^2P}{4T}\left[1-\left(\frac{r}{a}\right)^2\right] \qquad \text{A-50}$$

Note that the center deflection at $r = 0$ is expressed as

$$\eta_{r=0} = \eta_0 = \frac{a^2P}{4T} \qquad \text{A-51}$$

Therefore, equation (A-50) can be written in final form as

$$\eta = \eta_o \left[1 - \left(\frac{r}{a} \right)^2 \right] \qquad \text{A-52}$$

A plot of this relationship is shown in Figure 29.

APPENDIX B

ACOUSTICAL SYSTEM

Helmholtz Resonator

In acoustics, the term resonator has come to mean a simple vibrating system consisting of a compressible fluid contained in a rigid enclosure communicating with the external medium through an aperture of restricted area.

The theory of resonators has been developed in detail by Helmholtz, for whom they are named after, but only a simplified treatment will be presented here. Figure 25 shows two simple Helmholtz resonators. The exact form of the resonator is unimportant as long as the smallest dimension is considerably larger than the dimension of the aperture. A simple resonator, as described above, is analogous to that of a mechanical system with one degree of freedom having lumped mechanical elements of mass, stiffness and resistance. (It is also analogous to a series RCL circuit.) This analogy provides the simplest physical interpretation of the system. In Helmholtz's as well as Rayleigh's (Reference 8) development of the theory of such a resonator, the gas in the aperture is considered to move as a unit and provides the mass element of the system. The motion of the gas in the aperture acts like a reciprocating piston compressing and rarifying the air contained in the cavity. The influx and efflux of gas through the aperture provides the stiffness element (i.e., the stiffness is due to the volumetric compression, $s_c = -\frac{dV}{V}$, within the cavity). The resistance element is provided by the radiation of energy into the surrounding medium (dependent upon the cross sectional area of aperture) and by the dissipation of energy due to viscous damping (dependent on the length of the aperture, i.e., effects of tubing).

Before proceeding further with the analysis of the acoustic system, the following assumptions must be stated:

Assumptions

i) The wave length, λ, of the vibration of free air is large compared with the dimension of the cavity. This implies that at any instant, the condensation will be uniform throughout the cavity.

ii) Adiabatic compression

iii) Uniform volume flow

iv) The tube length (aperture) must be sufficiently short so that the dead time ℓ/c can be neglected.

As previously stated, the resistance element is a function of the dimension of the aperture and on this basis, the analysis will be carried out in two parts.

I. The first case to be considered is that in which the length of the aperture is negligible compared to its diameter. This case is shown in Figure 2.5a. The motion in the system is mainly confined to the air in the aperture (or neck). If the cross-sectional area and length of the aperture are S and ℓ respectively, and ρ in the density (mass/vol) of the gas in the neck, then the mass of air in the neck is $\rho\ \ell\ S$. A force balance carried out on the air in the aperture shows that the acceleration force is given as $f_a = (\rho\ \ell\ S)\ddot{\eta}$, where η is the displacement of the unit air mass. The stiffness force or excess pressure that results when a volume of gas, $dV = S\eta$, flows through the aperture

is developed as follows:

The bulk modulus of elasticity, B, of a fluid is defined as the negative of the ratio of the incremental pressure dP to the strain dV/V.

$$B_1 = - \frac{dP}{dV/V}$$

or

$$B_1 = - \frac{dP}{s_1}$$

where s_1 is the condensation equal to $- dV/V_0$. Now the general definition of incremental pressure dP is identical with the acoustic definition of excess pressure, p. Hence

$$p = dP$$

letting

$$c^2 = \frac{B}{\rho} \quad ; \quad p = \rho c^2 s_1$$

substituting for s

$$p = - \rho c^2 \frac{dV}{V}$$

and

$$p = - \frac{c^2 \rho}{V} S\eta$$

Therefore, the resulting stiffness force acting on the mass is given by

$$f_s = pS = - \frac{c^2 \rho}{V} S^2 \eta \qquad \text{B-1}$$

The resistive force for this case is due only to the radiation of energy and is given by Rayleigh (Reference 8) as

$$f_R = \frac{\rho c K_1^2 S^2}{2\pi} \dot{\eta} \qquad \text{where} \quad K_1 = \frac{2\pi}{\lambda} = \frac{\omega}{c} \qquad \text{B-2}$$

Summing forces the complete equation of motion is obtained

$$f_a + f_R + f_s = f_d$$

or $$\rho \ell S \ddot{\eta} + \frac{\rho c K_t^2 S^2}{2\pi} \dot{\eta} + \frac{\rho c^2 S^2}{V} \eta = S P e^{j\omega t} \qquad B-3$$

where $S P e^{jwt}$ is an externally applied force and P is its pressure amplitude. Thus, it is seen that this acoustical system can be described by a second order linear differential equation with an undamped natural (or fundamental) frequency of

$$\omega_{nR} = c\sqrt{\frac{S}{\ell V_o}} \qquad B-4$$

and a damping ratio (due to radiation) equal to

$$\zeta_R = \frac{c K_t^2}{4\pi \omega_{nR} \ell} \frac{S}{} = \frac{K_t^2}{4\pi}\sqrt{\frac{S V_o}{\ell}} \qquad B-5$$

Now in an actual resonator this damping term is very small and has little effect on the vibration of the system. Thus, it can be assumed that the damped and undamped natural frequencies are approximately the same.

II. In the second case to be considered, the length of the aperture is comparable or larger than its diameter. This case takes into account the effects of a long length of tubing connected to the resonator, thus extending the length of the aperture. A simple resonator of this type is shown in Figure (2.5b). The analysis in this case will treat the system as a pneumatic system. Thus, it will be necessary to define a new set of terms. The objective of the treatment of this case is to arrive at a transfer function (P_c/P_d) for the system.

Resistance - R: The resistance in the system for this present case is assumed to be due only to the resistance offered to the motion of the viscous fluid in the tubing. The pressure drop, P_r, in the tube

due to flow resistance is given by the Hagen-Poiseuille Law as:

$$\dot{Q} = \frac{\pi r_1^4}{8 \mu l} P_r \qquad r_1 = \text{radius of tubing}$$

where the pneumatic resistance coefficient is defined as

$$R = \frac{8 \mu l}{\pi r_1^4} \qquad B-6$$

hence

$$P_r = R \dot{Q} \qquad B-7$$

The value of R varies with absolute viscosity which is assumed to be essentially constant for small temperature and pressure change. The relationship only holds for laminar flow.

Capacitance - C: Pneumatic capacitance is defined as the time integral of the volumetric flow into a vessel divided by its internal pressure. Starting from a special form of the general gas equation (equation 8-8), a value for the capacitance of the system presently under study can be formulated as follows:

$$C = -\frac{dV}{dP_2} \qquad B-8$$

Now the volume flow into the cavity or reservoir is equal to the decrease in volume of the gas originally in the cavity; hence,

$$dQ = -dV$$

therefore

$$C = \frac{dQ}{dP_2} \qquad B-9$$

Assuming adiabatic compression in the cavity

$$P_2 V^{\gamma} = K_s \qquad \text{WHERE: } \gamma = \text{ratio of specific heats}$$

differentiating

$$V^{\gamma} dP_2 + P_2 \gamma V^{\gamma-1} dV = 0$$

hence

$$\frac{dV}{dP_2} = -\frac{V}{P_2 \gamma}$$

Substituting this relationship into equation (B-8) a value for capacity is obtained

$$C = \frac{V}{P_2 \gamma} \qquad \text{B-10}$$

and hence equation (B-9) becomes

$$\frac{dQ}{dP_2} = C = \frac{V}{P_2 \gamma} \qquad \text{B-11}$$

Inertance - J: If the motion of the fluid is assumed to be confined to the tubing then the accelerating force on the mass element, $\rho S \ell$, in the tubing is given as

$$S P_J = (\rho S \ell) a$$

where P_J is the pressure drop necessary to accelerate the fluid and may be written as

$$P_J = \rho \ell a \qquad \text{B-12}$$

Now "a", the acceleration of the fluid in the tube, can be expressed pneumatically as

$$a = \frac{\ddot{Q}}{S}$$

hence

$$P_J = \frac{\rho \ell}{S} \ddot{Q} \qquad \text{B-13}$$

or

$$P_J = J \ddot{Q} \qquad \text{B-14}$$

where the inertance (J) of the system is defined from equation (B-14) as

$$J = \frac{\rho \ell}{S} \qquad \text{B-15}$$

This term is proportional to the density of the fluid and for small pressure changes, it is essentially constant.

Thus, having defined the terms necessary to work with, an equation of motion can be obtained for the system by making a pressure balance on the mass element of air in the tubing as follows:

$$P_J + P_r + P_2 = P_1 \qquad \text{B-16}$$

and

$$P_J + P_r + P_2 - P_o = P_1 - P_o$$

letting P_d (disturbing pressure at mouth of tubing) = $P_1 - P_o$

P_c (pressure change in reservoir) = $P_2 - P_o$;

hence,

$$P_J + P_r + P_c = P_d \qquad \text{B-17}$$

Now by definition

$$P_r = R\dot{Q}$$

and

$$P_J = J\ddot{Q}$$

substituting into equation (B-17)

$$J\ddot{Q} + R\dot{Q} + P_c = P_d \qquad \text{B-18}$$

Now from equation (B-9)

$$dP_2 = \frac{dQ}{C}$$

taking the integral of both sides

$$\int dP_2 = \frac{1}{C}\int dQ$$

or

$$P_2 = \frac{Q}{C} + \text{CONSTANT} \qquad \text{B-19}$$

The constant term can be evaluated from the condition that when $Q = 0$, $P_2 = P_o$. Hence,

$$P_2 - P_o = \frac{Q}{C} = P_c \qquad \text{B-20}$$

Therefore, the equation of motion in final form becomes

$$J\ddot{Q} + R\dot{Q} + \frac{Q}{C} = P_d \qquad \text{B-21}$$

or substituting equation (B-20) into equation (B-21)

$$JC\ddot{P}_c + RC\dot{P}_c + P_c = P_d \qquad \text{B-22}$$

This again is a second order differential equation which may be written in the more familiar form

$$\frac{1}{\omega_{nR}^2}\ddot{P}_c + \frac{2\zeta_R}{\omega_{nR}}\dot{P}_c + P_c = P_d \qquad \text{B-23}$$

The undamped natural frequency is

$$\omega_{nR} = \sqrt{\frac{1}{JC}} = c\sqrt{\frac{S}{\ell V}} \qquad \text{B-24}$$

which is the same as in the previous case. The damping ratio for this case, due to viscous damping is

$$\zeta_R = \frac{R}{2}\sqrt{\frac{C}{J}} = \frac{8\mu\ell}{2\pi r^4}\sqrt{\frac{\pi r^2 V}{\rho \ell \gamma P_o}} \qquad \text{B-25}$$

Finally, by Laplace transformation of equation (B-23), the transfer function for a Helmholtz resonator in which the length of the aperture is larger than its diameter is given as

$$\frac{P_c(s)}{P_d(s)} = \frac{1}{\frac{S^2}{\omega_{nR}^2} + \frac{2\zeta}{\omega_{nR}}S + 1} \qquad \text{B-26}$$

APPENDIX C

ANALYSIS OF BRIDGE NETWORK

In Figure 3 is shown the general circuitry of a bridge network. For this bridge to be balanced, i.e., no output voltage, the following relationship must be true

$$I_A Z_1 = I_B Z_2 \qquad C-1$$

$$I_A Z_3 = I_B Z_4 \qquad C-2$$

hence

$$Z_2 Z_3 = Z_1 Z_4 \qquad C-3$$

In the particular case under study, the bridge has two active elements, z_2 and z_4. These elements produce a differential output such that a $+\Delta z$ in one element produces a $-\Delta z$ in the other and thus the net result is $|2\Delta z|$. A transfer function for this network will now be formulated in general terms under the assumption that $R_i \simeq 0$ and $0 < R_L < \infty$.

Using Kirchoff's Current Law

Σ currents at Node #2

$$\frac{V_2}{Z_2} + \frac{(V_2 - V_3)}{R_L} + \frac{(V_2 - V_1)}{Z_4} = 0$$

or

$$\left[\frac{1}{Z_2} + \frac{1}{R_L} + \frac{1}{Z_4}\right] V_2 - \frac{V_3}{R_L} = \frac{V_E}{Z_4} \qquad C-4$$

similarly

Σ currents at Node #3

$$-\frac{V_2}{R_L} + \left[\frac{1}{Z_1} + \frac{1}{Z_3} + \frac{1}{R_L}\right] V_3 = \frac{V_E}{Z_3} \qquad C-5$$

Now solving equation (C-4) and (C-5) simultaneously for V_2 and V_3

$$V_2 = \frac{\begin{vmatrix} \frac{V_E}{Z_4} & -\frac{1}{R_L} \\ \frac{V_E}{Z_3} & +\left[\frac{1}{Z_1}+\frac{1}{Z_3}+\frac{1}{R_L}\right] \end{vmatrix}}{\begin{vmatrix} \left[\frac{1}{Z_2}+\frac{1}{Z_4}+\frac{1}{R_L}\right] & -\frac{1}{R_L} \\ -\frac{1}{R_L} & \left[\frac{1}{Z_1}+\frac{1}{Z_3}+\frac{1}{R_L}\right] \end{vmatrix}}$$

or

$$V_2 = V_E\left[\frac{\frac{1}{Z_1Z_4}+\frac{1}{Z_2Z_4}+\frac{1}{Z_4R_L}+\frac{1}{Z_3R_L}}{\det}\right] \qquad C-6$$

where

$$\det = \frac{1}{Z_1Z_2}+\frac{1}{Z_2Z_3}+\frac{1}{Z_2R_L}+\frac{1}{Z_1R_L}+\frac{1}{Z_3R_L}+\frac{1}{Z_4R_L}+\frac{1}{R_L^2}+\frac{1}{Z_3Z_4}+\frac{1}{Z_4Z_1}-\frac{1}{R_L^2}$$

and

$$\det = \left[\frac{1}{Z_1Z_2}+\frac{1}{Z_2Z_3}+\frac{1}{Z_3Z_4}+\frac{1}{Z_4Z_1}\right]+\frac{1}{R_L}\left[\frac{1}{Z_1}+\frac{1}{Z_2}+\frac{1}{Z_3}+\frac{1}{Z_4}\right] \qquad C-7$$

and

$$V_3 = \frac{\begin{vmatrix} \left[\frac{1}{Z_2}+\frac{1}{R_L}+\frac{1}{Z_4}\right] & \frac{V_E}{Z_4} \\ -\frac{1}{R_L} & \frac{V_E}{Z_3} \end{vmatrix}}{\det}$$

or

$$V_3 = V_E\frac{\left[\frac{1}{Z_2Z_3}+\frac{1}{Z_3R_L}+\frac{1}{Z_3Z_4}+\frac{1}{Z_4R_L}\right]}{\det} \qquad C-8$$

Now from the bridge configuration

$$V_o = V_3 - V_2 \qquad C-9$$

therefore

$$V_o = V_E \frac{\frac{1}{Z_1 Z_4} + \frac{1}{Z_3 Z_4} + \frac{1}{Z_4 R_L} + \frac{1}{Z_3 R_L} - \frac{1}{Z_2 Z_3} - \frac{1}{Z_3 R_L} - \frac{1}{Z_3 Z_4} - \frac{1}{Z_4 R_L}}{\det} \qquad C-10$$

Now

$$Z_o = Z_1 = Z_3$$

$$\frac{V_o}{V_E} = \frac{\left[\frac{1}{Z_4} - \frac{1}{Z_2}\right]}{2\left[\frac{1}{Z_4} + \frac{1}{Z_2}\right] + \frac{Z_o}{R_L}\left[\frac{Z_2 + Z_4}{Z_2 Z_4}\right]}$$

and

$$\frac{V_o}{V_E} = \frac{R_L(Z_2 - Z_4)}{2R_L(Z_2 + Z_4) + 2Z_2 Z_4 + Z_o Z_2 + Z_o Z_4} \qquad C-11$$

Now assuming a differential variation in z_2 and z_4

$$Z_2 = Z_2 + \Delta Z_2 = Z^* + \Delta Z^*$$

$$Z_4 = Z_4 - \Delta Z_4 = Z^* - \Delta Z^*$$

where

$$Z^* = Z_2 = Z_4$$

Substituting this relationship into equation (C-11) and rearranging terms

$$\frac{V_o}{V_E} = \frac{\Delta Z^*}{2Z^* + \frac{Z^* Z_o}{R_L} + \frac{Z^* Z^*}{R_L} - \frac{\Delta Z^* \Delta Z^*}{R_L}} \qquad C-12$$

Now

$$\frac{(\Delta Z^*)^2}{R_L} \simeq 0$$

therefore

$$\frac{V_o}{V} = \frac{\frac{\Delta Z^*}{Z^*}}{2 + \frac{1}{R_L}\left[Z_o + Z^*\right]} \qquad C-13$$

This is thus the general transfer function for a Wheatstone bridge with two differential active arms. Now in particular, the elements of the bridge being used are capacitors as shown in Figure 4 . The transfer function for this particular bridge is obtained as follows

Letting

$$|Z_o| = \left|\frac{1}{\omega C_o}\right| \qquad \text{WHERE} \quad C_o = C_1 = C_3 \qquad C-14$$

and

$$|Z^*| = \left|\frac{1}{\omega C^*}\right| \qquad \text{WHERE} \quad C^* = C_2 = C_3 \qquad C-15$$

differentiating

$$dZ^* = -\frac{dC^*}{\omega (C^*)^2}$$

or

$$\Delta Z^* = \frac{-\Delta C^*}{\omega (C^*)^2}$$

substituting this result into equation (C-13)

$$\frac{V_o}{V_E} = \frac{\frac{\Delta C^*}{C^*}}{2 + \frac{1}{R_L}\left(\frac{1}{\omega C^*} + \frac{1}{\omega C_o}\right)} \qquad C-16$$

and

$$\frac{V_o}{V_E} = \frac{1}{2}\,\frac{\frac{\Delta C_o}{C_o}}{\left[1 + \frac{1}{\Omega R_L C_o}\right]} \qquad \text{WHERE} \quad C_o = C^*, \quad \omega = \Omega = \text{CONSTANT} \qquad C-17$$

the sensitivity, S, is defined as

$$S = \frac{\frac{V_o}{V_E}}{\frac{\Delta C_o}{C_o}} = \frac{1}{2}\,\frac{1}{1 + \frac{1}{\Omega R_L C_o}} \qquad C-18$$

Now, equation (D-11) of Appendix-D expresses to a first order in $\Delta d_o/d_o$, the change in capacitance of one side of the symmetrical capacitive transducer to a differential change in the electrode spacing

$$\Delta C_o = -\frac{1}{2} K' C_o \frac{\Delta d_o}{d_o} \qquad \text{WHERE} \qquad \Delta d_o = \eta_o$$

WHERE

$$K' = \left[\frac{a}{R'}\right]^2 \left\{ 1 - \left[1 - \left(\frac{R'}{a}\right)^2 \right]^2 \right\}$$

or

$$K' = 2 - \left(\frac{R'}{a}\right)^2$$

Thus, equation (C-15) can be expressed as

$$\frac{V_o}{V_\epsilon} = \frac{1}{2}\left[\frac{K'\Delta d_o}{2d_o}\right]\left[\frac{1}{1 + \frac{1}{\Omega R_L C_o}}\right] \qquad \text{C-19}$$

Now, in the "s" domain, equations (C-14), and (C-15) can be written in Laplace form as

$$Z_o = \frac{1}{sC_o} \qquad \text{C-20}$$

$$Z^* = \frac{1}{sC^*} \qquad \text{C-21}$$

Thus, equation (C-16) can be written in Laplace form as

$$\frac{V_o(s)}{V_\epsilon(s)} = \frac{\frac{\Delta C^* s}{sC^*}}{2 + \frac{1}{R_L}\left[\frac{1}{sC^*} + \frac{1}{sC_o}\right]}$$

and

$$\frac{V_o(s)}{V_\epsilon(s)} = \frac{1}{2}\frac{\Delta C^*}{C^*}\left[\frac{S}{S + \left[\frac{1}{2R_L C^*} + \frac{1}{2R_L C_o}\right]}\right] \qquad \text{C-22}$$

Now, as before

$$C_o = C^*$$

therefore

$$\frac{V_o(s)}{V_E(s)} = \frac{1}{2}\frac{\Delta C_o}{C_o}\left[\frac{S}{S+\frac{1}{R_L C_o}}\right] \qquad C\text{-}23$$

Substituting equation (D-11) into equation (C-23), the bridge transfer function is written as

$$\frac{V_o(s)}{\Delta d_o(s)} = \frac{K'}{4}\frac{V_E(s)}{d_o}\left[\frac{S}{S+\frac{1}{R_L C_o}}\right] \qquad C\text{-}24$$

or in Bode form

$$\frac{V_o(s)}{\Delta d_o(s)} = \frac{V_E(s)}{4 d_o}\frac{K'}{\alpha}\left[\frac{S}{\frac{S}{\alpha}+1}\right] \qquad \text{WHERE} \quad \alpha = \frac{1}{R_L C_o} \qquad C\text{-}25$$

Now, in particular

$$V_E = V_E \sin \Omega t$$

or in Laplace form

$$V_E(S) = V_E \frac{\Omega}{S^2+\Omega^2}$$

Substituting this relationship into equation (C-24), the transfer function can be written as

$$\frac{V_o(s)}{\Delta d_o(s)} = \frac{K' V_E}{4 d_o}\left[\frac{S}{S+\alpha}\right]\left[\frac{\Omega}{S^2+\Omega^2}\right] \qquad C\text{-}26$$

The response of this expression to a unit impulse is expressed in the time domain as

$$V_o(t) = \frac{\Delta d_o V_E K' \Omega}{4 d_o}\left[\frac{-\alpha}{\alpha^2+\Omega^2}e^{-\alpha t} + \frac{1}{\Omega}\sqrt{\frac{\Omega^2}{\alpha^2+\Omega^2}}\sin(\Omega t+\psi)\right] \qquad C\text{-}27$$

where

$$\psi = \tan^{-1}\frac{\alpha}{\Omega}$$

By exciting the bridge with a high frequency A.C. source, it can be assumed that $\Omega \gg \alpha$. Based on this assumption, equation (C-27) reduces to

$$V_o(t) = \frac{\Delta d_o V_E K'}{4 d_o} \sin(\Omega t + \psi) \qquad C-28$$

which, when rectified, becomes D.C. value

$$V_o(t) = \frac{\Delta d_o}{d_o} \frac{V_E K'}{4} \qquad C-29$$

OR IN LAPLACE FORM

$$\frac{V_o(s)}{\Delta d_o(s)} = \frac{K' V_E}{4 d_o} \qquad C-30$$

Thus, by assuming $\Omega \gg \alpha$, the output voltage is insensitive to small changes in the bridge frequency and the circuit resistance.

APPENDIX D

THEORETICAL ANALYSIS OF A VARIABLE CAPACITOR RELATING THE VARIATION IN CAPACITOR PLATE SPACING TO THE RESULTANT CHANGE IN CAPACITANCE $\frac{\Delta d_o}{\Delta C_o}$

Figure 30 is a cross sectional diagram of a diaphragm type (variable) capacitor. The capacitor consists of a deflectable diaphragm and a fixed electrode. The diaphragm is a metallic membrane of thickness h and is circularly clamped along its periphery. Its radius, measured from the inside edge of the clamp, is "a". The electrode is a circular metallic structure of radius R'. The diaphragm and the electrode have a common axis passing through their centers normal to their parallel surfaces and are separated by an air gap of thickness d_o.

When the diaphragm is at ground potential and the electrode is excited by an A.C. source, a capacitor is formed. The capacitance of a parallel plate capacitor is defined by the dimension of the gap between the parallel plate and by the medium in the gap. This is expressed as

$$C = \frac{k\epsilon_o A}{d} \quad (MKS) \qquad D\text{-}1$$

where A is the cross sectional area of the gap.

d is the plate separator.

ϵ_o is the permittivity constant separating the plate.

k is the dielectric constant.

Now, in particular, the capacitance of the diaphragm type capacitor when the diaphragm is in its equilibrium position is expressed as

$$C_o = \frac{k\epsilon_o(\pi R'^2)}{d_o} \qquad D\text{-}2$$

When the diaphragm is acted upon by a disturbing force, its displacement from its equilibrium position, as derived in Appendix A is given by equation (A-52)

$$\eta = \eta_o \left[1 - \left(\frac{r}{a}\right)^2 \right]$$

where η_0 is the center deflection. Figure 2.9 gives a graphical solution of this equation for $0 \leq r \leq a$.

Since the capacitance of a parallel plate capacitor is inversely proportional to the distance between the plate, the deflection, η, of the diaphragm from its equilibrium position results in a differential change in capacitance Δc.

An expression relating the diaphragm deflection to the resultant capacitance change has been derived by Lilly which will now be presented.

Derivation:

1) Consider the electrode surface as consisting of concentric rings of infinitesimally width. Let identical rings exist directly across the air gap on the diaphragm surface. Each ring has a width dr and a radius r measured from the center axis as shown in Figure 30 . Each pair of identical rings (one on electrode and one on the diaphragm) represents an elemental parallel annulus capacitor separated by a distance d_o. When the diaphragm is deflected a distance η, the capacitance of each elemental capacitor is directly proportional to its annulus surface area, $2\pi r dr$, and inversely proportional to the distance between the rings $d_o \pm \eta$. This is expressed as

$$C = \frac{k\epsilon_o 2\pi r\, dr}{(d_o \pm \eta)}$$

D-3

where the distance is $d_o - \eta$ if the diaphragm is deflected towards the fixed electrode and $d_o + \eta$ when deflected away from it.

The total capacitance of the diaphragm type capacitor, when the diaphragm is deflected, is equal to the summation of capacitance of each annular ring capacitor

$$C = \sum_{r=0}^{R'} \frac{k\epsilon_o 2\pi r\, dr}{(d_o \pm \eta)} \qquad \text{WHERE } \eta = \eta(r) \qquad \text{D-4}$$

or by integrating from r = 0 to r = R', an expression for the capacitance is obtained

$$C = \int_o^{R'} \frac{k\epsilon_o 2\pi r}{(d_o \pm \eta)}\, dr \qquad \text{D-5}$$

2) In particular, it is necessary to find the change in capacitance, ΔC, resulting from a diaphragm deflection. This is obtained by subtracting equation (D-3) from equation (D-5) as follows

$$\Delta C_o = C_o - C \qquad \text{OR} \qquad C_o \pm \Delta C_o = C$$

or, considering only the absolute value of each term

$$\Delta C_o + \frac{k\epsilon_o \pi R'^2}{d_o} = \int_o^{R'} \frac{k\epsilon_o 2\pi r}{(d_o \pm \eta)}\, dr \qquad \text{D-6}$$

multiplied by $\dfrac{d_o}{k\epsilon_o \pi R'^2}$

$$\frac{d_o}{k\epsilon_o \pi R'^2} \Delta C_o + 1 = \frac{d_o}{k\epsilon_o \pi R'^2} \int_o^{R'} \frac{k\epsilon_o 2\pi r}{(d_o \pm \eta)}\, dr$$

multiplied by $\left(\dfrac{R'}{a}\right)^2$

$$\frac{d_o}{k\epsilon_o \pi a^2} \Delta C_o + \left(\frac{R'}{a}\right)^2 = \frac{d_o}{k\epsilon_o \pi a^2} \int_o^{R'} \frac{k\epsilon_o 2\pi r}{(d_o \pm \eta)}\, dr \qquad \text{D-7}$$

Rearranging and letting $N = \left[\frac{R'}{a}\right]^2$ and

$$S_1 = \left[\frac{\Delta C_o}{\left(\frac{k\epsilon_o \pi a^2}{d_o}\right)}\right] = \frac{\Delta C_o}{\left(\frac{k\epsilon_o \pi R'^2}{d_o}\right)}\left(\frac{R'}{a}\right)^2 = \frac{\Delta C}{C_o} N$$

Equation (D-7) can be written as

$$S_1 = \frac{\Delta C_o}{C_o} N = \frac{d_o}{k\epsilon_o \pi a^2}\int_o^{R'} \frac{k\epsilon_o 2\pi r}{(d_o \pm \eta)} dr - N \qquad \text{D-8}$$

This expression is identical to that derived by Lilly except that equation (D-8) is in the rationalized MKS system while Lilly's derivation is in the cgs system. The two systems differ only by a factor $\frac{1}{4\pi k\epsilon}$.

Integrating equation (D-8), Lilly obtained the following relationship for two cases

Approach $(d_o - \eta)$: $S_1 = \left[\left(\frac{1}{2}\right)(1-H^3)W + \frac{1}{3}(1-H^3)W^2 + \ldots\right]$ D-9

Recession $(d_o + \eta)$: $S_1 = \left[-\frac{1}{2}(1-H^2)W + \frac{1}{3}(1-H^3)W^2 - \ldots\right]$ D-10

where

$$H = (1-N) = \left[1 - \left(\frac{R'}{a}\right)^2\right]$$

and

$$W = \left[\frac{\eta_o}{d_o}\right] = \frac{\Delta d_o}{d_o} \qquad \eta_o = \Delta d_o$$

3) In conclusion, to a first order approximation in $W = \frac{\Delta d_o}{d_o}$ the differential change in capacitance is expressed as

$$\frac{\Delta C_o}{C_o} = \pm \frac{1}{2} K' W = \pm \frac{1}{2} K' \frac{\Delta d_o}{d_o} \qquad \text{D-11}$$

where K' is a function of gauge geometry

$$K' = \frac{1}{N}\left[1 - H^2\right] \qquad \text{D-12}$$

or

$$K' = 2 - \left(\frac{R'}{a}\right)^2 \qquad \text{D-12a}$$

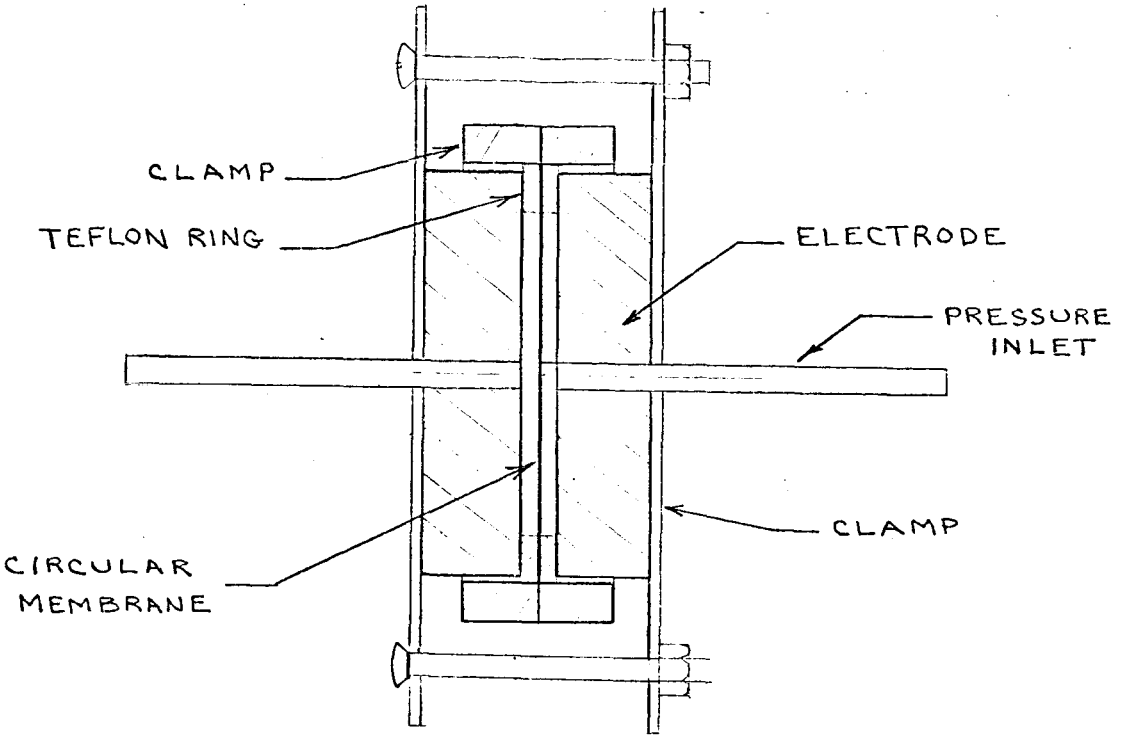

Fig. 1. CROSS SECTION OF A CAPACITIVE PRESSURE TRANSDUCER

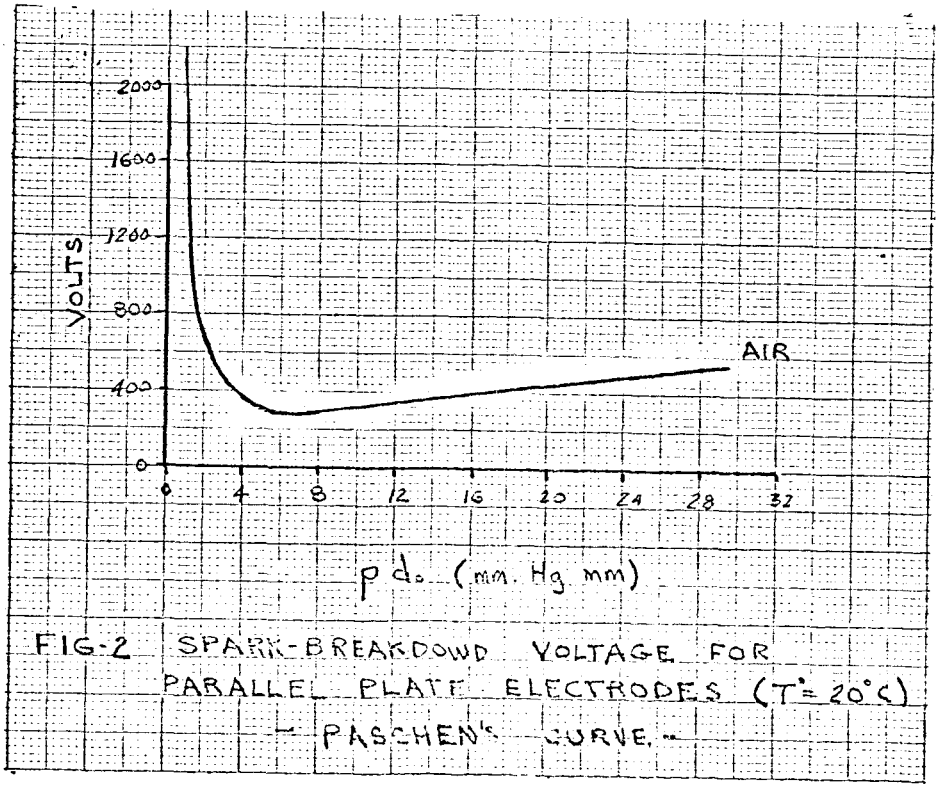

FIG-2 SPARK-BREAKDOWN VOLTAGE FOR PARALLEL PLATE ELECTRODES ($T = 20^{\circ}C$) — PASCHEN'S CURVE. —

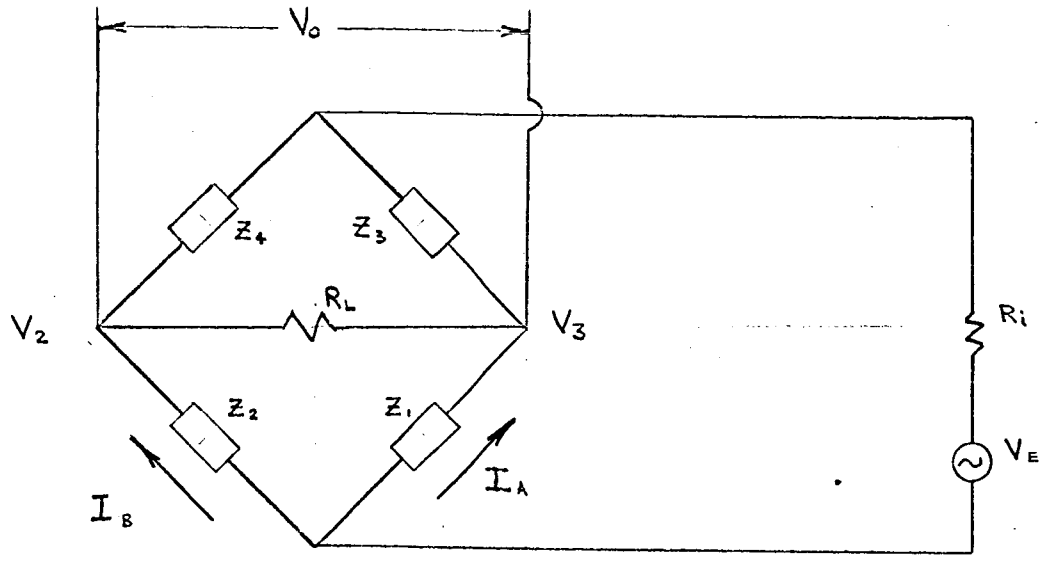

Fig. 3 GENERAL BRIDGE NETWORK

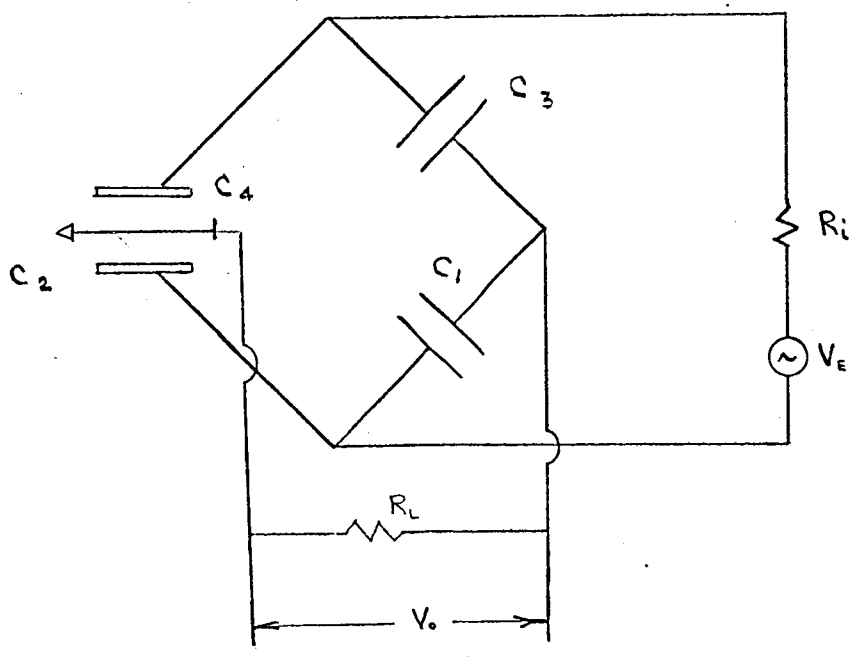

Fig. 4 CAPACITANCE BRIDGE NETWORK

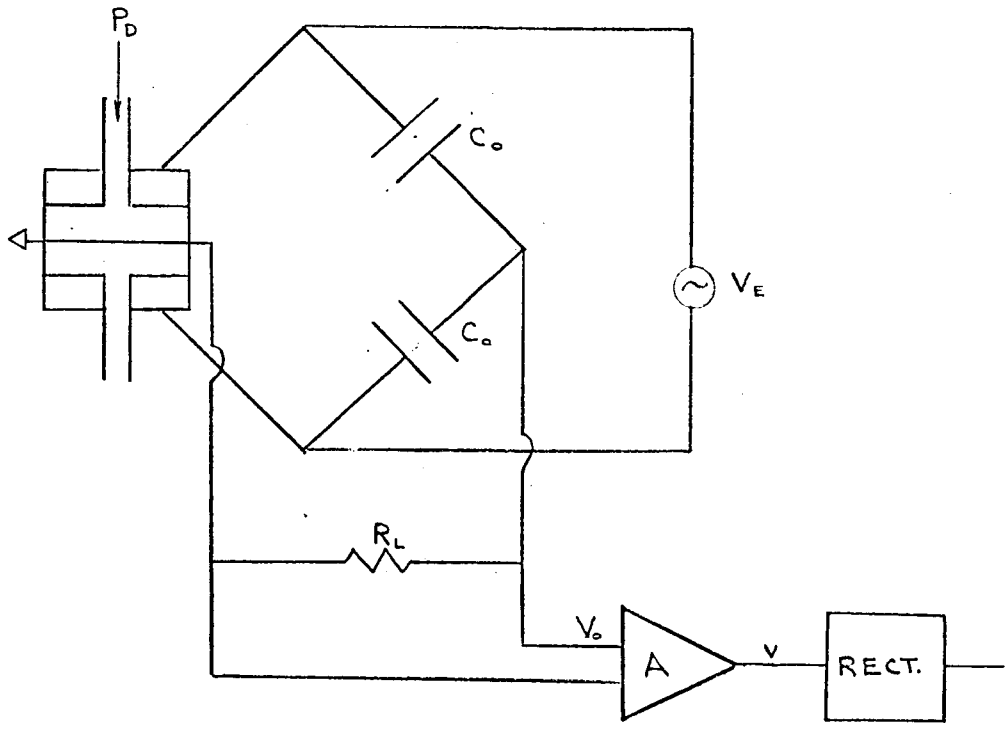

Fig. 5 SCHEMATIC REPRESENTATION OF THE UNCOMPENSATED FORWARD LOOP SYSTEM

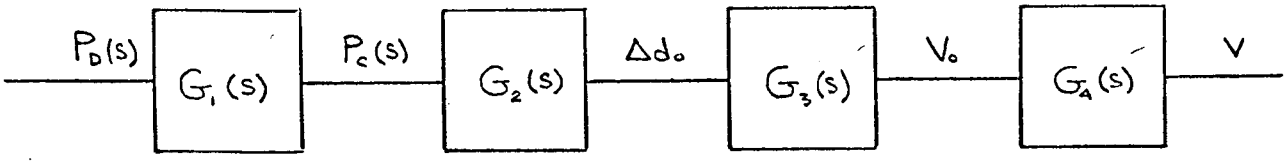

Fig. 6 BLOCK DIAGRAM OF FORWARD LOOP

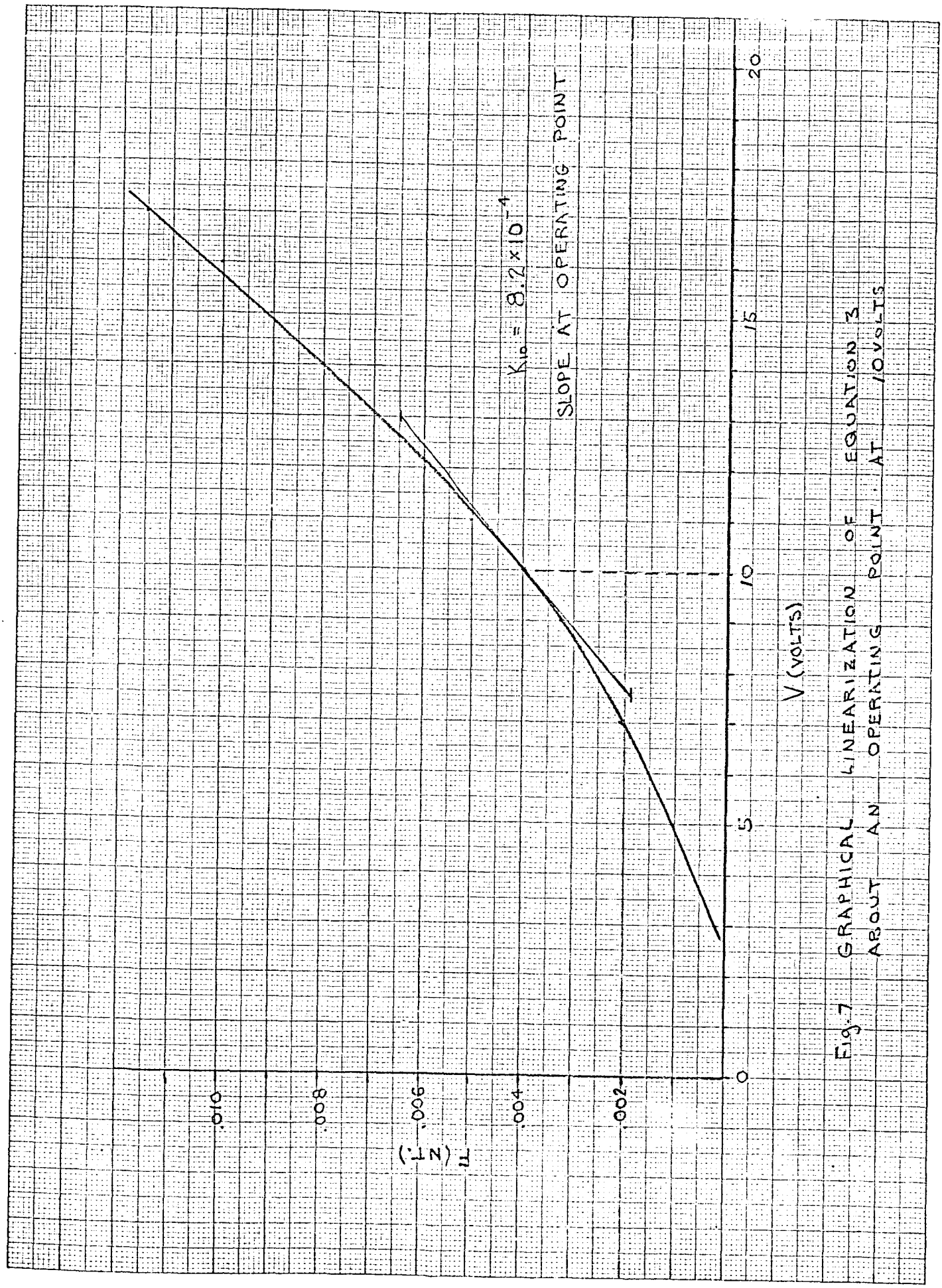

Fig. 7 GRAPHICAL LINEARIZATION OF EQUATION 3 ABOUT AN OPERATING POINT AT 10 VOLTS

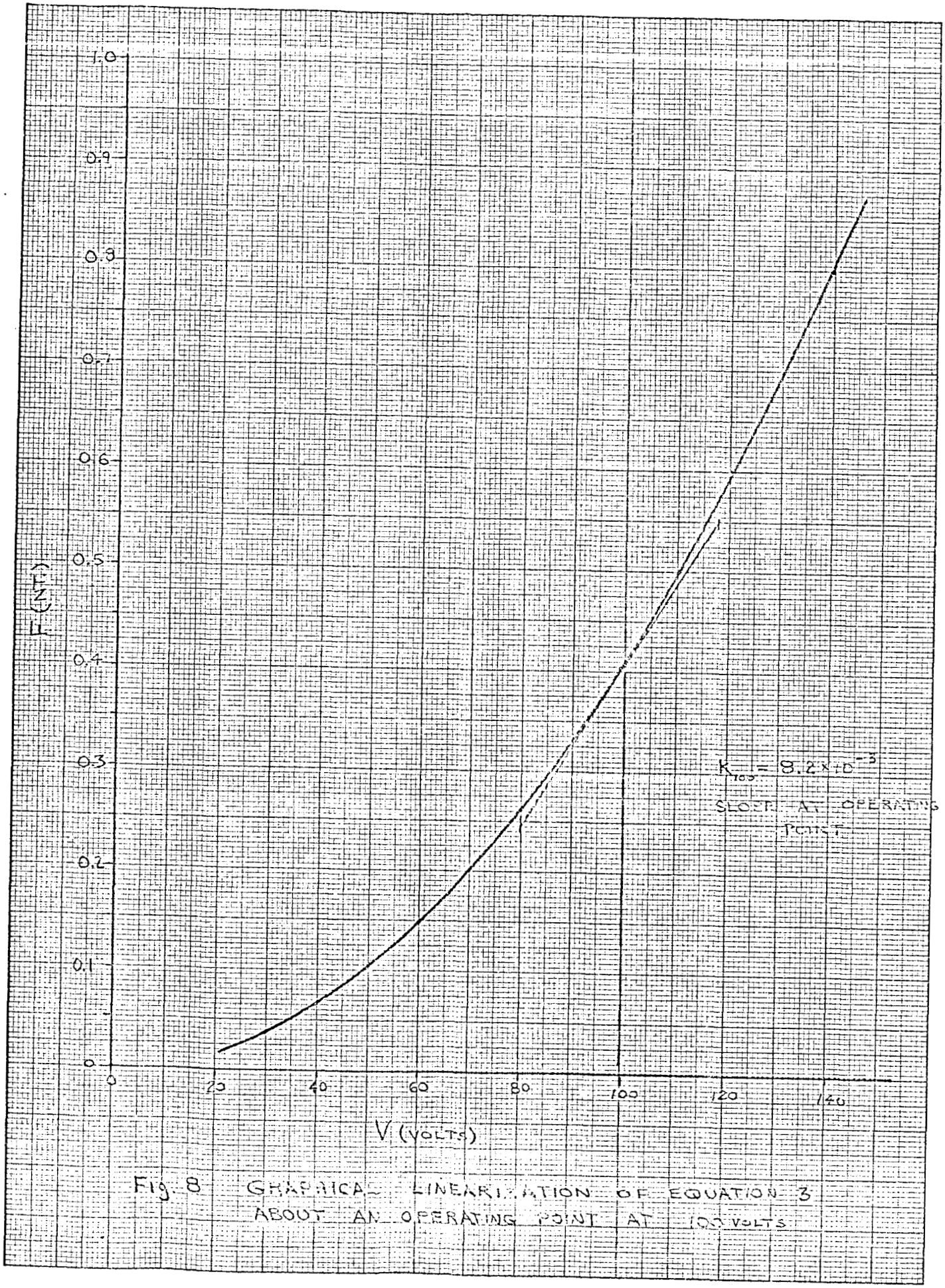

Fig. 8 GRAPHICAL LINEARIZATION OF EQUATION 3 ABOUT AN OPERATING POINT AT 100 VOLTS

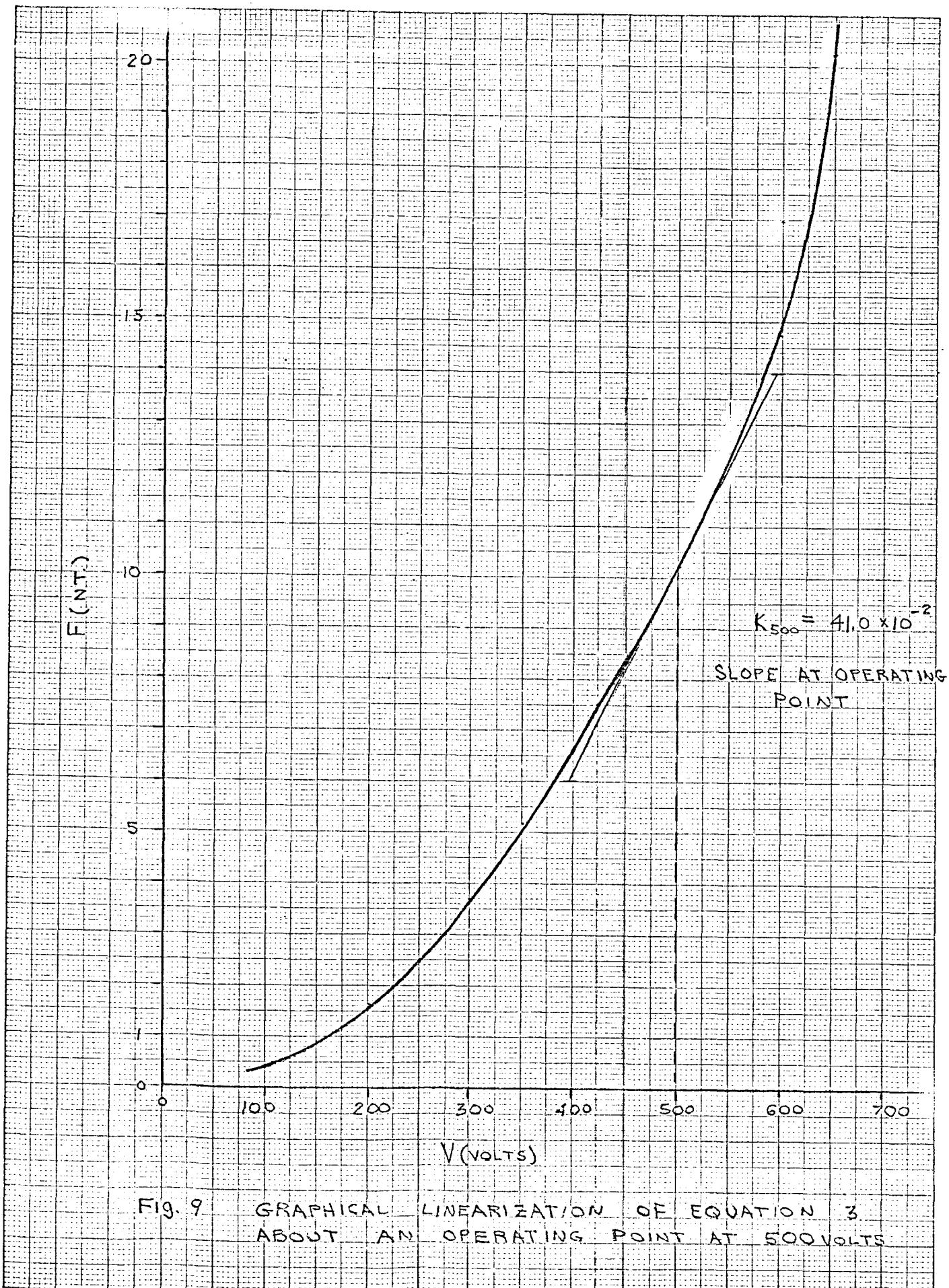

Fig. 9 GRAPHICAL LINEARIZATION OF EQUATION 3 ABOUT AN OPERATING POINT AT 500 VOLTS

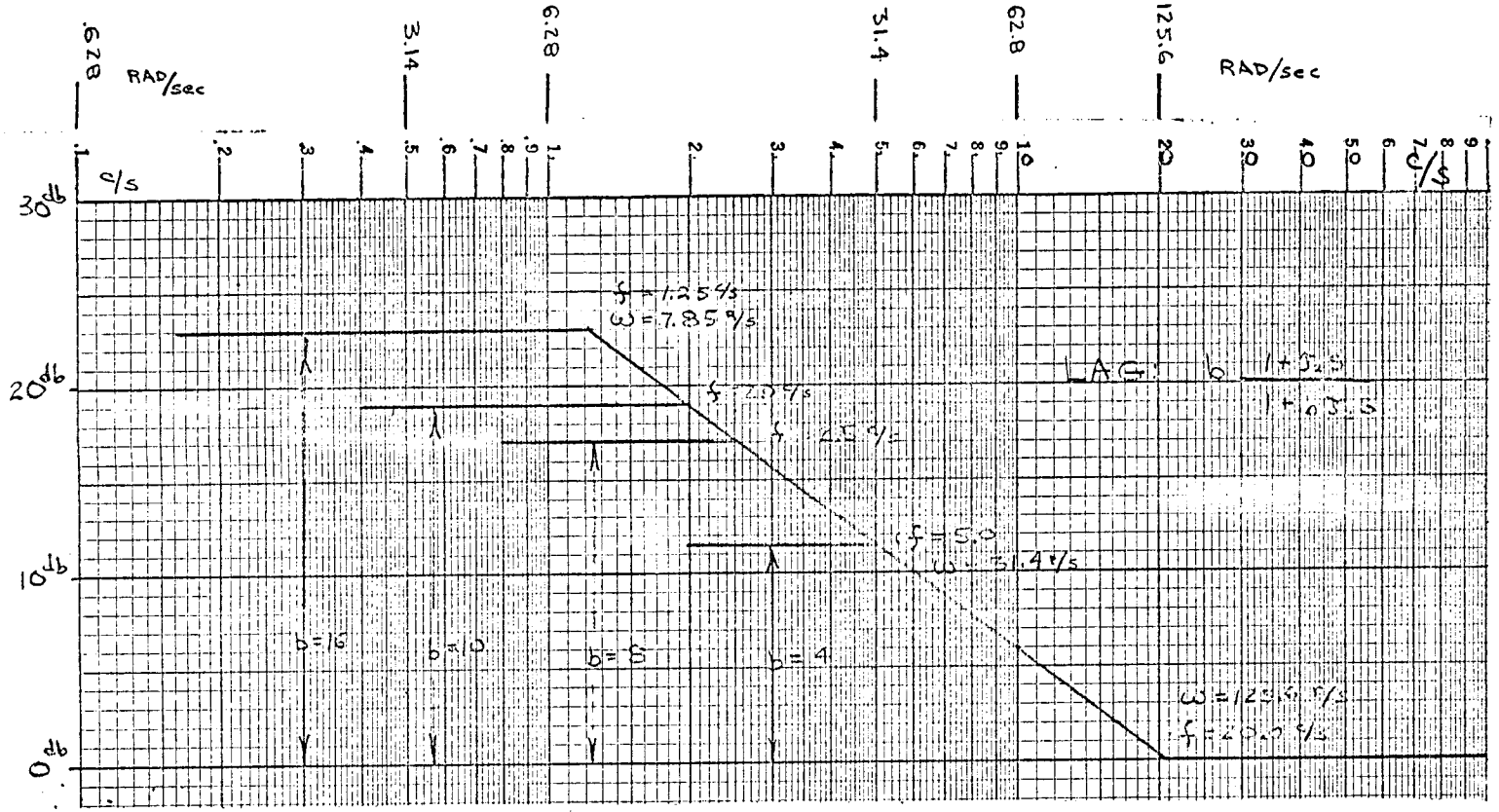

Fig. 10 AMPLITUDE RESPONSE FOR PHASE LAG ELEMENT

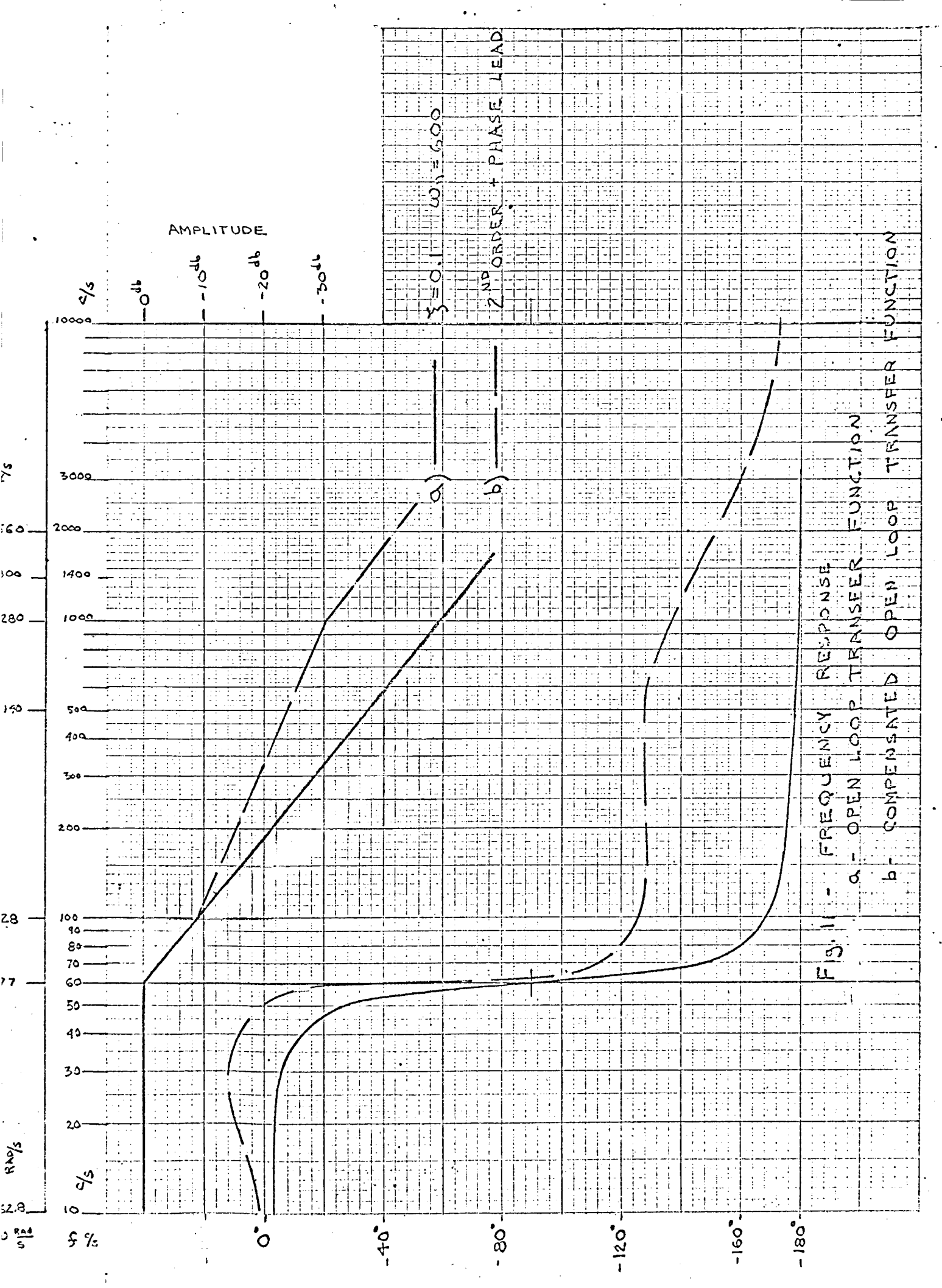

Fig. 11 - FREQUENCY RESPONSE
a - OPEN LOOP TRANSFER FUNCTION
b - COMPENSATED OPEN LOOP TRANSFER FUNCTION

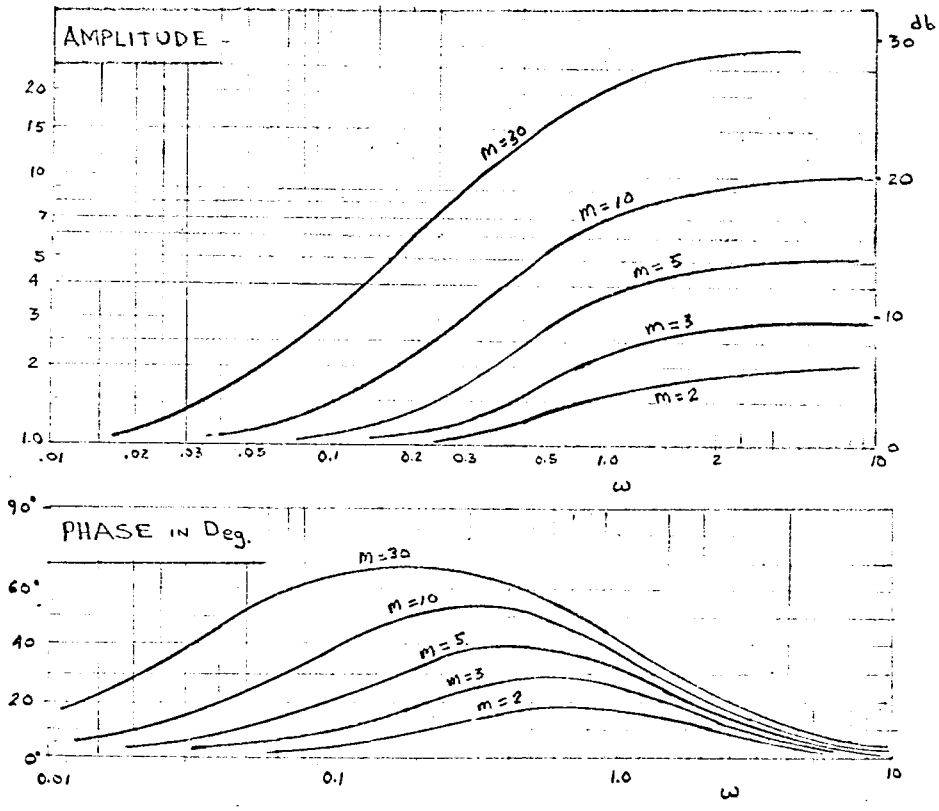

Fig 12 Amplitude and Phase Response of Phase Lead Controller

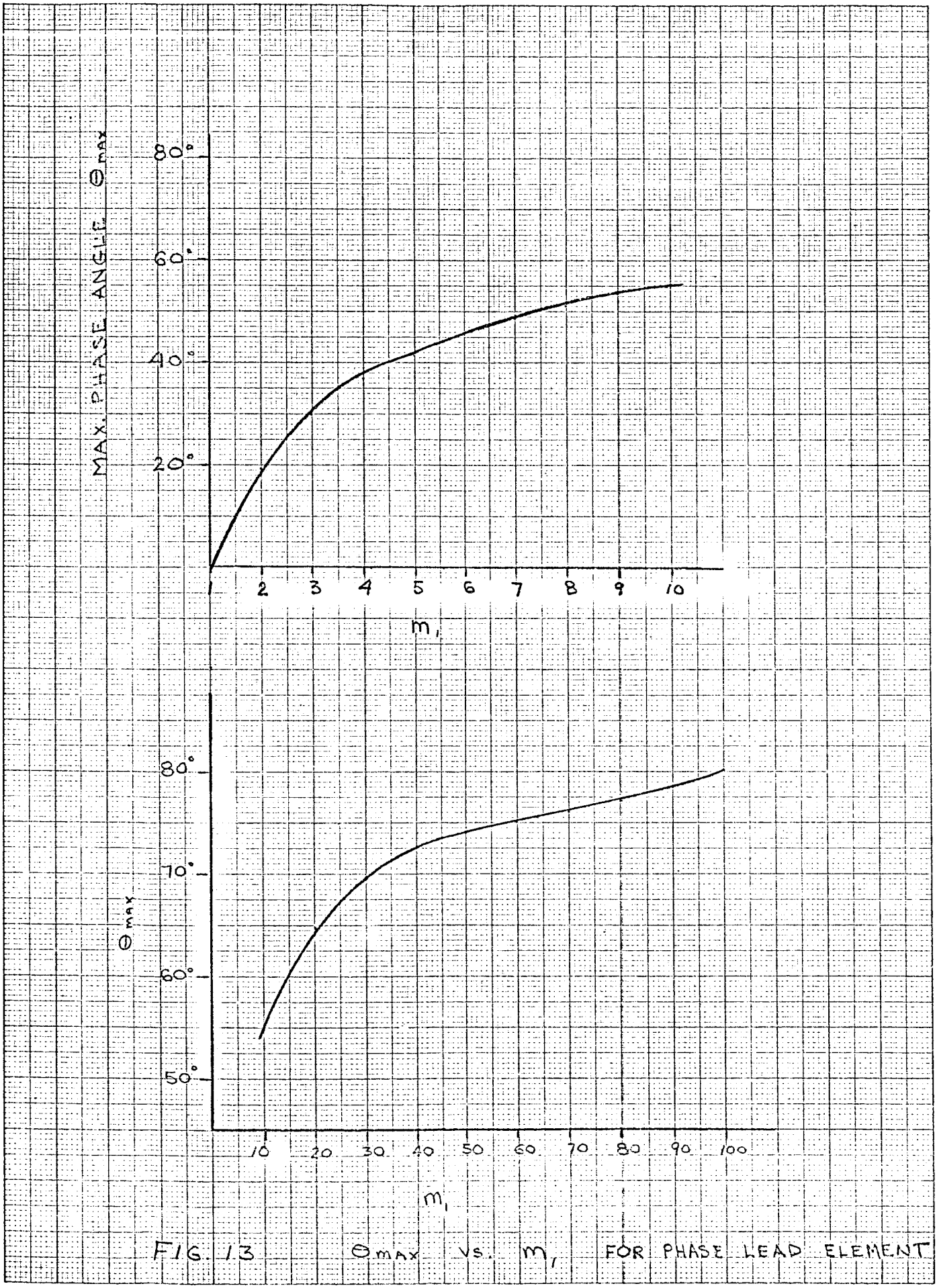

FIG. 13 θ_{MAX} VS. m_1 FOR PHASE LEAD ELEMENT

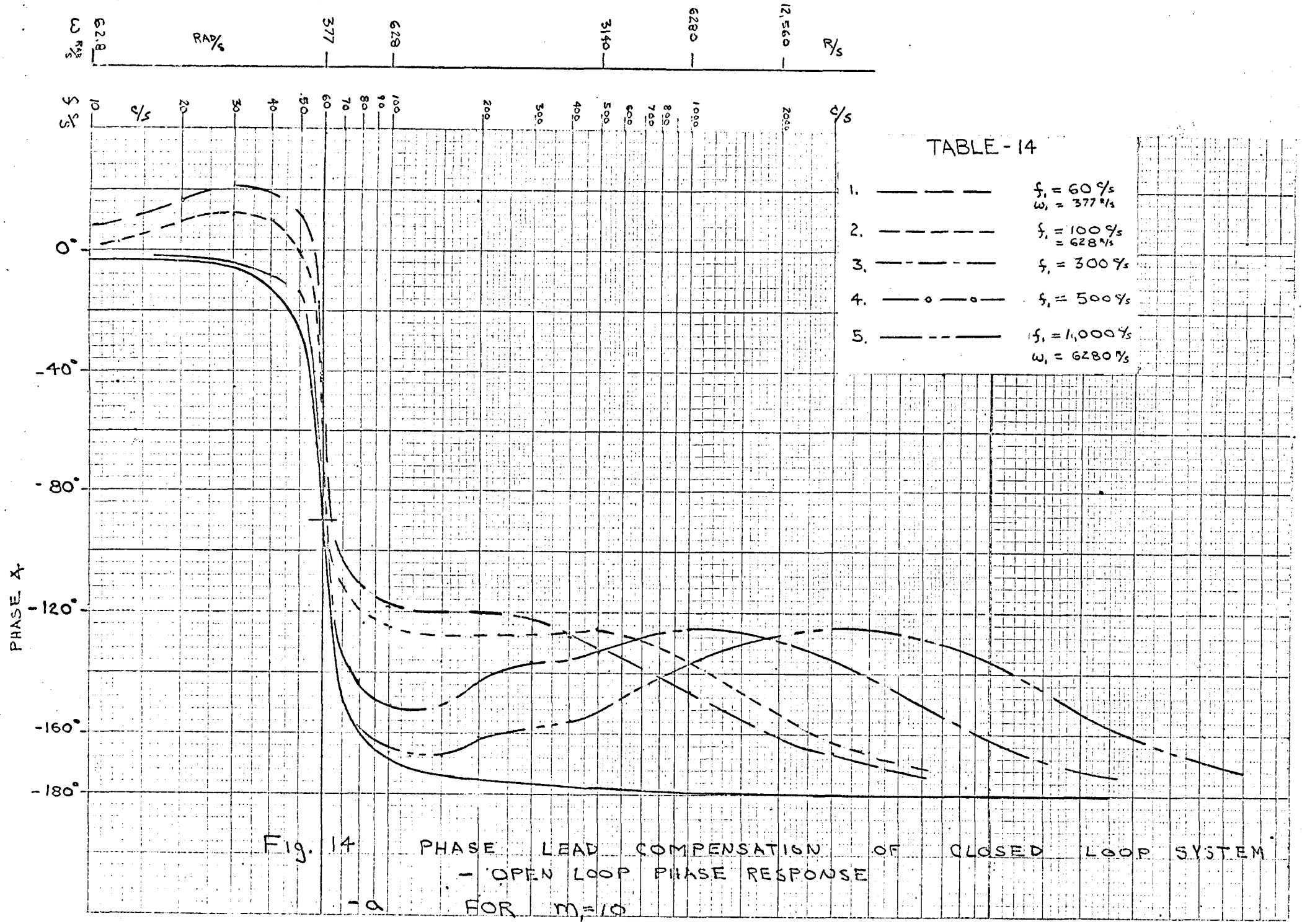

Fig. 14 PHASE LEAD COMPENSATION OF CLOSED LOOP SYSTEM - OPEN LOOP PHASE RESPONSE FOR m=10

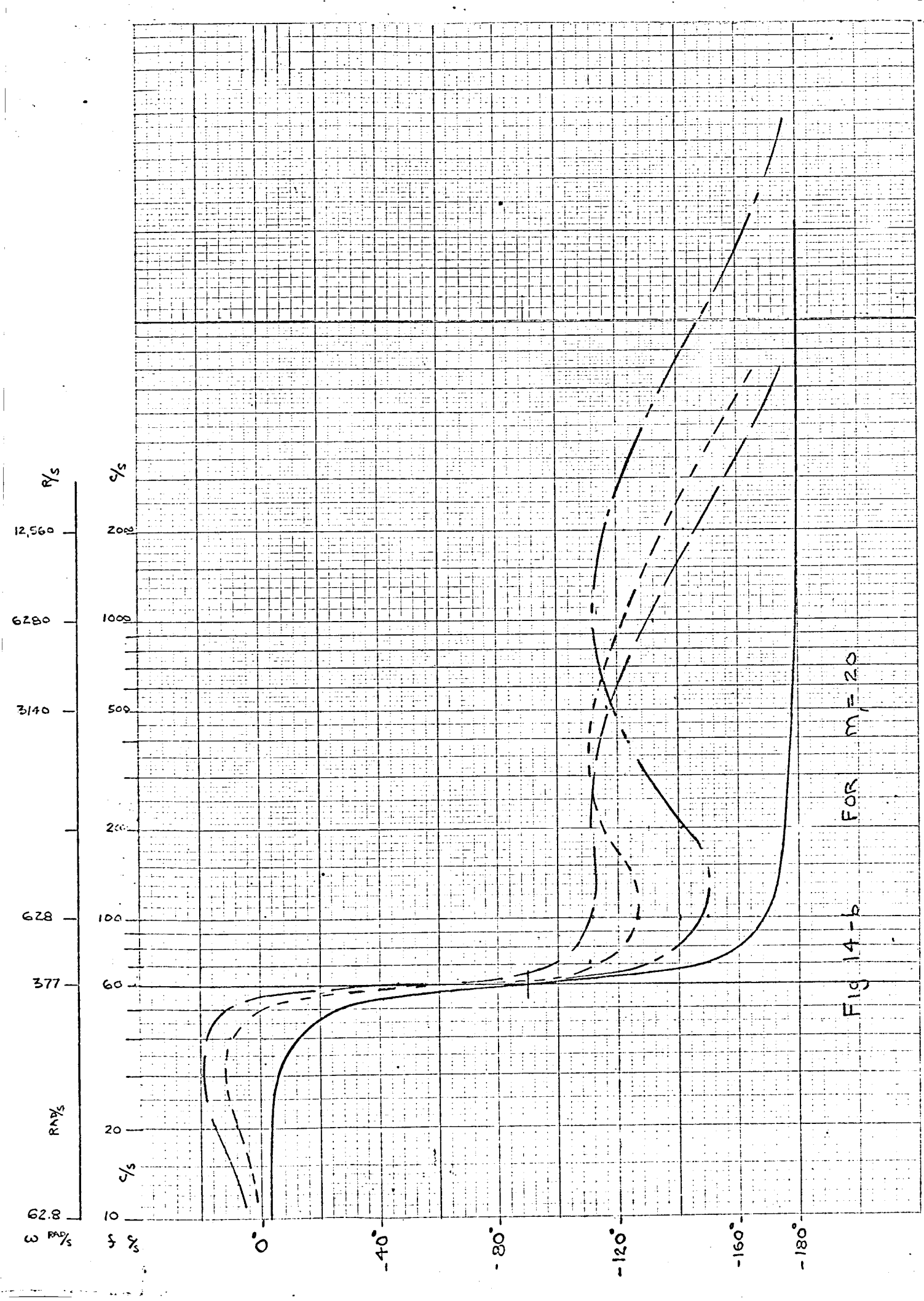

FOR M = 20

Fig 14-6

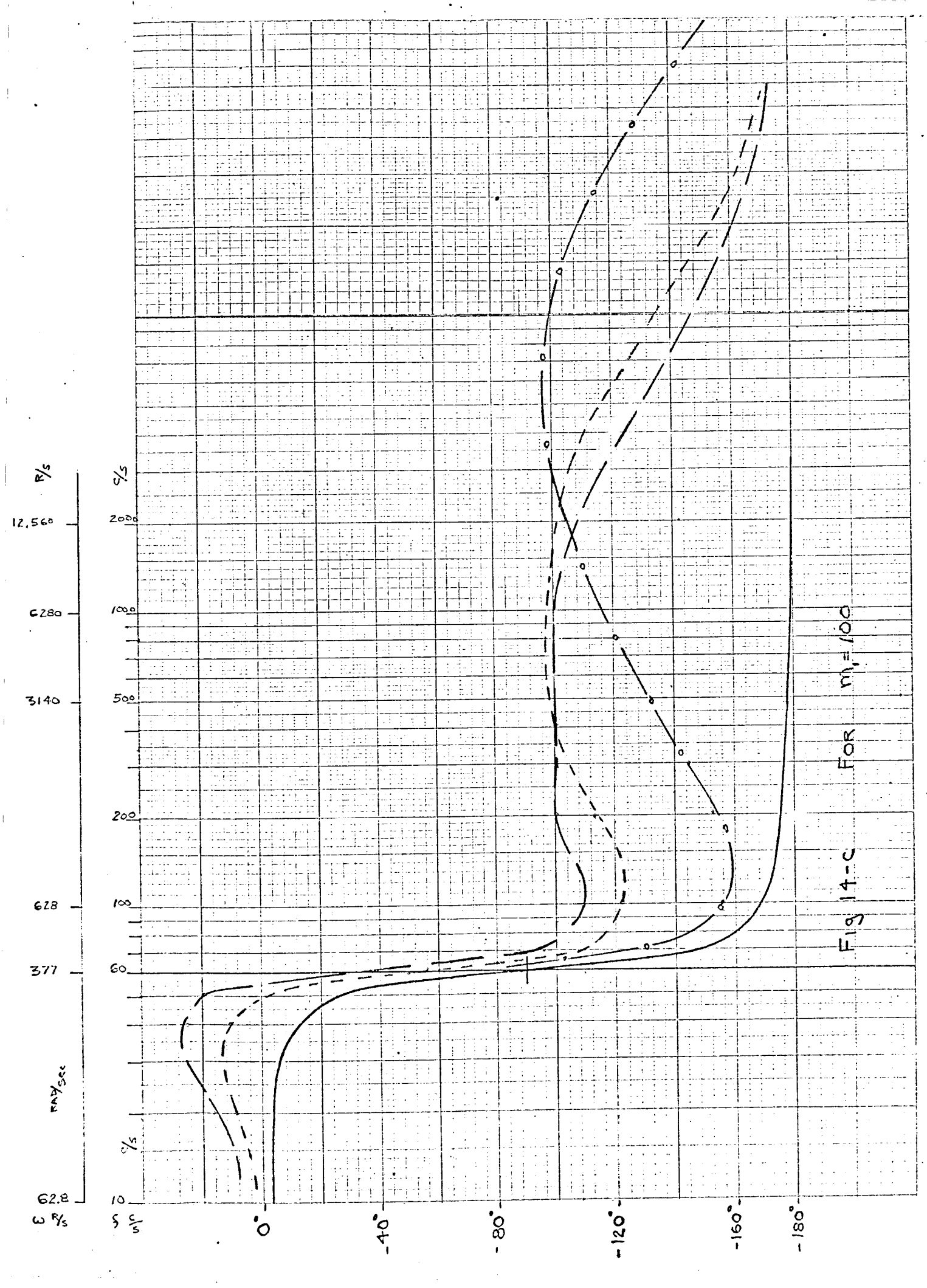
R/s
12,560
6280
3140
628
377
62.8
ω R/s
c/s
2000
1000
500
200
100
60
10
c/s
rad/sec
δ c/s
0°
-40°
-80°
-120°
-160°
-180°
For m1 = 100
Fig 14-c

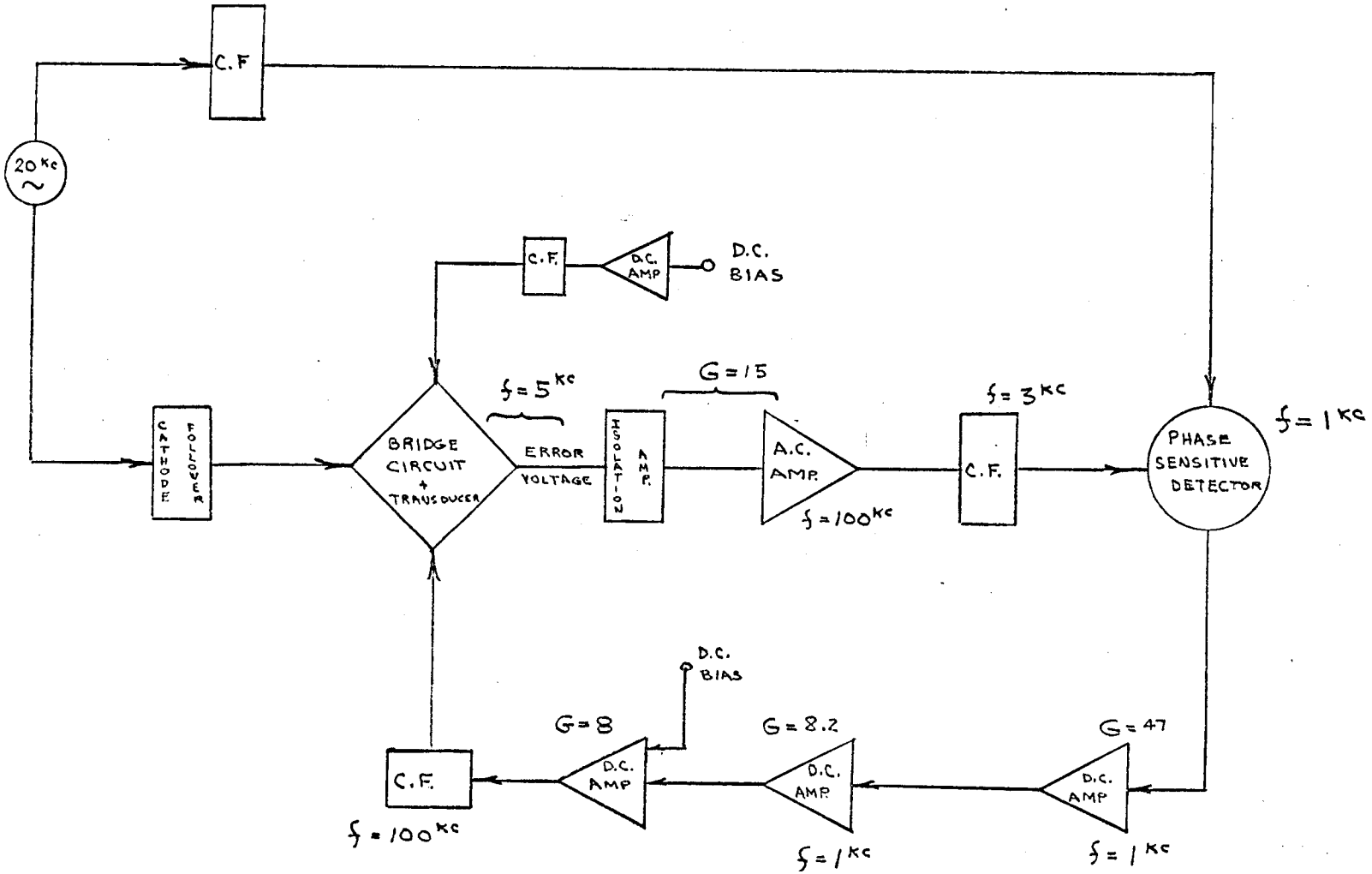

Fig. 15 BLOCK DIAGRAM OF THE EXPERIMENTAL SYSTEM

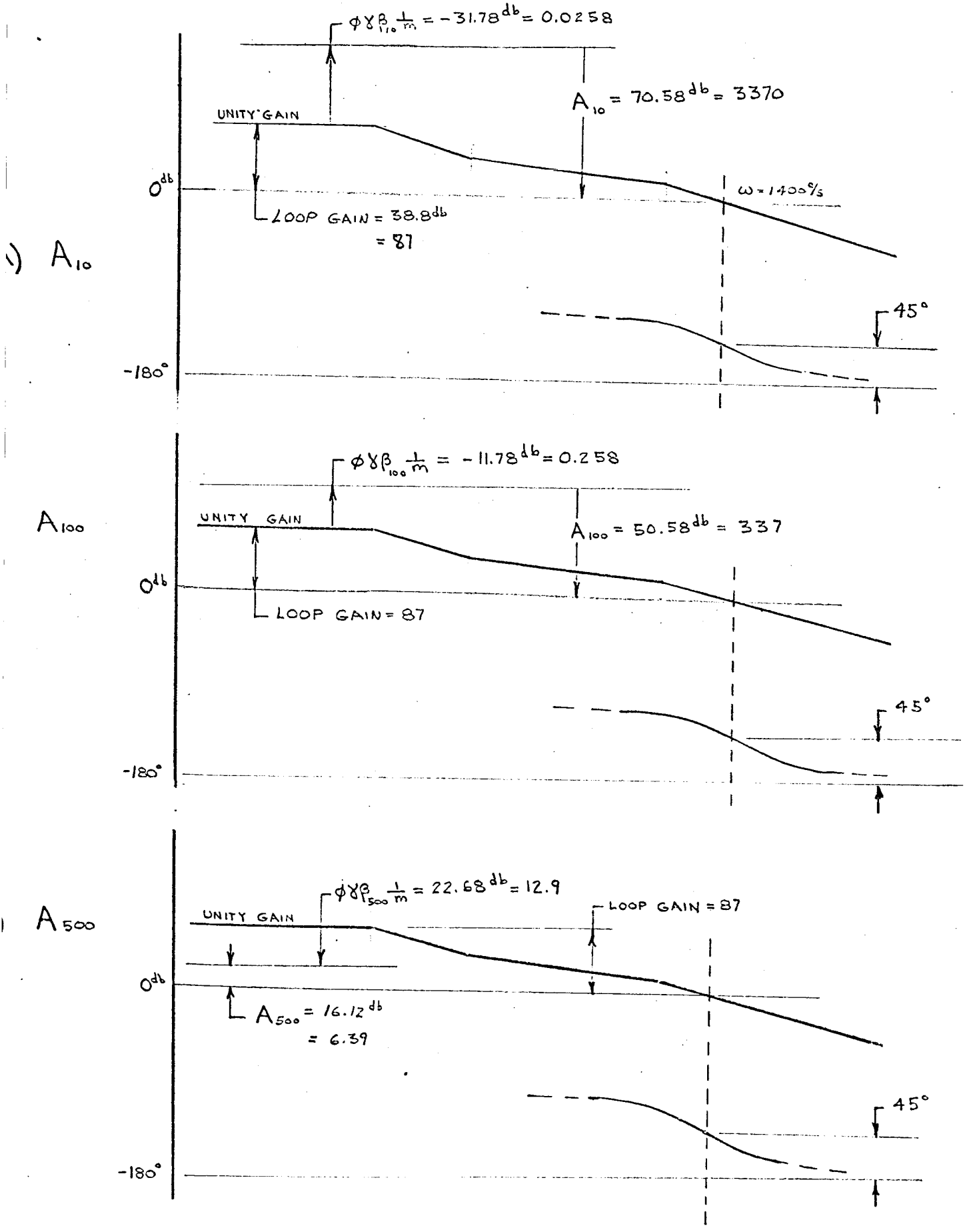

Fig 16 GRAPHICAL EVALUATION OF A_i

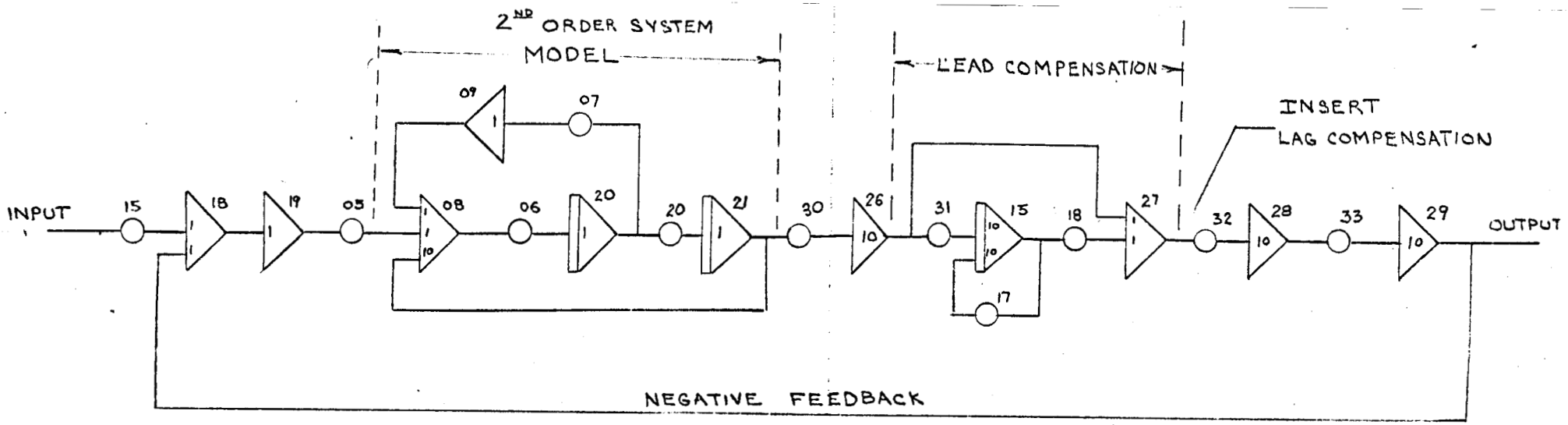

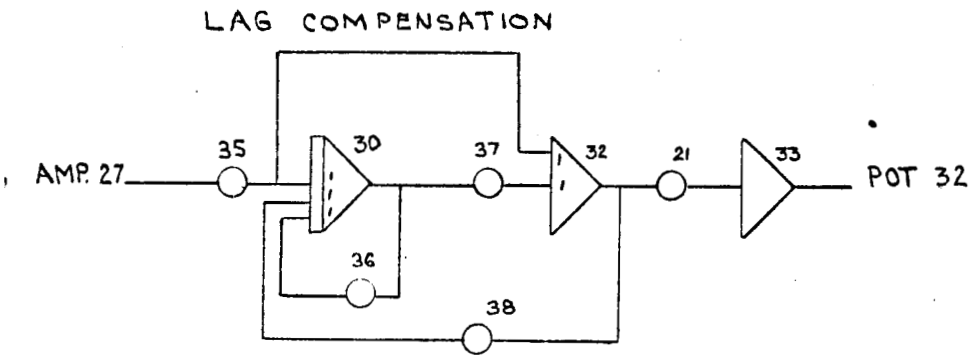

TABLE- 18

POT	SETTING
05	0.5
06	0.6
07	0.2
15	INPUT = .5
17	1.0
18	1.0
20	0.6
21	VAR. GAIN
30	1.0
31	1.0
32	0.87
33	VAR.
35	↓
36	
37	
38	

Fig. 17 ANALOG CIRCUIT FOR THE COMPENSATED CLOSED LOOP SYSTEM

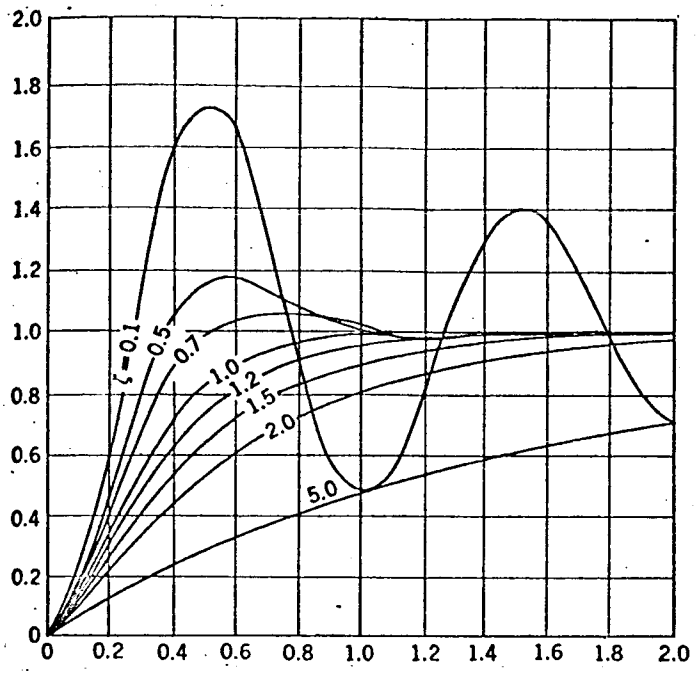

Fig 18 - STEP RESPONSE TO A 2ND ORDER SYSTEM

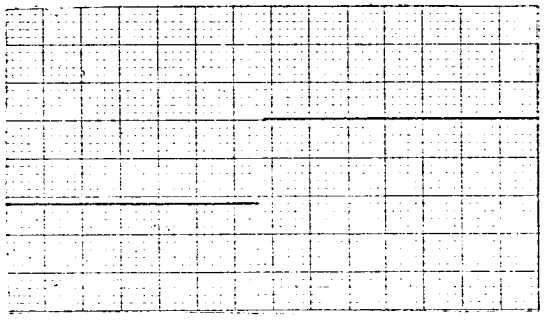

STEP INPUT

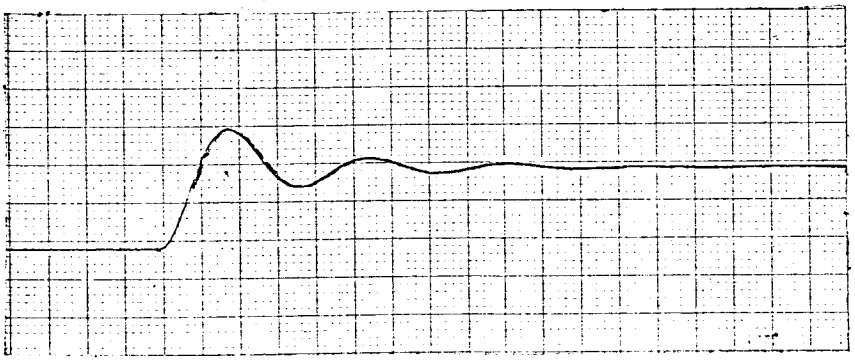

25mm/Sec

Fig 19 - TIME RESPONSE OF CLOSED LOOP SYSTEM WITH PHASE LEAD COMPENSATION FOR GAIN OF 87

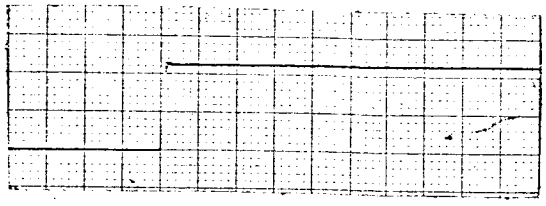

STEP INPUT

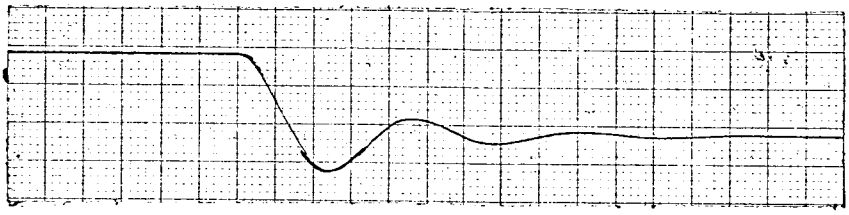

50 mm/s

a.

GAIN = 87(3/4)

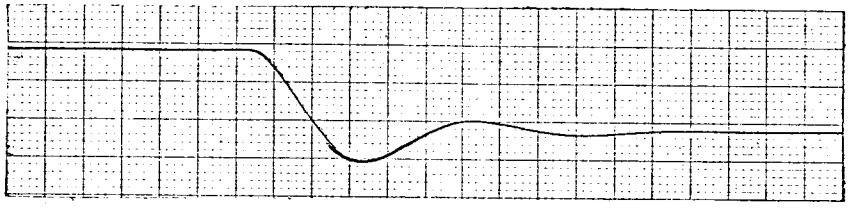

50 mm/s

b.

GAIN = 87(1/2)

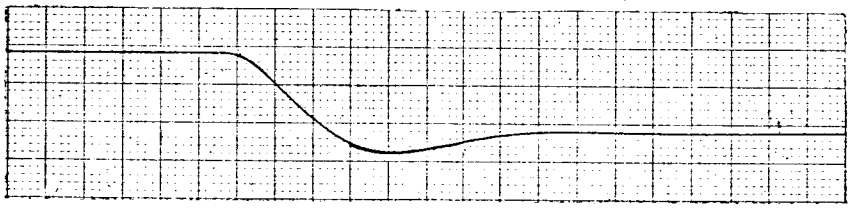

50 mm/s

c.

GAIN = 87(1/4)

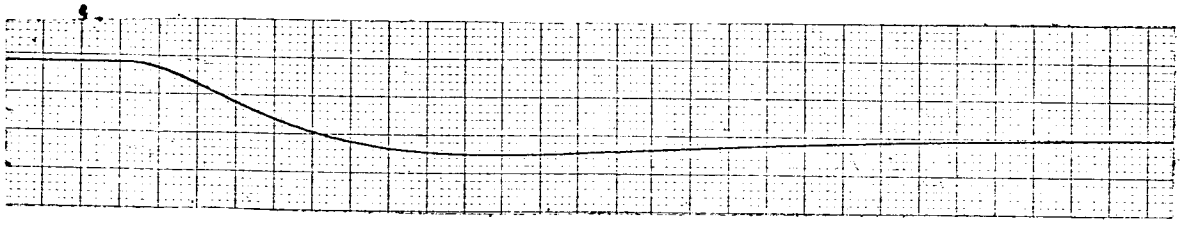

50 mm/s

d.

GAIN = 87 (1/10)

Fig. 20 TIME RESPONSE OF CLOSED LOOP SYSTEM WITH PHASE LEAD COMPENSATION FOR VARIOUS GAINS

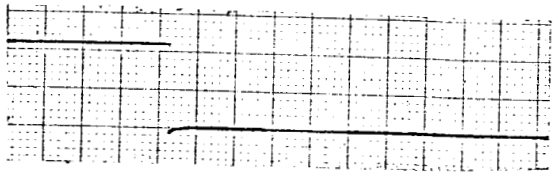

STEP
INPUT

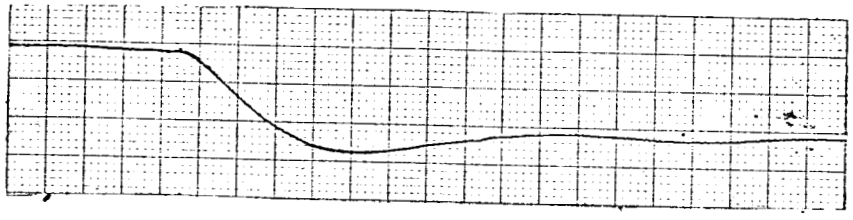

50 mm/sec

a.

GAIN = $4\left(\frac{87}{4}\right)$

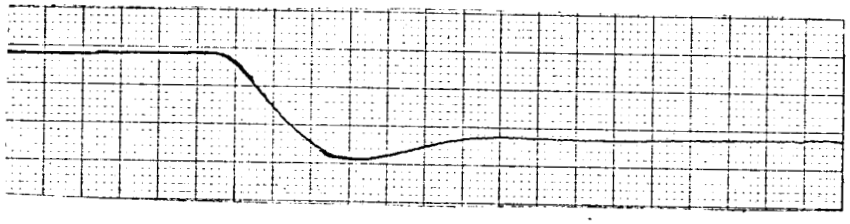

50 mm/sec

b.

GAIN = $8\left(\frac{87}{4}\right)$

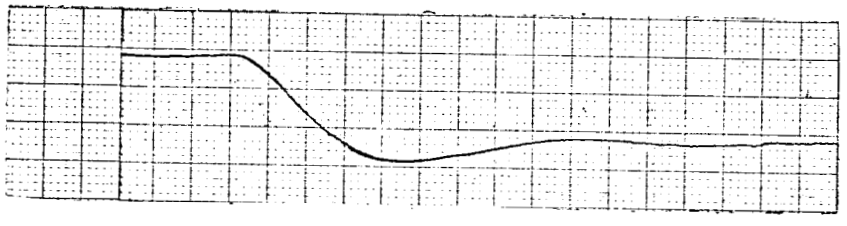

50 mm/sec

c.

GAIN = $10\left(\frac{87}{4}\right)$

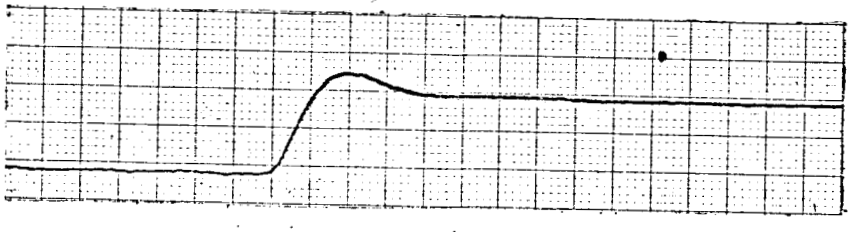

25 mm/sec

d.

GAIN = $16\left(\frac{87}{4}\right)$

Fig. 21 TIME RESPONSE OF CLOSED LOOP SYSTEM WITH LAG AND LEAD COMPENSATION FOR VARIOUS GAINS

Fig. 22 -

Y_{os} vs. ζ

For 2ND ORDER System

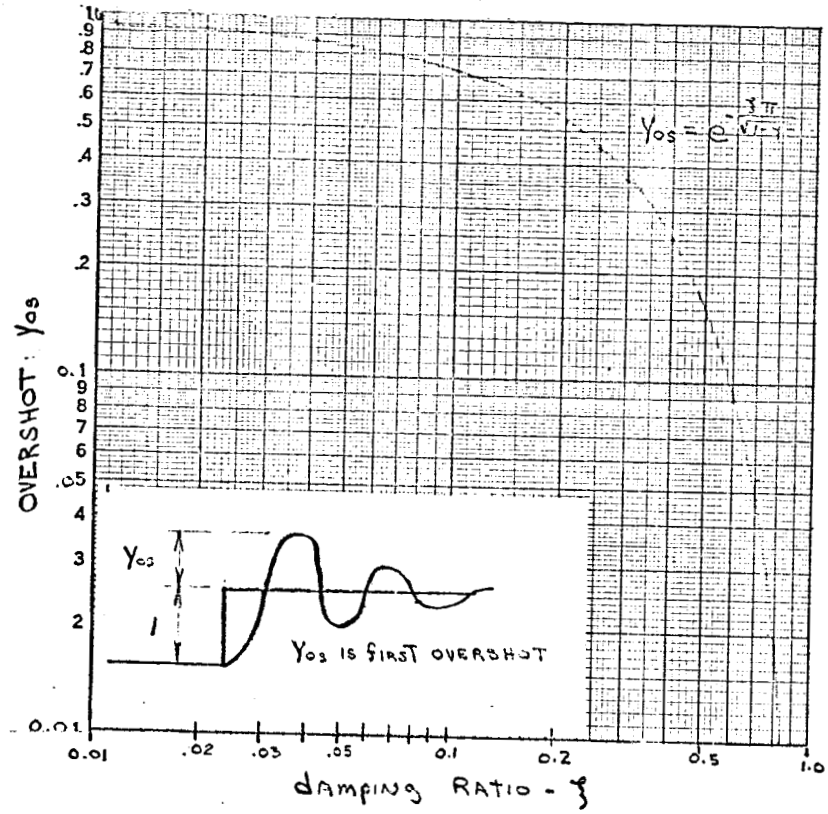

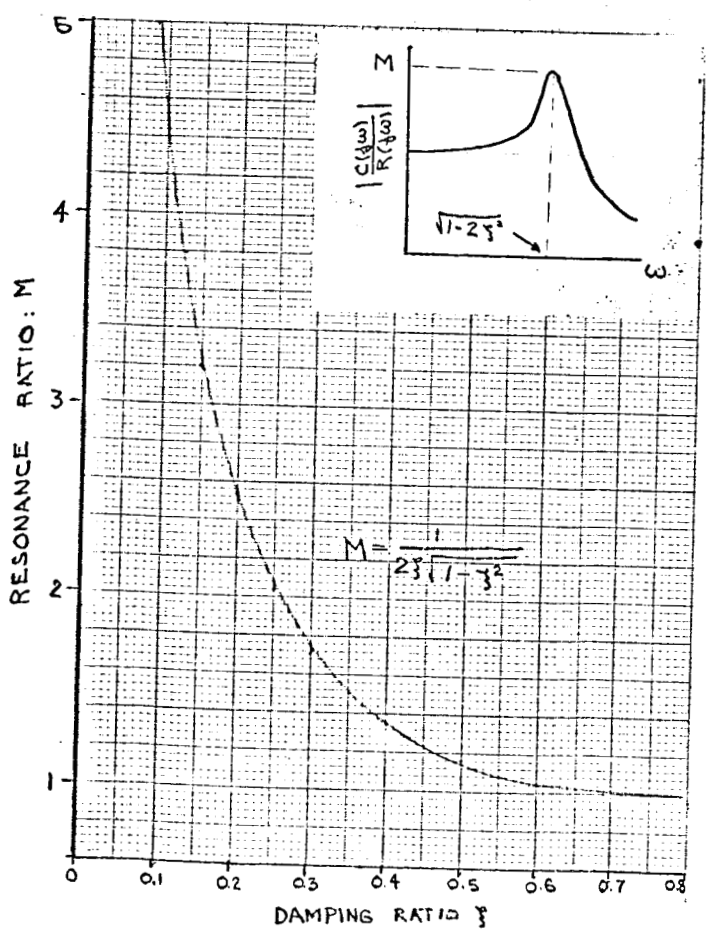

Fig. 23 M_m vs. ζ

For 2ND ORDER System

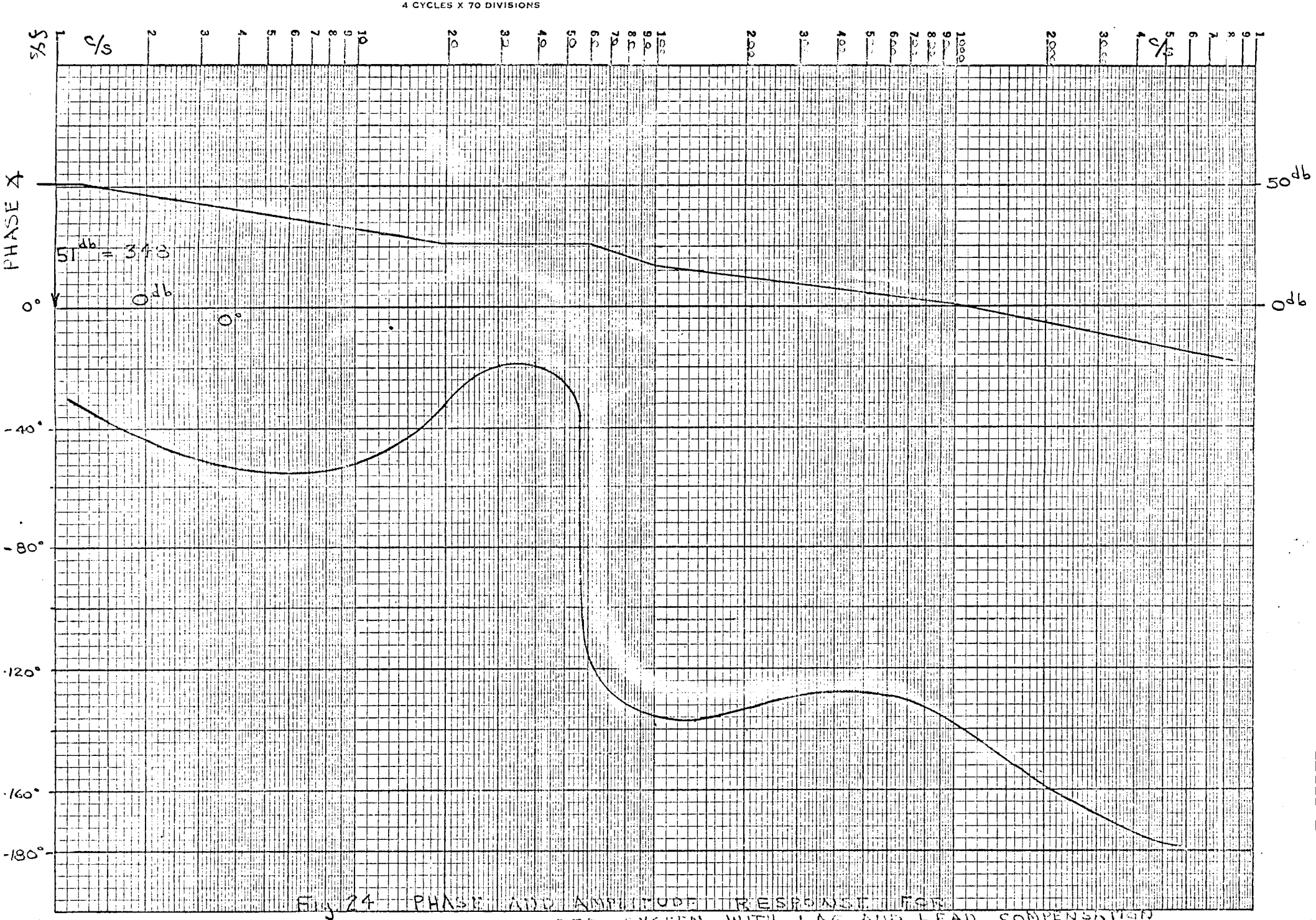

Fig 24 PHASE AND AMPLITUDE RESPONSE FOR SECOND ORDER SYSTEM WITH LAG AND LEAD COMPENSATION

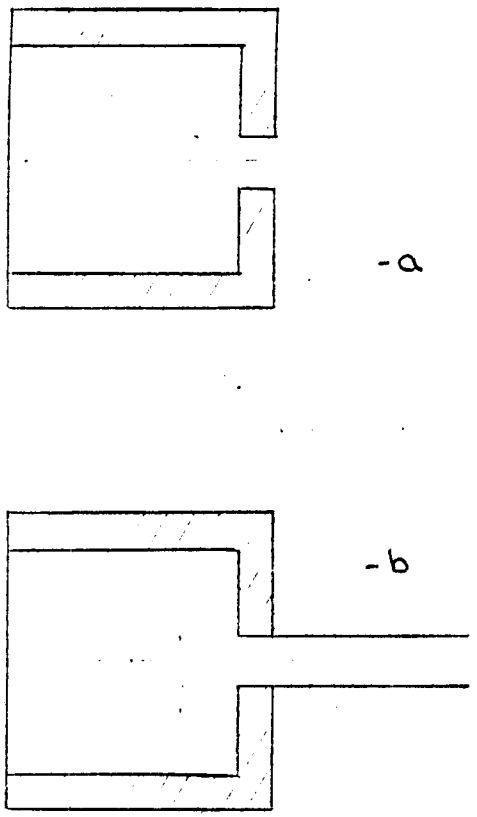

Fig. 25 ACOUSTICAL RESONATOR

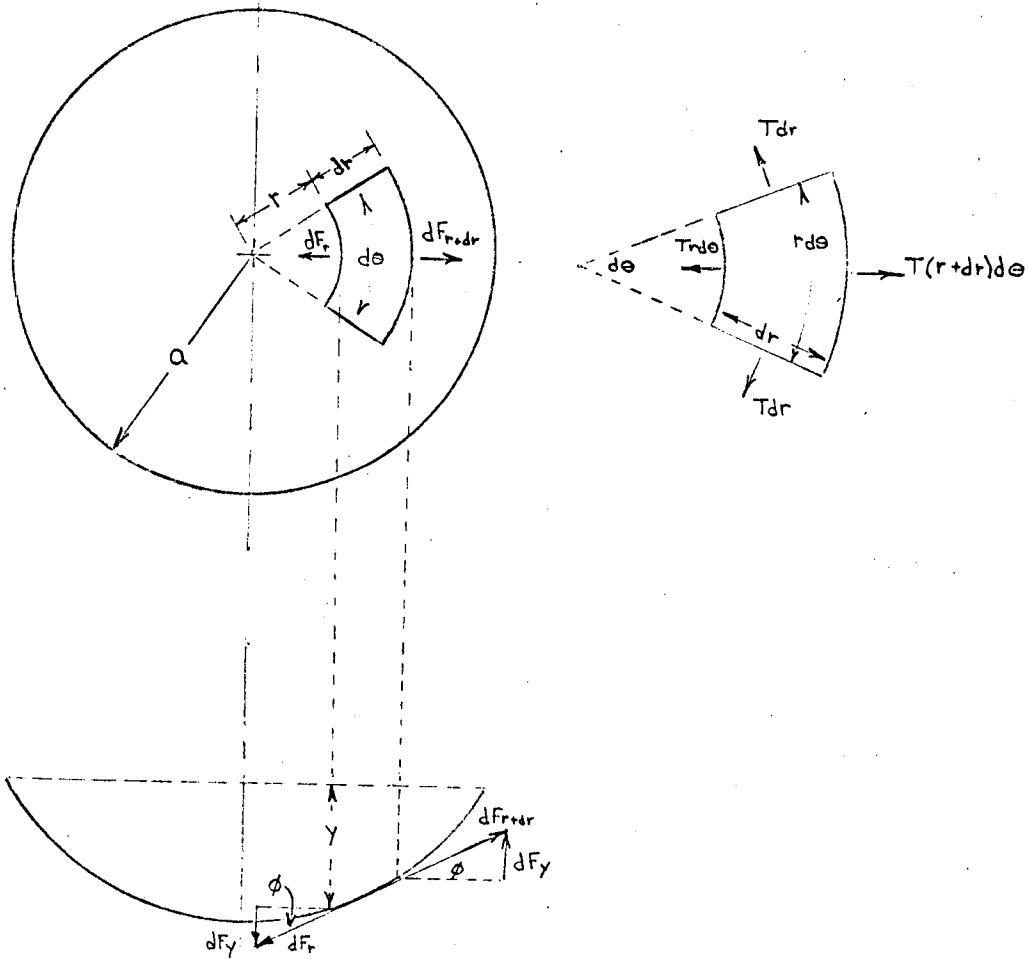

Fig. 26 FORCES ACTING ON AN ELEMENTAL AREA OF A CLAMPED CIRCULAR MEMBRANE IN A DEFLECTED STATE

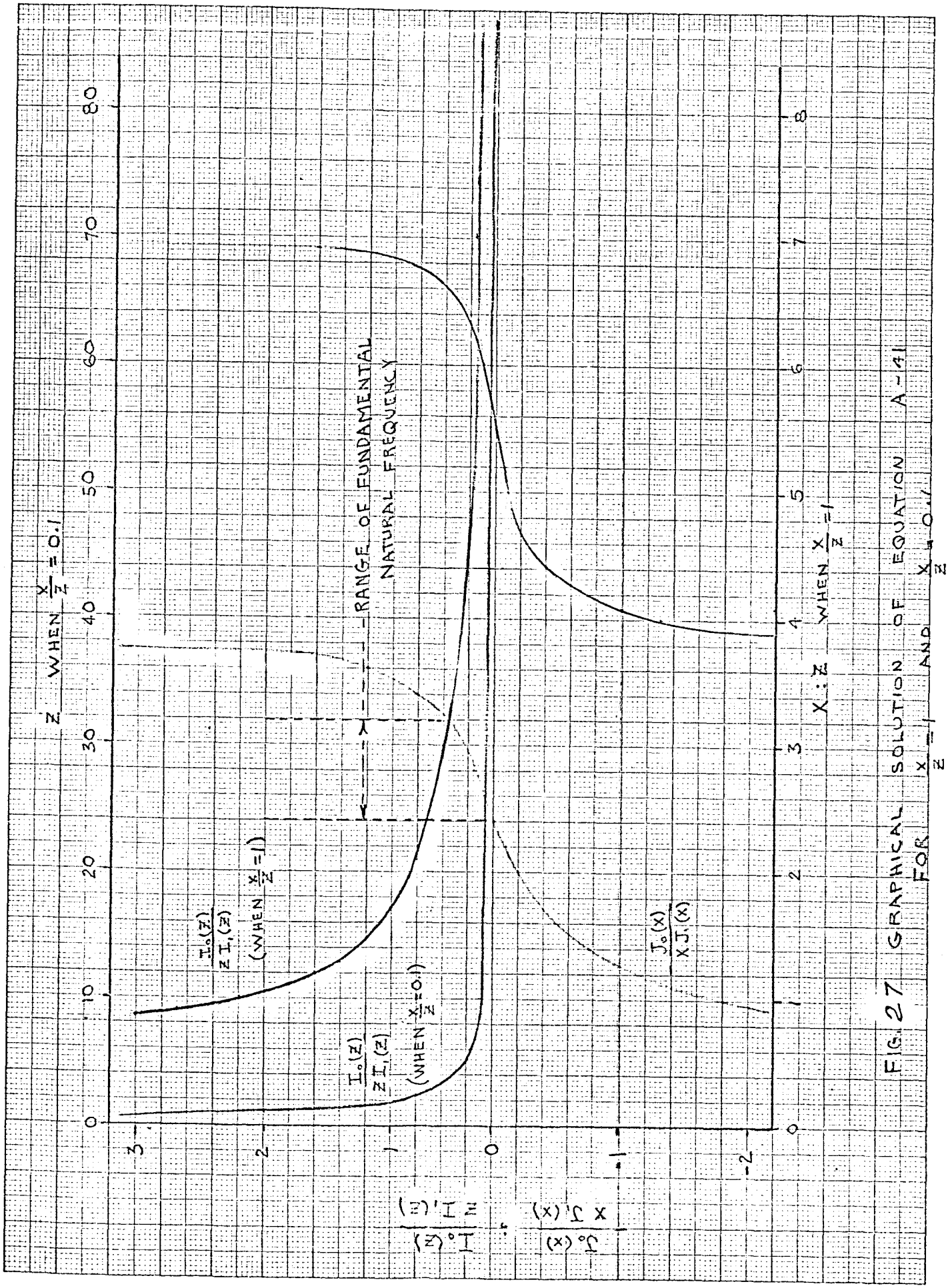

FIG. 27 GRAPHICAL SOLUTION OF EQUATION A-141 FOR $\frac{x}{z}=1$ AND $\frac{x}{z}=0.1$

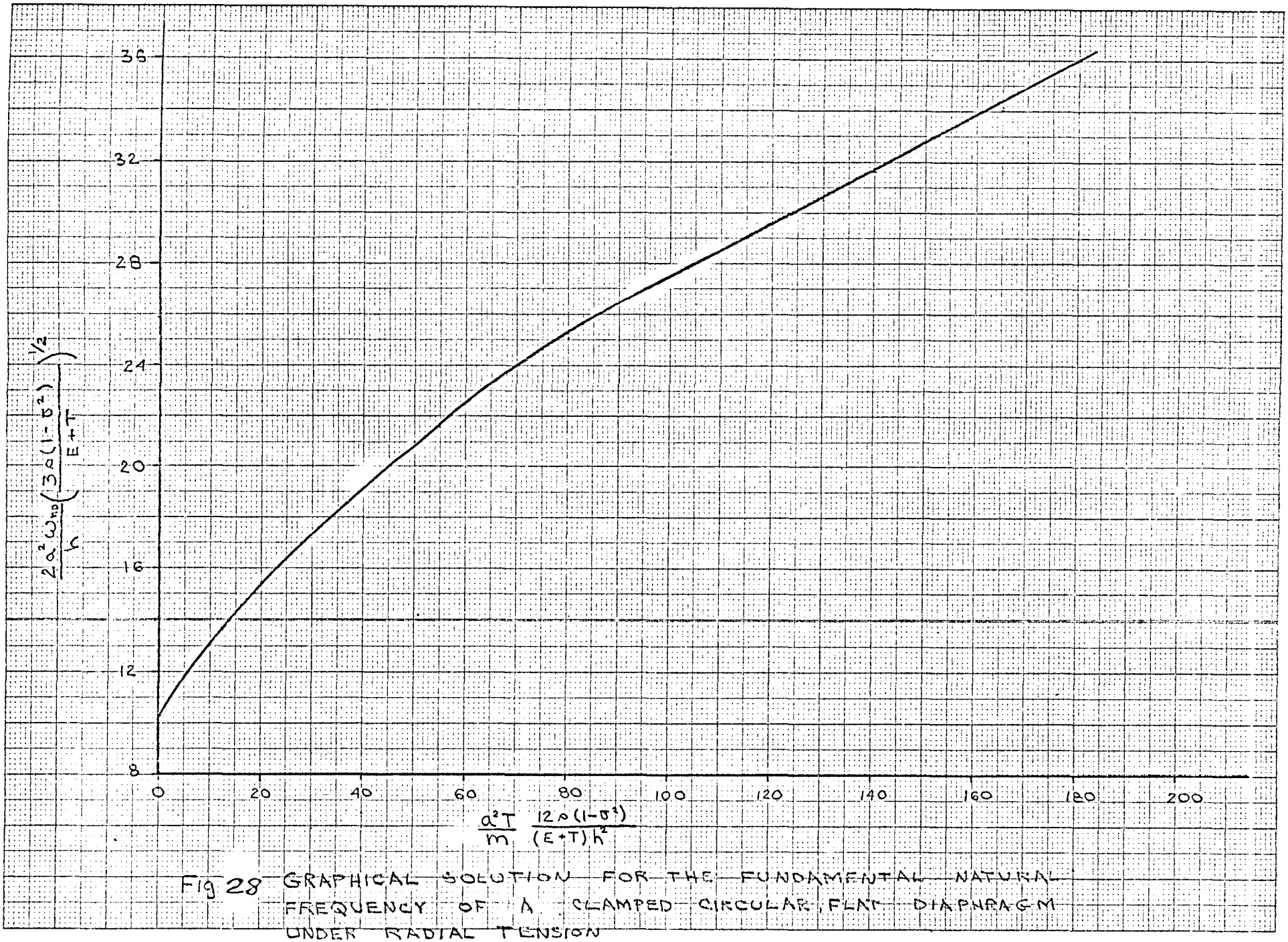

Fig 28 GRAPHICAL SOLUTION FOR THE FUNDAMENTAL NATURAL FREQUENCY OF A CLAMPED CIRCULAR FLAT DIAPHRAGM UNDER RADIAL TENSION

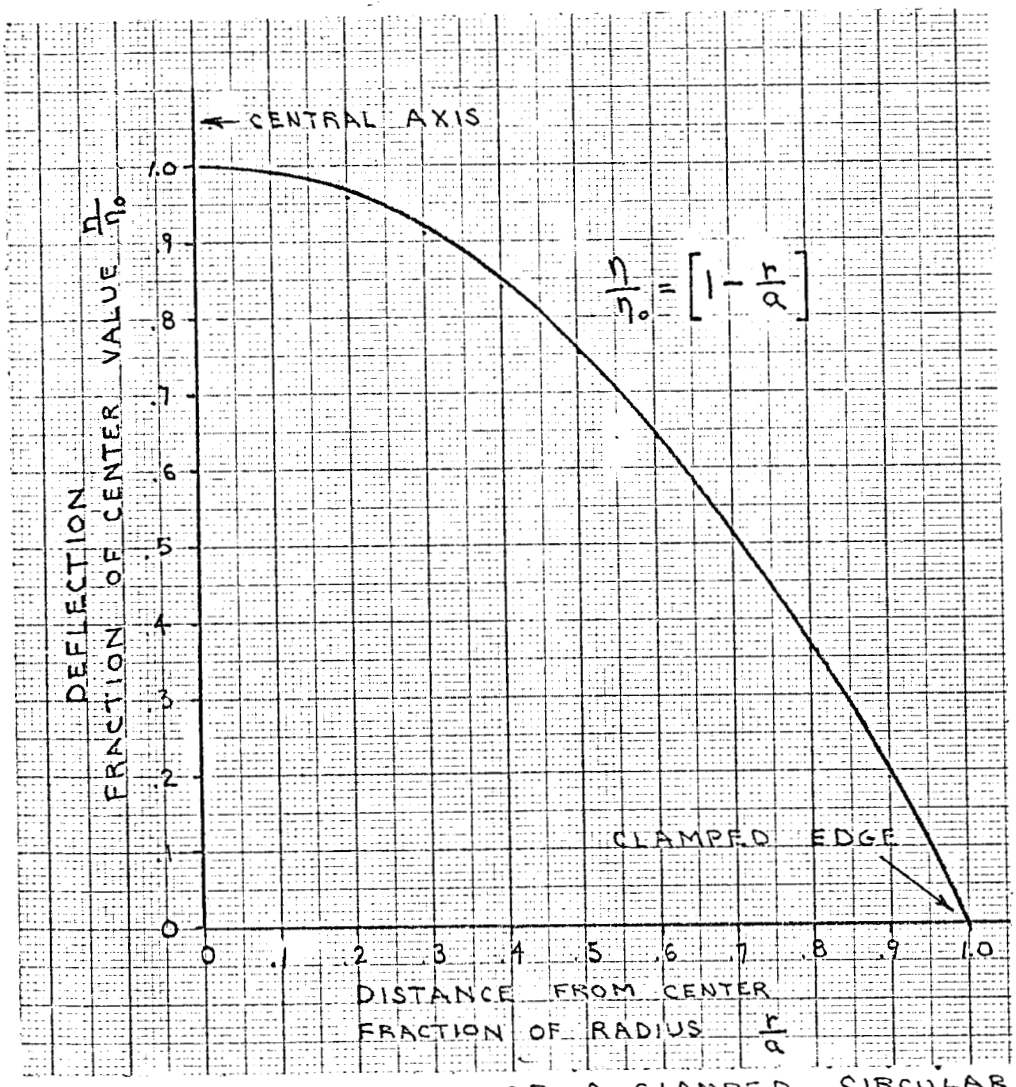

Fig. 29 DEFLECTION OF A CLAMPED CIRCULAR MEMBRANE VS. RADIAL DISTANCE FROM CENTER

a -

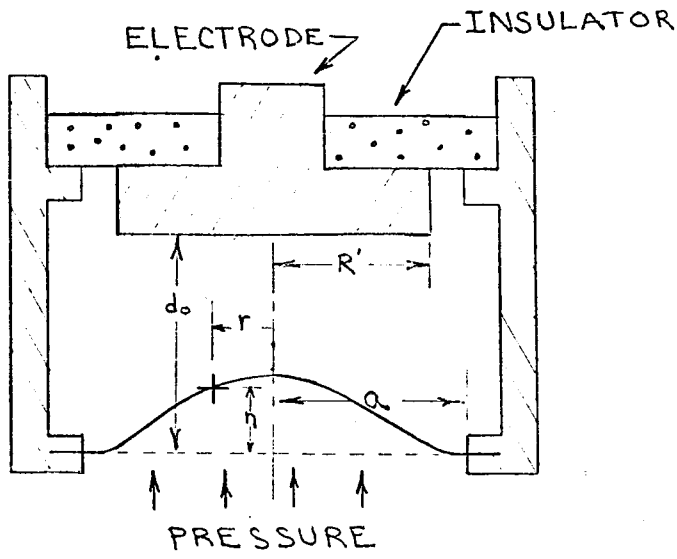

b -

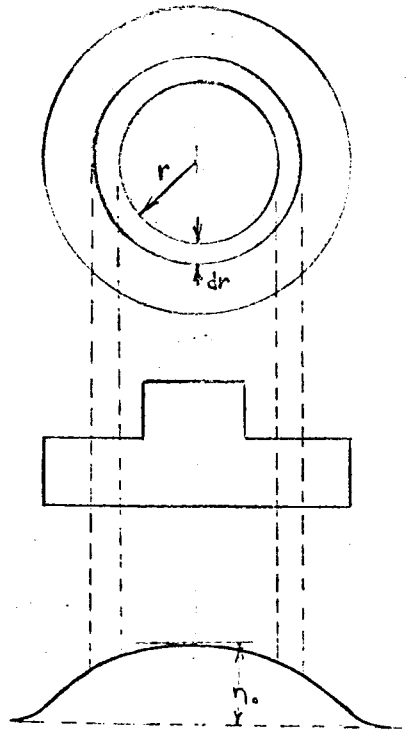

TOP VIEW

FRONT VIEW

Fig 30 CROSS SECTION OF A VARIABLE CAPACITOR

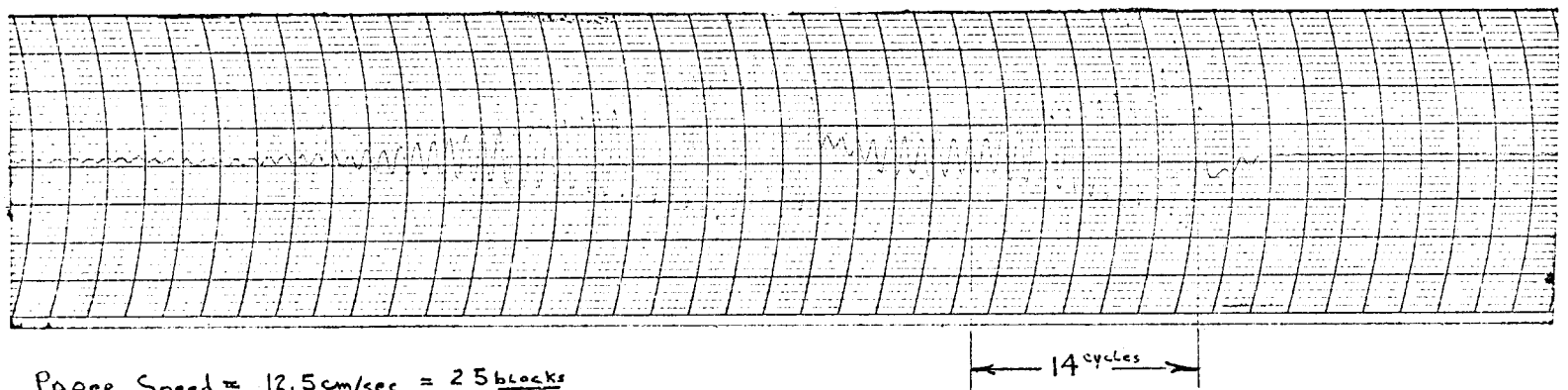

Paper Speed = 12.5 cm/sec = 2 5 $\frac{\text{blocks}}{\text{sec}}$

$$f_{nD} = \frac{14 \text{ cycles}}{6 \text{ blocks}} \times \frac{25 \text{ blocks}}{\text{sec}} = 58 \text{ c/s} \simeq 60 \text{ c/s}$$

$$\omega_{nD} = 2\pi f_{nD} = 377 \text{ RAD/sec}$$

Fig. 31 - NATURAL FREQUENCY OF THE DIAPHRAGM EXPERIMENTALLY DETERMINED UNDER VACUUM CONDITIONS

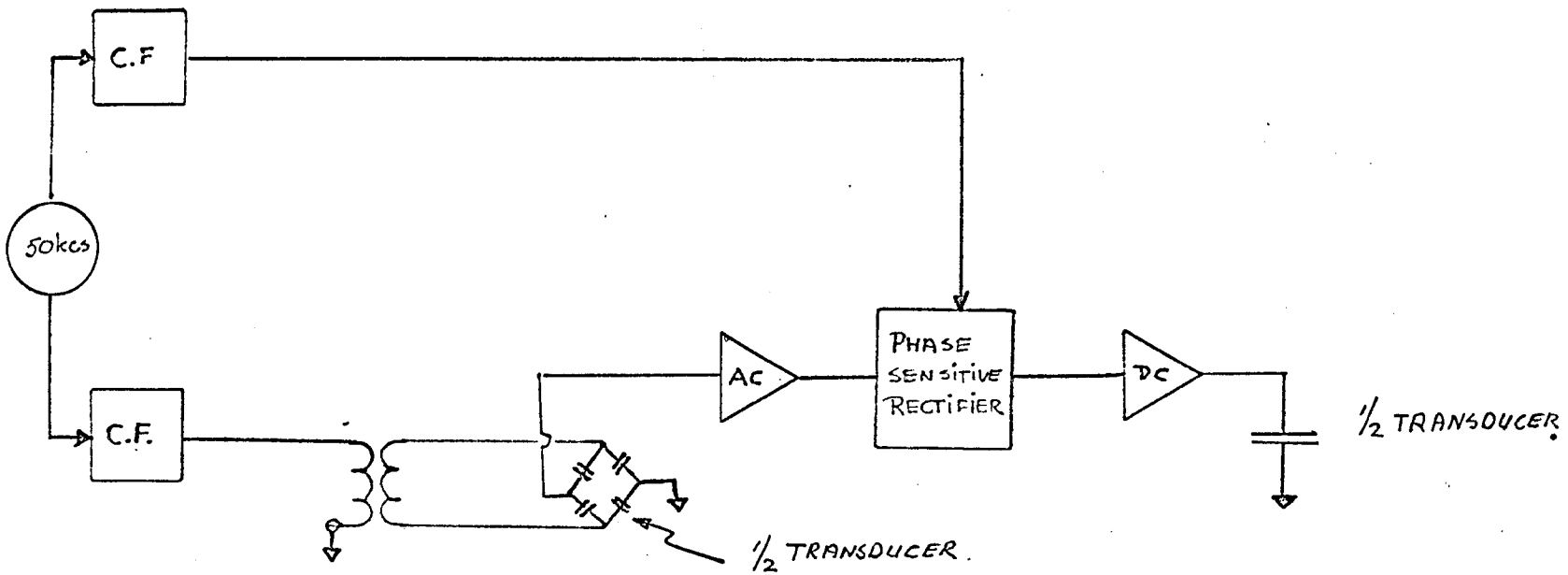

FIG 32 SCHEMATIC DIAGRAM OF EXPERIMENTAL SYSTEM

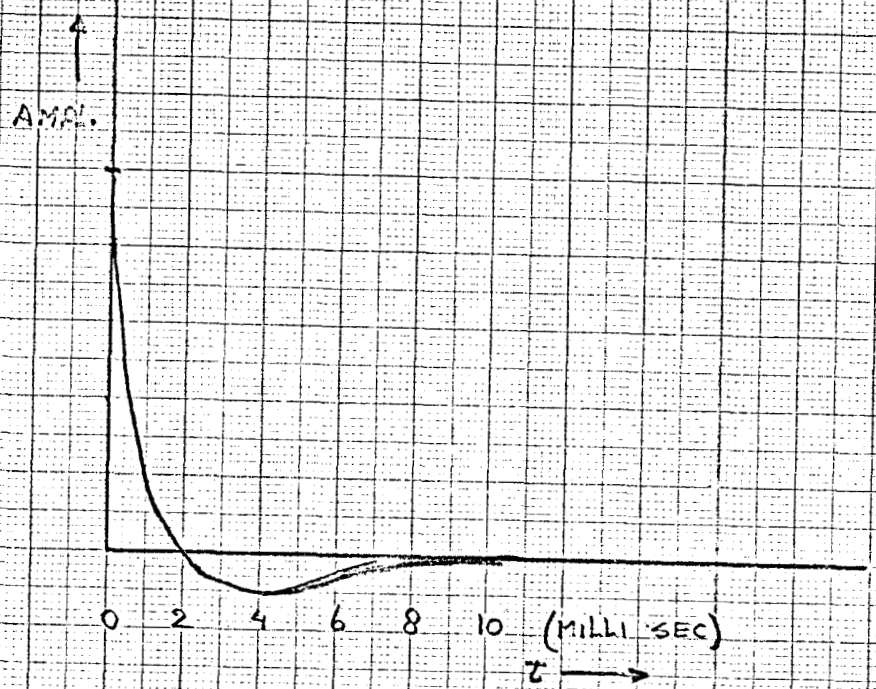

Fig 33 Typical STEP RESPONSE of closed loop system (this case G=10)

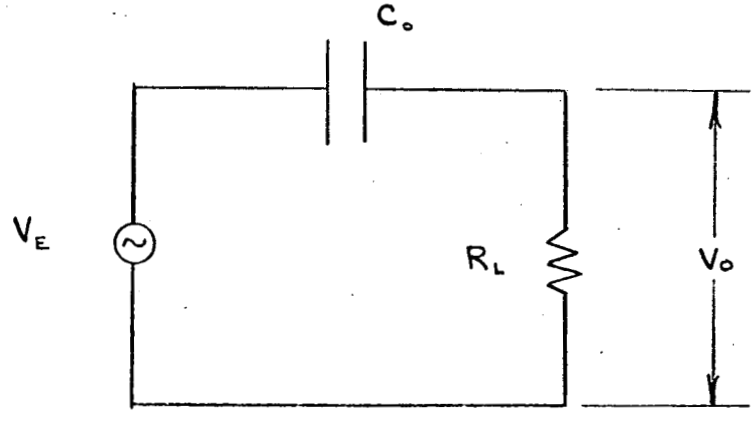

Fig. 34 THÉVENIN CIRCUIT

TABLE 1

V_i	K_i	$\phi \gamma \beta_i \frac{1}{m}$	A_i	LOOP GAIN
10	8.2×10^{-4}	0.0258	3370.	87
100	8.2×10^{-3}	0.258	337.	87
500	41×10^{-2}	12.9	6.4	87

TABLE 2.

TABULATED VALUES OF THE GRAPHICAL SOLUTION FOR THE FUNDAMENTAL UNDAMPED NATURAL FREQUENCY OF ANY CIRCULAR, CLAMPED, FLAT DIAPHRAGM UNDER RADIAL TENSION

x/z	x	z	$\frac{xz}{2a^2\omega_n\sqrt{3\rho(1-\sigma^2)}/h\sqrt{E+T}}$	$\frac{z^2-x^2}{12a^2T(1-\sigma^2)/mh^2(E+T)}$
[a]1.0	3.1962	3.1962	10.22	0
.95	3.170	3.337	10.58	1.086
.9	3.143	3.492	10.98	2.317
.85	3.114	3.664	11.41	3.725
.8	3.083	3.854	11.88	5.347
.75	3.051	4.068	12.41	7.240
.7	3.018	4.311	13.01	9.480
.65	2.983	4.589	13.69	12.16
.6	2.947	4.912	14.48	15.44
.55	2.909	5.281	15.36	19.43
.5	2.869	5.738	16.46	24.69
.45	2.828	6.284	17.77	31.50
.4	2.786	6.965	19.40	40.75
.35	2.742	7.834	21.48	53.86
.3	2.696	8.987	24.23	73.49
.25	2.649	10.60	28.07	105.3
.2	2.602	13.01	33.85	162.5
.15	2.553	17.02	43.45	283.2
.1	2.505	25.05	62.75	621.2
.075	2.480	33.07	82.01	1087.3
.05	2.455	49.10	120.5	2405
.025	2.430	97.20	236.2	9442
[b]0	2.4048	∞	∞	∞

[a]Plate without tension

[b]Infinitely thin membrane

SENSING ELEMENT	SENSITIVITY TO PRESSURE "S"	SENSITIVITY TO A CONSTANT ACCELERATING FORCE	$\frac{\text{SIGNAL}}{\text{NOISE}} = \frac{\left(\frac{\Delta d}{d_o}\right)_{\text{Pressure}}}{\left(\frac{\Delta d}{d_o}\right)_{\text{ACCELERATION}}}$	FREQUENCY RESPONSE "ω"	LINEARITY	OTHERS
① THIN PLATE $S = \frac{12(1-\sigma^2)}{E h^3}\left[\frac{r^4+a^4}{64} - \frac{a^2 r^2}{32}\right]$ $\omega = \frac{(3.2)^2 h}{a^2}\sqrt{\frac{E}{12\rho(1-\sigma^2)}}$	LOW (E is Large)	LOW		HIGH	GOOD (SMALL DEFLECTIONS)	DEPENDENCE ON MECHANICAL PROPERTIES
② WEAKLY STRESSED MEMBRANE $S = \frac{a^2}{4T}\left[1-\left(\frac{r}{a}\right)^2\right]$ $\omega = \frac{2.405}{a}\sqrt{\frac{T}{m}}$	INCREASED	NO CHANGE $m <$ $k <$		DECREASED – LOW –	DECREASED (LARGER DEFLECTIONS)	
③ MECHANICALLY HIGHLY STRESSED MEMBRANE $T \to \infty$ ASSUME: STIFFNESS OF ③ = STIFFNESS OF ①	DECREASED – SAME AS ①	DECREASED – LESS THAN ① Because $m \to 0$	INCREASED	INCREASED	INCREASED	NEED TO MONITOR OTHER PARAMETERS i.e. TEMP.
④ ELECTRICALLY STRESSED MEMBRANE ASSUME: $T_{ELECT.} = T_{MECH.}$ NOTE: CLOSED LOOP	SAME AS ②	SAME AS ③	SAME AS ② AND ③	SAME AS ②	INCREASED NOT f(MECH. PROP.)	NOT A FUNCTION OF MECHANICAL PROPERTIES

TABLE-3 COMPARISON OF SENSING ELEMENTS FOR OPEN LOOP CAPACITIVE PRESSURE TRANSDUCER